A STUDY OF THE SEDIMENT TRANSPORT
IN ALLUVIAL CHANNELS

by

James R. Barton and Pin-Nam Lin
Assistant Professors

Civil Engineering Department
Colorado A & M College
Fort Collins, Colorado

Prepared for the
Corps of Engineers
Department of the Army
Omaha, Nebraska

Under Contract No. DA-25-075-eng-2632
March, 1955

Report No. 55JRB2

A STUDY OF THE SEDIMENT TRANSPORT IN ALLUVIAL CHANNELS

by

James R. Barton and Pin-Nam Lin
Assistant Professors

Prepared for the
Corps of Engineers
Department of the Army
Omaha, Nebraska

[illegible] Contract No. DA-25 [illegible] 3632
[illegible]

FOREWORD

This report presents the results of a study made with the 70-foot tilting flume in the hydraulics laboratory at Colorado Agricultural and Mechanical College. The experiments were performed during late 1953 and early 1954 under the direct supervision of the authors.

All data collected are summarized in the Appendix so that the original data may be readily available to other investigators in the field of sediment transportation.

The study was sponsored by the Corps of Engineers, Department of the Army, through the Research Foundation of Colorado Agricultural and Mechanical College. Mr. Don C. Bondurant represented the sponsor. The cooperation and assistance rendered by him and his staff are greatly appreciated.

The project was conceived by Dr. M. L. Albertson, Head of Fluid Mechanics Research, who also offered many suggestions in the course of the study and thoroughly reviewed the manuscript of this report. Dr. D. F. Peterson, Head of the Department of Civil Engineering, made helpful comments in the preparation of the report. For the encouragement and assistance of both, the authors are much indebted.

Prof. T. H. Evans, Dean of the School of Engineering, is the Chairman of the Research Foundation of the Colorado Agricultural and Mechanical College.

The following staff members of the Department of Civil Engineering contributed in either collection of data or construction of equipment:

Messrs. D. J. Sadar, R. V. Asmus, A. R. Chamberlain, R. E. Bruce, and Prof. Maxwell Parshall.

TABLE OF CONTENTS

Chapter		Page
	LIST OF SYMBOLS.	iv
	LIST OF FIGURES.	vi
I	INTRODUCTION	1
II	REVIEW OF LITERATURE	2
	Resistance of Alluvial Channels	2
	Analysis by Einstein, Barbarossa and Banks	2
	Ali's study of alluvial channels	3
	Gilbert's observations of wave formation	3
	Shields' study of wave formation and channel resistance	3
	Kármán's analysis of desert dunes.	4
	Anderson's analysis of sediment waves.	4
	Tison's study of wave formation.	4
	The Mechanics of Suspended Load Transport	5
	Turbulent transfer of sediment and momentum.	5
	Mixing length concept.	6
	Theory of vertical distribution of sediment.	7
	Experimental studies	8
	Relationship between Z and Z_1	10
	Discharge of suspended load.	10
	Chien's analysis of sampling efficiency.	12
III	THEORETICAL ANALYSIS	13
	Kármán Constant	13
	Richardson Number	15
	Resistance of Alluvial Channels	17
	Dimensional Analysis.	18
	Non-dimensional Chezy's coefficient.	19
	The Kármán constant.	19
	Total discharge of bed material.	21
	Distribution of Sediment in a Vertical.	22
IV	EXPERIMENTAL EQUIPMENT AND PROCEDURE	24
	General Description of the Flume.	24
	Circulation System.	24
	Measuring Devices	26
	Discharge measurements	26
	Slope measurements	26
	Velocity measurements.	26
	Suspended sediment measurements.	26

TABLE OF CONTENTS

Chapter		Page
	Total sediment load measurements	27
	Bed roughness measurements	27
	Average depth.	27
	Temperature measurements	28
	Description of the Sediment	28
	Operation and Sampling Procedure.	28
	Sampling Methods.	29
V	DISCUSSION AND ANALYSIS OF DATA.	31
	Terms Used to Describe the Bed Conditions	31
	Variation of Bed Conditions with Mean Velocity of Flow.	32
	Resistance of an Alluvial Channel	33
	Kármán Constant	35
	Sediment Distribution in a Vertical Section	36
	Total Bed-Material Discharge.	36
	Sediment Sampling Efficiency	37
VI	SUMMARY AND SUGGESTIONS FOR FUTURE STUDY	39
	Summary	39
	Future Study.	40
	BIBLIOGRAPHY	41
	FIGURES	
	APPENDIX	

LIST OF SYMBOLS

Symbol	Dimensions	Definition or description
a	ft	A reference level measured from the bed
b	ft	Width of flume
c	%	Concentration of sediment by dry weight in percent of sample weight
c_a	%	c at the reference level "a"
c_m	%	Average c above level "a"
c_t	%	$q_t/\gamma q$
C	$ft^{1/2}/sec$	Chezy's coefficient in the formula $U_m \; C\sqrt{RS}$
d	mm	Median diameter of the sediment
D	ft	Mean depth of flow
E_1	$\frac{ft\text{-}lb}{sec} / ft^3$	Energy per unit flow volume required to over the difference in weight
E_2	$\frac{ft\text{-}lb}{sec} / ft^3$	Energy per unit volume extracted from mean motion by secondary motion
f	--	Darcy-Weisbach resistance coefficient
Fr	--	Froude number
g	ft/sec^2	Gravitational acceleration
G	lb/sec	Total sediment discharge
k	--	Kármán constant
K	ft	Height of the bed roughness a. For smooth bed - K equals the grain diameter of which 65% is finer b. For dunes - K equals the average height of the dunes as measured along a longitudinal line traverse
ℓ	ft	Mixing length
L	ft	Average length of dunes
M	slugs/sec	Bed-material discharge by mass
n	$ft^{1/6}$	Manning's roughness coefficient
q	$ft^3/sec/ft$	Water discharge per foot of width

Symbol	Dimensions	Definition or description
q_t	lb/sec/ft	Bed-material discharge per foot of width
Re	--	Reynolds number
Ri	--	Richardson number
S	--	Slope of the energy line
t	^{o}C	Temperature
U	ft/sec	Temporal mean velocity at a point
U_m	ft/sec	Mean of U in a vertical
U_{max}	ft/sec	Maximum value of U in a vertical
U_*	ft/sec	Shear velocity - $U_* = \sqrt{\tau_o/\rho}$
w	ft/sec	Fall velocity of median sediment size
y	ft	Distance above mean bed level
Z	--	Exponent in sediment distribution equation $Z = w/kU_*$
Z_1	--	Value of Z measured from empirical sediment distribution curve
β	--	Z_1/Z
γ	lb/ft^3	Specific weight of water
γ_s	lb/ft^3	Specific weight of sediment
ϵ_m	ft^2/sec	Turbulent momentum transfer coefficient
ϵ_s	ft^2/sec	Turbulent sediment transfer coefficient
μ	$lb\text{-}sec/ft^2$	Dynamic viscosity of water
ν	ft^2/sec	Kinematic viscosity of water
ρ	$lb\text{-}sec^2/ft^4$	Mass density of water
ρ_s	$lb\text{-}sec^2/ft^4$	Mass density of sediment
σ	mm	Standard deviation of sediment size distribution
τ	lb/ft^2	Shearing stress within the fluid
τ_o	lb/ft^2	Shearing stress at the boundary

LIST OF FIGURES

Fig. No.	Title
1	Distribution of a transferable characteristic
2	Schematic velocity distribution curves
3	Schematic sediment distribution curve
4	Schematic fall velocity distribution curve
5	Schematic diagram of the flume
6	Schematic diagram of pitot tube and sediment sampler
7	Schematic diagram of sampler for total sediment load
8	Views of flume equipment
9	Views of measuring equipment
10	Views of sampling equipment
11	Views of typical dune patterns
12	Views of typical sandbar patterns
13	Views of typical plane bed
14	Variation of resistance coefficient with Reynolds number— relative roughness as third variable
15	Variation of resistance coefficient with Richardson number and bed conditions
16	Variation of resistance coefficient with relative roughness
17	Variation of Kármán Constant with Richardson number and relative fall velocity
18	Typical velocity distribution curves
19	Typical sediment distribution curves
20	Variation of resistance coefficient with concentration of total sediment load
21	Variation of sampling efficiency with Reynolds number

CHAPTER I

INTRODUCTION

Within the last twenty years the field of sediment transportation has attracted considerable attention, and many papers have been written on the behavior of alluvial streams. Increased activity in the design and construction of hydraulic structures has brought on an urgent realization of the many problems which arise in the construction of any project that involves an alluvial channel. Canals scour or silt up, reservoirs fill up with sediment, excessive scour occurs downstream from dams, and dangerous sandbars form in navigation channels. These and many other problems confront the engineer who is faced with designing an efficient and lasting hydraulic structure.

Without a knowledge of the fundamental principles involved, the engineer is forced to rely on past experience as his guide. Unfortunately, however, past experience sometimes offers no clue to the solution of his special problem, and the results of his design are often discouraging. In order to alleviate this situation numerous research programs have been launched in the past 25 years to study in the laboratory and in the field the very complex problem of sediment moving in flowing water. Government agencies, educational institutions, private industries, and individuals have all made contributions to the present state of knowledge of the sediment problem, but the progress has been slow and many phases of the problem are not yet understood.

With this background, the present study, sponsored by the Corps of Engineers of the United States Army, was made at Colorado A & M College for the purpose of studying the specific problem of roughness in alluvial channels. Since the roughness of alluvial channels is inherently related to other problems not commonly thought of as channel roughness problems, some time was devoted to a study of these related subjects.

Thirty seven runs were made during a testing period of about six months and an analysis of the resulting data included information on the following topics:

(1) The roughness of an alluvial channel,

(2) The von Kármán constant which is closely related to the velocity distribution,

(3) The sampling efficiency involved in determining the amount of sediment moving through a given cross section of the flow,

(4) The distribution of suspended sediment.

The data involved in topic (4) have not been completely analyzed and therefore the results do not appear in this report, but will be made available later.

The results of the present experiments tend to emphasize the fact that the problem of sediment transportation is extremely complex and the final answers to all the numerous ramifications of the problem may require a great deal of time to obtain. However, it is hoped that the results obtained in these experiments will prove useful in helping to explain some of the problems which are not clearly understood at the present time.

Chapter II

REVIEW OF LITERATURE

Literature in the field of sediment transportation and open channel roughness is very extensive. Papers dealing with sediment motion in open channels date back as far as the experiments of Dubuat in 1786. These and other early experiments are described in an interesting manner by Hooker (15). Roughness of a fixed bed in open channels was investigated by Bazin as early as 1865. Since these early experiments, hundreds of laboratory and field studies have been made. This review of literature includes only certain of the more important contributions made in the field of sediment transportation and roughness of alluvial channels.

Resistance of Alluvial Channels

In addition to the possible effect of sediment on the resistance of flow, the study of resistance of alluvial channels is further complicated by the fact that the boundary "roughness" itself depends on the flow. The formation of sediment waves, therefore, plays an important role in the mechanics of resistance of alluvial channels. In this section, papers related to the study of resistance of alluvial channels are reviewed. The effect of sediment suspension on the turbulence of flow, however, will be dealt with later under "The mechanics of suspended load transport."

Analyses by Einstein, Barbarossa and Banks--In 1951, Einstein and Barbarossa (9) proposed to resolve the channel roughness into two classes, namely that of the grain and that of the bed waves. The so-called grain friction is given by

$$\frac{U}{U_*'} = \frac{U}{\sqrt{gR'S}} = 5.75 \log_{10}(12.3\frac{R'}{d_{35}}) , \quad (1)$$

where R' is so defined that $\rho U_*'^2 = \gamma R'S$ gives the part of shearing stress transmitted to the bed by grain roughness, and d_{35} is the grain size of the bed material of which 35% by weight is coarser. According to Einstein and Banks (10), "many experimenters in laboratories have observed that the shape of the bars seems to be a function of the sediment transport, more exactly of the bed-load transport." Consequently, the resistance due to bed waves is taken as a function of the parameter

$$\psi' = \frac{\rho_s - \rho_f}{\rho_f}\frac{d_{35}}{R'S} ,$$

which is the parameter of flow intensity in Einstein's bed load equation. From experimental data, a plot of U/U_*'' against ψ' can be prepared. Here $U_*'' = \sqrt{\tau_0''/\rho}$, τ_0'' being the shearing stress transmitted to the bed through the drag on the sand waves. In practical application of this method to compute, say Manning's n, the first step is to compute R' from the known values of U and S by means of Eq 1. With R' known,

ψ' can be computed. A plot of U/U_*'' against ψ' will then enable one to obtain U_*'' and R''. The hydraulic radius of the channel is taken as $R = R' + R''$, and the computation of n can then be completed by means of the Manning formula where n is now the only unknown.

The foregoing method is based on the premise that, in a system involving several components of resistance, the resultant resistance is simply the arithmetic sum of the components. In other words,

$$U_*^2 = \sum_{i=1}^{n} U_{*i}^2 = \sum_{i=1}^{n} (gRS)_i .$$

That this step is practicable has been demonstrated by Einstein and Banks (10, 11) on the condition that, of any two boundary protrusions of different types, one must not be less than 5 to 10 times the size of the other.

<u>Ali's study of alluvial channels</u>--Said Ali and M. L. Albertson (1) conducted an analysis of a large quantity of data published by various agencies and found that the data indicated

$$\frac{C}{\sqrt{g}} = \phi\left(\frac{U_m R}{\nu}, \frac{d}{R}\right), \tag{2}$$

where d is the median diameter of the bed material. Graphs have been prepared by Ali and Albertson on the basis of Eq 2. According to these graphs, there is, for a given value of d/R, a Reynolds number corresponding to the maximum resistance coefficient for the channel. As Reynolds number is further increased, the resistance coefficient decreases, eventually approaching the limit of a plane bed.

<u>Gilbert's observations of wave formation</u>--Gilbert (13) first observed the three regimes of sediment waves. Starting with a plane bed, when the velocity was low, only movement of grains at isolated spots would occur. Gilbert observed, however, that even under such conditions, dunes would develop. These dunes existed for a certain range of velocity. As the velocity was increased beyond this range, Gilbert observed that the dunes would "rather abruptly" disappear, leaving behind a plane bed.

It is not clear to the authors whether Gilbert observed the regime of sandbars described later in this report although he did state in his discussion of the "rhythm" or periodic disturbance in his flow system that "associated with the dunes were greater debris waves, also traveling downstream and each involving the volume of many dunes." Unfortunately, the authors cannot find any information in Gilbert's paper (13) regarding the appearance of these large "debris waves" in a plan view or the appearance of the water surface when these large "debris waves" occurred.

<u>Shields' study of wave formation and channel resistance</u>--Shields (32) found with particles of uniform size that the pattern of sediment waves, which formed when general movement of the bed began, varied with d/δ', where δ' is the thickness of the laminar sub-layer. In the order of increasing d/δ', the initial bed may have ripples, short bars, diagonal bars, and shallow undulations.

His measurements also indicated that for a given material, the resistance coefficient is a function of slope and the Reynolds number.

Kármán's analysis of desert dunes— In 1947, Kármán (18) presented expressions for the length of dunes in a desert. If v is the average turbulent velocity fluctuation in the vertical, then the maximum height a particle will attain is proportional to $v^2/2g$ and the time of travel may be taken as proportional to, say $2v/g$. The horizontal distance a particle would travel will then be of the order of $2Uv/g$, U being the mean velocity near the boundary. Assuming $v \propto U_*/\sqrt{2}$, one obtains for the length of the dunes approximately

$$L \cong \frac{U\ U_*}{\sqrt{2}g} . \tag{3}$$

A similar equation was also derived by Kármán, who assumed that the velocity of flow along the wavy surface was constant, and that the surface was of sinusoidal form. The consideration of a small disturbance then led to

$$L = 2\pi U\sqrt{\frac{\delta}{g}} , \tag{4}$$

where δ is the thickness of the layer in which most of the material is concentrated. (This layer is comparable to the saltation layer as proposed by Danel, Durand and Condolios (6). If $\delta \propto v^2/2g$, Eq 4 is reduced to an equation similar to Eq 3.

Anderson's analysis of sediment waves—By postulating that a surface wave induces the formation of a bed wave, Anderson (2) ignored viscosity and derived by successive approximation the stream function for flow over a bed of sand waves. This stream function may be used to obtain an expression of D/L, the ratio of the depth of flow to the length of sediment waves, as a function of the Froude number $U_m/\sqrt{gD}$. The resultant expression was found by Anderson to follow available data very well. The authors wish to point out, as Vanoni has done (35), that Anderson's treatment cannot apply to the formation of sediment waves in the desert or on the floor of a deep ocean where a free surface does not exist or is at a great distance above the bed. According to Menard (22), ripple marke have been photographed on the ocean floor at a depth of 792 ft and, in some cases have been found at a depth as great as 4500 ft.

Tison's study of wave formation—With experiments carried out in a flume with oils, Tison (33) showed that dunes could not form in a laminar flow over a bed of sediment. When a transverse sandbar was artificially molded across the upstream end of the flume, he observed that scour and deposition would take place downstream as a result of the modification in the initial flow pattern by the sandbar. However, as long as the flow remained laminar, dunes did not form. Similarly, when a vertical cylinder was placed in the flow, a pattern of scour and deposition similar to that around a cylindrical pier was observed; but again as long as the flow was laminar, no dune formation took place.

The Mechanics of Suspended Load Transport

In this section, certain fundamental topics in the mechanics of suspended load transport are outlined.

Turbulent transfer of sediment and momentum--Let the case of uniform turbulent flow carrying sediment in a wide channel be considered. Disregarding the formation of secondary circulations, one may take the temporal mean of the velocity at any point of the flow as parallel to the axis of the channel. Velocity fluctuations due to turbulence, however, may exist in all three directions. Because of the requirement of continuity of flow, any instantaneous flow caused by turbulent fluctuation in a certain direction must be accompanied by a flow of equal discharge in the opposite direction.

Velocity fluctuations due to turbulence, therefore, give rise to exchange or mixing in the flow. Whenever a gradient of a transferable entity exists in the flow, exchange of fluid at equal rates of volume naturally transfers the entity under question in the direction of decreasing gradient. Thus, because of turbulence, sediment will be constantly transferred, on a statistical basis, from more concentrated to less concentrated regions; and, likewise, momentum will be transferred toward the boundaries where the velocities are low. In the case of flow in a wide channel mentioned above, mean gradients of velocity and concentration exist only in the vertical direction. It is in this direction that turbulent transfer plays an important role.

Vertical transfer of momentum tends to speed up the low-velocity zone and to slow down the high-velocity zone. The effect is the same as having a shearing stress acting at each point of the flow. Thus it is often said that shearing stress in a turbulent flow is transmitted by momentum transfer. It can be seen that more momentum will be transferred when there is a greater difference in momentum distribution over a given distance, so that the shearing stress transmitted by momentum transfer is expected to be proportional to the gradient of momentum, i. e., $d(\rho U)/dy$. Boussinesq (3) first proposed an equation for the shear in fully turbulent flow of the form

$$\tau = \rho \epsilon_m \frac{dU}{dy} , \qquad (5)$$

where $\rho\epsilon_m$ has the same dimensions as the coefficient of viscosity, and is often called the eddy viscosity.

In 1925, Schmidt (30) introduced the term transfer (or exchange) coefficient in his study of the vertical transfer of dust in the atmosphere, and developed an expression for the rate of sediment transfer per unit area as

$$q_s = -\epsilon_s \frac{dC}{dy} , \qquad (6)$$

where ϵ_s is the coefficient of sediment transfer. Obviously, this expression is similar to Eq 5 . In these two equations, τ corresponds to q_s , ρU to C , and ϵ_m to ϵ_s . The term ϵ_m is thus known as the coefficient of momentum transfer.

Mixing Length Concept--By the analogy between molecular and eddy motion, Prandtl (14) postulated a certain length ℓ' , similar to the mean free path in molecular diffusion. The hypothesis proposed by Prandtl is that ℓ' is a unique length which characterizes the local intensity of the turbulent mixing at any level, but which, unlike the mean free path, may vary from point to point and may even depend on U and possibly other variables. According to this hypothesis, transfer of a characteristic in a turbulent flow is effected by the motion of elements of fluid, each of which leaves one layer and moves in a direction transverse to the mean flow through the distance ℓ' . At this point, each element is supposed to mix with the surrounding fluid so that its characteristic becomes identical with the mean characteristic in that region. Let Θ be the mean value of a transferable characteristic dependent on y only. The mean flow is assumed to be in the x-direction. Then according to the mixing length hypothesis, the instantaneous rate of transfer of Θ into a unit area in the layer at y_2 is given by

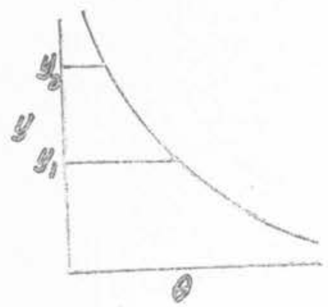

Fig. 1 Distribution of a transferable characteristic

$$v' \left[\Theta(y_1) - \Theta(y_2)\right] .$$

Expanding this in terms of a Taylor series and taking the first approximation when either $(y_2 - y_1)$ or $\frac{d\Theta}{dy}$, or both, is small, one has the mean rate of transfer per unit area

$$q_\Theta = \overline{-v' (y_2 - y_1) \frac{d\Theta}{dy}}$$

$$= - \overline{v' (y_2 - y_1)} \frac{d\Theta}{dy}$$

$$= - \ell' \sqrt{\overline{v'^2}} \frac{d\Theta}{dy} ,$$

where ℓ' is so defined that $\ell' \sqrt{\overline{v'^2}} = \overline{v' (y_2 - y_1)}$.

Obviously, if momentum is the characteristic being transferred, then

$$\Theta = \rho U \quad \text{and} \quad \epsilon_m = \ell' \sqrt{\overline{v'^2}} ,$$

so that

$$\tau = \rho \ell' \sqrt{\overline{v'^2}} \frac{dU}{dy} . \qquad (7)$$

Prandtl (14) further proposed that $\ell' \sqrt{\overline{v'^2}} = \ell^2 \left|\frac{dU}{dy}\right|$. Therefore,

$$\tau = \rho \ell^2 \left|\frac{dU}{dy}\right| \left(\frac{dU}{dy}\right) \qquad (8)$$

ℓ is also known as the mixing length. It should be noted, however, that in general ℓ' is not equal to ℓ .

Theory of vertical distribution of sediment--If the sediment concentration by volume is interpreted as the fraction of area occupied by the sediment particles per unit area, the volume of sediment settling through a unit area per unit time is simply (wc)(1), where w is the fall velocity of the uniform sediment. Under steady conditions of flow, the rate at which sediment is being transferred upward through a horizontal plane must be equal to the rate at which sediment settles through the same plane by gravity. Thus setting $q_s = wc$, one has

$$wc + \epsilon_s \frac{dc}{dy} = 0 , \qquad (9)$$

which was first obtained by O'Brien (24) . Assuming that $\epsilon_s = \epsilon_m$, one may write

$$\epsilon_s = \epsilon_m = \frac{\tau}{\rho} \Big/ \frac{dU}{dy} . \qquad (10)$$

For uniform mean flow in a channel,

$$\frac{d\tau}{dy} = \gamma \frac{dh}{dx} = -\gamma S , \qquad (11)$$

where h is the piezometric head. Since the slope S is constant, integration of Eq 11 leads to

$$\tau = -\gamma Sy + \text{const}$$

when $y = D$, $\tau = 0$; so that

$$\tau = \gamma S\,(D-y)$$

$$= \tau_0 \left(\frac{D-y}{D}\right), \qquad (12)$$

where τ_o is the shearing stress at the bed. Now according to Kármán, in a turbulent flow

$$\frac{dU}{dy} = \frac{1}{ky} \sqrt{\frac{\tau_o}{\rho}} \quad , \tag{13}$$

k being the Kármán constant. Substituting from Eqs 12 and 13 in Eq 10 leads to

$$\epsilon_m = \frac{\frac{\tau_o}{\rho} \frac{D-y}{D}}{\frac{1}{ky}\sqrt{\frac{\tau_o}{\rho}}} = k \sqrt{\frac{\tau_o}{\rho}} \frac{D-y}{D} y \ .$$

Eq 9 is consequently reduced to

$$wc + kU_* \frac{D-y}{D} y \frac{dc}{dy} = 0 \ .$$

Separating variables,

$$\int_{c_a}^{c} dc = -\frac{wD}{kU_*} \int_{a}^{y} \frac{dy}{y(D-y)} \ ,$$

which, on reduction, leads to

$$\frac{c}{c_a} = \left(\frac{D-y}{y} \frac{a}{D-a} \right)^Z \ , \tag{14}$$

where

$$Z = \frac{w}{kU_*} = \frac{w}{k\sqrt{gDS}} \ .$$

Eq 14 was first derived around 1936 by A. T. Ippen at the suggestion of von Kármán and was presented by Rouse (26) in 1937. It gives the concentration at an arbitrary point at a distance y above the bed, when c_a at some distance "a" above the bed is known.

Experimental studies--In 1946, Vanoni (35) presented the results of a series of elaborate tests in a flume. He found that Eq 14 was of the right form; but, in order to fit the experimental data, the exponent Z had to be modified. By letting the modified value of Z be Z_1, then in general $Z_1 < Z$, i.e., the actual distribution of sediment is more unifrom than the theoretical distribution. This was taken by Vanoni as an indication that sediment and momentum transfer coefficients were not equal. By comparing Z and Z_1, he concluded that for fine material the coefficient of sediment transfer tends to exceed the coefficient of momentum transfer, and for coarser sediment the tendency was reversed. In his tests, apparently only a small amount of sand was present on the bed of the flume. Both the

Kármán constant k and the resistance coefficient f were observed to be reduced by the presence of suspended load. The discrepancy between the calculated and measured distributions and the reduction in k and f were considered by Vanoni to be related essentially to three effects that occurred in the flow in the presence of the sediment: (1) the sediment appears to damp out the turbulence in such a way that the momentum transfer is reduced, (2) random turbulence, which is not a factor in the transfer of momentum, contributes to the transfer of sediment, and (3) the "slip" between the fluid and the sediment tends to make the sediment transfer coefficient less than the momentum transfer coefficient.

In a paper published in 1951, Ismail (16) extended Vanoni's studies. Besides verifying Vanoni's findings, Ismail observed that the coefficient of friction for a stream carrying suspended sediment exceeded that for clear flow only when dunes formed on the bed.

Later in 1953, Vanoni (34, 36) reported more data obtained from flume experiments. It is of particular interest to note that even in the occasional presence of dunes, the resistance coefficient f was observed by Vanoni (34) to be invariably reduced. It is also of interest to note that an examination of Nikuradse's data by Vanoni shows that over a range of wall roughness varying from 1/15 to 1/507 of the pipe radius, the Kármán constant changes from 0.324 to 0.415. The average of all experimental values was 0.374, so that the maximum and the minimum values of k were within about 10% of the average. From the new data, Vanoni found that the ratio of Z to Z_1, may be greater or less than unity (34:150).

Measurements of k made at the Iowa Institute of Hydraulic Research (23) in clear water flowing over a very rough bed (roughness up to about 1/5 of the depth of flow) show also a reduction of k to about 0.3. These tests clearly indicate that k can be influenced by factors other than the presence of the suspended load.

Regarding damping of turbulence by the presence of sediment, attention should be called to a parameter proposed by Einstein and Chien (12). This parameter may be expressed as

$$\left(1 - \frac{\gamma}{\gamma_s}\right) \frac{\sum cw}{U_m S},$$

where the summation sign is to extend over the entire vertical. It is in fact the sum of the ratios of the power per unit width required to keep the sediment in suspension,

$$(\gamma_s - \gamma) \sum \frac{c}{\gamma_s} w,$$

to the power of flow per unit width dissipated in turbulence, $\gamma U_m S$.

Relationship between Z and Z_1—In a report prepared for the Missouri River Division, Corps of Engineers, Einstein and Chien (12) treated at great length the problem of obtaining a closer approximation to the solution of the suspended load theory. Of the six possible cases they presented, five were based on the probability distribution of the quantity $\ln(1 + Bk)$, which was called by Einstein and Chien as the mixing length. In this expression, B is a constant and k is the Kármán constant. The case considered by Einstein and Chien as having the best possibilities is briefly described.

In this case, the Kármán finding that the frequency distribution of turbulent velocity is approximately normal is adopted along with the probability distribution mentioned above. Ergodic transformation then yields

$$q_v = \int v' dA = \int_0^{\infty} v' p dv' = \frac{\sigma}{\sqrt{2\pi}} ,$$

where p is the probability for the fluctuating velocity to be v'. Assuming that the velocities of upward and downward fluctuations are equal and that the fluctuations take place through the entire area, Einstein and Chien obtained the equation of sediment exchange in a flow assumed to be of infinite depth as

$$\int_w^{\infty} c_u(v' - w) p dv' - \int_{-w}^{\infty} c_d(v' + w) p dv' = 0 , \qquad (15)$$

where w is the fall velocity and c_u and c_d are respectively the average concentrations of the upward and downward flows through the area under consideration. Solution of Eq 15 then led to

$$Z_1 = \frac{Z}{e^{-L^2 Z^2/\pi} + ZL \frac{2}{\sqrt{2\pi}} \int_0^{-\sqrt{2/\pi}\, LZ} e^{-x^2/2}\, dx} . \qquad (16)$$

Discharge of suspended load—Several methods are available to estimate the discharge of suspended load. Lane and Kalinske (20) stated that the ratio c_a/c_b for a size interval having a fall velocity w is a function of w/U_*. Here c_a is the concentration of the material in suspension at a certain point just above the bed, and c_b is the concentration of that material in the bed. A curve relating c_a/c_b to w/U_* was prepared by Lane and Kalinske (20) on the basis of field data. Later Kalinske and Hsia (17) considered, in addition, the case of fine material under the action of weak shear. In this case, viscosity may be an important variable in the mechanism of sediment entrainment. Consequently, Kalinske and Hsia proposed that c_a/c_b was a function of both w/U_* and $\frac{U_* d}{\nu}$. In order to apply the results of these studies to practical calculation of suspended load discharge, one must determine the value of "a" . Rouse (27, 28) suggested that "a" be of the order of the bed roughness k .

Another method proposed by Lane and Kalinske (21) consists in using the mean value of the transfer coefficient to compute the discharge of suspended load. Using the Karman-Prandtl equation of velocity distribution, one has

$$\epsilon_m = kU_*y \left(1 - \frac{y}{D}\right),$$

the mean of which over a vertical is

$$\overline{\epsilon}_m = \frac{DU_*}{15} . \qquad (17)$$

Substituting from Eq 17 in Eq 9, and integrating,

$$\frac{c}{c_a} = e^{-15\frac{w}{DU_*}(y - a)},$$

therefore,

$$q_s = \int_0^D Ucdy = qc_aP_e^{15\frac{a}{y}\frac{w}{U_*}}, \qquad (18)$$

where P is a function of w/U_* and $U_*/U_m = 3.8\left(n/D^{1/6}\right)$. With w/U_* and $n/D^{1/6}$ ascertained, P may be evaluated by a plot given by Lane and Kalinske (21).

In 1950, Einstein (8) presented a procedure for estimating the discharge of suspended load. He assumed the thickness of the bed layer was 2d . If q_B was the discharge of bed load, then the concentration of grains of a given size within this layer was taken by Einstein to be proportional to

$$\frac{q_B i}{2U_B d},$$

where i = the fraction of q_B having a size interval with an average diameter of d , and U_B = the flow velocity at the bed. Assuming further, $U_B \ll U_*$, Einstein obtained the equation

$$c_a = c_{2d} = \frac{q_B i}{23.2dU_*} .$$

With c_a known, the concentration of suspended sediment at any other point in the flow may be computed by means of Eq 14. The discharge of suspended sediment is then given by

$$q_s = \gamma_s \int_{2d}^{D} Ucdy .$$

Chien's analysis of sampling efficiency--In 1952, Chien applied the method proposed by Einstein (4) for the computation of total sediment discharge and derived the following expression:

$$i_{sa}q_{sa} = \int_{a}^{D} c_{2d} \left(\frac{D-y}{y} \times \frac{2d}{D-2d} \right)^{Z} Pdy ,$$

where $i_{sa}q_{sa}$ gives the fraction of suspended load in the size interval d that is being transported in the upper portion of the flow having a thickness of $(D - a)$, c_{2d} is the sediment concentration at a distance of 2d above the bed, and P represents $5.75\ U_*' \log 30.2\ \frac{y}{K}$.
The term U_*' here is the so-called shear velocity with respect to the grain size. Applying again the method proposed by Einstein, one can obtain an expression for the fraction i_t of the total sediment discharge q_t in the size range d . Sampling efficiency is then given by $\frac{i_{sa}\ q_{sa}}{i_t\ q_t}$.

Chien found that for ordinary rivers, P varied from 9 to 12, and that within this range of P , assuming constancy of P would cause an error of about 5%, which may often be considered as acceptable. By assuming further that d and U_*' may be replaced by w/U_*' , Chien was able to compute a set of curves relating Z to the sampling efficiency, $i_{sa}q_{sa}/i_tq_t$, with the depth of flow D as the third variable.

Chapter III

THEORETICAL ANALYSIS

The present chapter deals principally with the following subjects:

(1) Variation of the resistance coefficient in an alluvial channel.

(2) Variation of the Kármán constant in sediment-laden flow.

(3) The transport of total bed-material load.

(4) The distribution of non-uniform sediment in a vertical section.

When relatively coarse sediment is being transported in suspension in a uniform flow, owing to the greater specific gravity of sediment, more sediment will be found in the neighborhood of the bed than in the region close to the surface, so that the concentration of sediment decreases with vertical distance above the bed. A vertical density gradient is thus said to exist. The influence of such a density gradient on turbulent transfer will be examined in detail in connection with the first two topics mentioned above.

Because of the existence of a vertical gradient of density, the mechanics of sediment-laden flow is not always identical with the hydraulics of homogeneous liquids. For instance, in the idealized case of perfectly uniform flow in a channel having parallel, vertical walls, in which waves do not exist, the Froude number according to the hydraulics of homogeneous liquids, is not a significant parameter. Nor is the Froude number considered a significant parameter in the study of pipe flow in the absence of sediment. These observations, rightly made with flow of homogeneous liquids, are not necessarily true when a vertical density gradient exists in a flow. Further discussions will be made elsewhere in this chapter.

The available theory of sediment distribution in a vertical (see Chapter II Section 2) is based on several assumptions, one of these assumptions being that the sediment is uniform in size. When the size distribution is such that the sediment may not be considered as uniform, the theory of sediment distribution in a vertical must be extended to account for the effect of size variation. An equation involving an integral will be presented.

<u>Kármán Constant</u>

There are two ways to define the Kármán constant k . According to Kármán's theory of mechanical similarity (14), it may be defined as

$$\ell = k \frac{\frac{\partial U}{\partial y}}{\frac{\partial^2 U}{\partial y^2}} ,$$

where ℓ is the mixing length. The Kármán-Prandtl equation of velocity distribution leads to another expression for k ,

$$\frac{dU}{dy} = \frac{U_*}{ky} \tag{19}$$

In the present discussion, the latter expression will be used. Let curve (1) in Fig. 2 represent the velocity profile for flow of homogeneous fluids, for which the Kármán constant is often taken as 0.4 on the basis of Nikuradse's work (14).

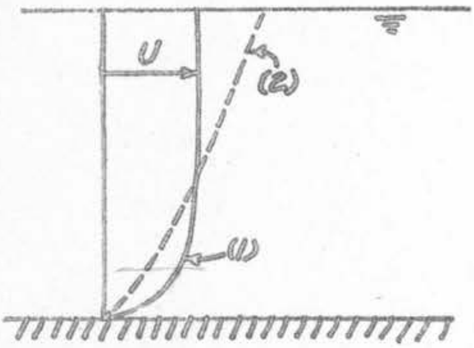

Fig. 2 Schematic Velocity Distribution Curves

If now the intensity of mixing is somehow reduced, the velocity distribution will be less uniform, and may take on a form like curve (2). The value of U_* corresponding to curve (2) is smaller than that in the case of curve (1), whereas the value of $\frac{dU}{dy}$ in the turbulent zone of curve (2) is greater than that in the case of curve (1). Since Eq 19 has been found by many investigators (35, 16) to be in good accord with experimental data, it is only possible to conclude that the Kármán constant k decreases when the rate of mixing is reduced. Similarly, when the rate of mixing is increased (e.g., turbulent flow over a heated plate), U_* will be increased whereas $\frac{dU}{dy}$ will be reduced, so that the Kármán constant is increased. Therefore, the Kármán constant may be regarded as an index of the rate of turbulent transfer. It varies directly with the rate of turbulent transfer of momentum. Under special conditions, values of k up to 0.61 have been observed by Sheppard (31).

For flow wherein the density decreases with vertical distance above the bed, turbulent transfer in a vertical invariably requires work done against gravitation to raise heavier material upward and to force lighter material downward. In this process, part of the kinetic energy available in turbulence is converted to potential energy, thereby reducing the amount of kinetic energy available for mixing. Thus when there is a gradient of density decreasing with height, the rate of turbulent mixing or transfer may be expected to decrease, and the value of k likewise may be expected to decrease.

Basically, in the absence of a gravitation field, vertical density gradient would not have any effect on the turbulent transfer in a vertical section. It is to overcome the gravitation field that some kinetic energy of turbulence is converted into potential energy. Therefore, the influence of vertical density gradient on turbulent mixing is basically a result of gravitation, and some form of the Froude number may be a significant parameter in the study of flow having a vertical density gradient. Thus, contrary to the hydraulics of homogeneous fluids, even for perfectly uniform flow enclosed in pipes or between vertical, parallel walls, some form of the

Froude number may be a significant parameter, provided that there is a vertical density gradient in the flow. This may explain why in the study of sediment transportation in pipes, a form of the Froude number is sometimes found to be a basic parameter (5, 7).

It should be pointed out, however, that for the case of uniform flow with respect to the longitudinal direction, Froude number could be important only when there is a vertical gradient of density. In view of this fact, it is logical to combine the Froude number and parameters characterizing density gradients in such a manner that the resultant parameter vanishes when either the density gradient or the gravitational force vanishes. The result is the Richardson number (25).

In summary, then, the Kármán constant may be regarded as an index of momentum transfer by turbulence. The greater the rate of momentum transfer, the greater will be the value of k. Since the rate of momentum transfer is influenced by the existence of a density gradient in the direction concerned, the Kármán constant is expected to depend on the Richardson number, which determines the reduction of the rate of momentum transfer by stabilizing density gradients, and possibly some other parameters which characterize the energy received from the mean flow.

Richardson Number

Whenever there is a vertical density gradient normal to the main flow, turbulent transfer in a vertical will involve exchange of matter of different density, so that work is done either on or by the eddies responsible for the exchange. To express the effect of gravitation in such a case, Richardson proposed a dimensionless parameter which was deduced by considering the ratio of work done against the density gradient (in the case of density decreasing with height above the solid boundary) to the energy of turbulence received from the main flow. A form of the number as presented by Prandtl (24) is

$$Ri = \frac{\frac{g}{\rho}\frac{\partial \rho}{\partial y}}{\left(\frac{\partial U}{\partial y}\right)^2}$$

However, for the study of sediment transport by suspension, it is more convenient to use a form of Richardson number as deduced in the following:

Let γ be the weight per unit volume of the water-sediment mixture. Then over an individual mixing length (24) of ℓ, a small element of fluid prior to being mixed will have its weight differing from that of the surrounding medium by

$$-\ell \frac{d\gamma}{dy},$$

In the case of a density decreasing with height above the bed, this difference in weight always opposes the motion, so that work has to be done to overcome the difference in weight. The rate at which the work is done by a unit volume of the fluid is

$$-w'\ell \frac{d\gamma}{dy} = - w'\ell \frac{dc}{dy} .$$

The temporal mean of this quantity is taken as

$$E_1 = \gamma_w \overline{w'\ell} \frac{dc}{dy} = - \gamma_w \epsilon_s \frac{dc}{dy} .$$

Now the energy of turbulence is received from the mean flow through the work done by the Reynolds stresses. In the present study, the pertinent component of the Reynolds stresses is the shearing stress acting in horizontal planes. Therefore, energy is extracted by the secondary motion from the mean motion at a rate of

$$E_2 = \tau \frac{dU}{dy} \qquad \text{per unit volume.}$$

The last two equations may be combined to give the following ratio which indicates the percentage of the energy in turbulence that is being converted to potential energy:

$$\frac{E_1}{E_2} = - \frac{\gamma_w \epsilon_s \frac{dc}{dy}}{\frac{dU}{dy}} . \tag{20}$$

Since $$wc + \epsilon_s \frac{dc}{dy} = 0 ,$$

and $$\tau \frac{dU}{dy} = \tau_o \left(1 - \frac{y}{D}\right) \frac{U_*}{ky} ,$$

Eq 20 is reduced to

$$\frac{E_1}{E_2} = \frac{\gamma_w wc}{\tau_o\left(1 - \frac{y}{D}\right)\frac{U_*}{ky}}$$

$$= \frac{gDwc}{U_*^3\left(1 - \frac{y}{D}\right)} \frac{ky}{D}$$

$$= \frac{wc}{U_* S} k \frac{\frac{y}{D}}{\left(1 - \frac{y}{D}\right)} . \tag{20a}$$

From a dimensional viewpoint, the significant parameter in the foregoing expression is $\frac{wc}{U_* S}$ as computed at a given value of y/D. This group, being of the nature of a Richardson number, will be denoted by Ri in this report.

It should be pointed out that the Richardson number used in the present report is very similar to a parameter proposed by Einstein and Chien (See Chapter II, Section 3), namely,

$$\frac{\rho_s - \rho}{\rho_s} \sum \frac{wc}{U_m S} .$$

The difference between the Richardson number used in this report and the Einstein and Chien parameter lies in the fact that Ri in Eq 20a is based on local values and includes U_* in the expression, whereas the latter is computed on the basis of the entire cross-section and uses the mean velocity in the parameter.

Resistance of Alluvial Channels

In the present report, a dimensionless form of the Chezy coefficient $C/\sqrt{g}$ will be used as an index of channel resistance. From the Chezy equation for two dimensional flow

$$U_m = C\sqrt{DS} ,$$

it follows that

$$U_m = C\sqrt{gDs}/\sqrt{g} ,$$

so that

$$\frac{C}{\sqrt{g}} = \frac{U_m}{U_*}$$

From this expression, it is clear that, being equal to the ratio of mean velocity to shear velocity, $C/\sqrt{g}$ must depend, among other things, on the velocity distribution in a vertical. This is to say that, since velocity distribution depends on the turbulent transfer in a vertical section, one may expect the Richardson number to be a controlling factor of $C/\sqrt{g}$.

For uniform flow of homogeneous liquids, one can deduce from the Kármán-Prandtl resistance equations

$$\frac{C}{\sqrt{g}} = f \text{ (Re, relative roughness)} .$$

In the range of experiments reported herein and also in the range of field data, the Reynolds number is often of such magnitude that the flow is of the so-called fully-rough type. For this type of flow, Reynolds number may be of secondary importance. Granting that this is the case and that the liquid is homogeneous, one has

$$\frac{C}{\sqrt{g}} = f_1 \text{ (relative roughness)} .$$

When there is a vertical density gradient in the flow, however, the foregoing equation should be modified to include the Richardson number, leading to

$$\frac{C}{\sqrt{g}} = f_2 \text{ (Ri, relative roughness)} .$$

But for flow having appreciable vertical density gradients in alluvial channels, the boundary roughness is a function of the flow and sediment characteristics, so that

$$\frac{C}{\sqrt{g}} = f_3 \text{ (Ri, relative sediment size)} .$$

The variation of $C/\sqrt{g}$ as well as that of the Kármán constant will be dealt with somewhat more formally in the following dimensional analysis.

Dimensional Analysis

Let the channel be very wide and be composed of relatively fine and cohesionless materials. Then for a uniform flow of given liquid property and at a given depth and mean velocity, not only will the total amount of sediment being transported be uniquely determined, but also the distribution of sediment and velocity in a vertical section. Thus, one may write the following equations: discharge

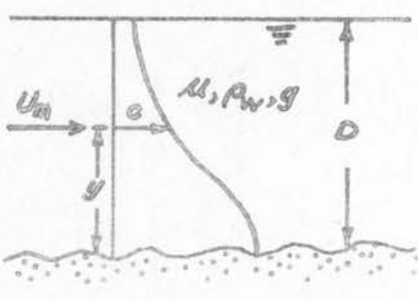

Fig. 3 Schematic sediment distribution curve

The bed-material discharge

$$G = f_1 (U_m, D, \rho_w, \mu, g, w), \tag{21}$$

the sediment concentration at a height y

$$c = f_2 (U_m, D, \rho_w, \mu, g, w, y), \tag{22}$$

the shear velocity (which depends on the velocity distribution)

$$U_* = f_3 (U_m, D, \rho_w, \mu, g, w), \tag{23}$$

and the Kármán constant (which also depends on the velocity distribution)

$$k = f_4 \, (U_m, D, \rho_w, \mu \, , g, w) \tag{24}$$

Non-dimensional Chezy's coefficient--Starting from these expressions, various flow variables will be discussed. By virtue of Eq 22, one may write

$$U_* = f_3 \, (U_m, D, \rho_w, \mu \, , g, w)$$

$$= f_5 \, (U_m, D, \rho_w, c, g, w, y),$$

so that on applying the Pi-theorem to f_3, one obtains

$$\frac{C}{\sqrt{g}} = \frac{U_m}{U_*} = f_6 \left(\frac{U_m D}{\nu} \, , U_m/\sqrt{gD} \, , w/U_m \right) \tag{25}$$

and on understanding that c is the value at a given y/D, the Pi-theorem applied to f_5 with U_*, D and ρ_m as the repeating variables results in

$$\frac{C}{\sqrt{g}} = \frac{U_m}{U_*} = f_7 \, (c, \, U_*/\sqrt{gD} \, , w/U_*) \tag{26}$$

However, the Froude number $U_*/\sqrt{gD}$ alone **will** not have any influence on $C/\sqrt{g}$ unless there is a density gradient in the vertical direction. Nor should the concentration alone be a significant variable unless a gravitational field exists or unless the concentration is so high as to materially change the effective density and viscosity of the sediment-laden water. In view of these considerations as well as the fact that the concentration of sediment transported by flow in open channels is usually low, it appears reasonable that Eq 26 may be given the special form

$$\frac{C}{\sqrt{g}} = f_8 \, (\frac{wc}{U_* S} \, , \frac{w}{U_*}) \tag{27}$$

where the first parameter is the Richardson number as previously explained and has been obtained here by combining the three dimensionless parameters on the right-hand side of Eq 26. The second parameter in Eq 27 may be regarded as a parameter characterizing the sediment property. Obviously, more than one parameter will be needed to accurately represent the sediment properties. For a preliminary study, the median fall velocity is used.

The Kármán constant--Using Eq 23, one may rewrite Eq 24 as

$$k = f_9\ (U_*,\ D,\ \rho_w, \mu,\ g,\ w)\ .$$

Dimensional analysis then leads to

$$k = f_{10}\ (c,\ S,\ \frac{w}{U_*})\ .$$

Consideration of the effect of density gradient again gives rise to the use of the Richardson number, so that one has the tentative form

$$k = f_{11}\ (\frac{wc}{U_* S}, \frac{w}{U_*})\ . \qquad (28)$$

When the flow is such that practically no sediment is in suspension, there are two possible cases in the study of the Kármán constant. First, the bed load transport may remain active, so that the channel may still be regarded as alluvial, and the bed roughness K is a variable governed by other flow parameters, i.e.,

$$K = f_{12}\ (U_m,\ D,\ \rho_w,\ \mu\ ,\ g,\ w) \qquad (29)$$

Substituting from Eq 29 into Eq 24

$$k = f_{13}\ (U_m,\ D,\ \rho_w,\ \mu\ ,\ g,\ K) \qquad (30)$$

so that

$$k = f_{14}\ (U_m D/\nu\ ,\ U_m/\sqrt{gD}\ ,\ K/D)$$

Since the Froude number cannot have influence on the velocity distribution in a uniform flow of clear water,

$$k = f_{15}\ (U_m D/\nu\ ,\ K/D) \qquad (31)$$

For large values of $U_m D/\nu$, the velocity distribution is essentially independent of the Reynolds number. As a result, one may write

$$k = f_{16}\ (\frac{K}{D})\ . \qquad (32)$$

It should be noted that Eq 32 is deduced on the basis that the Froude number may be ignored. This elimination of Froude number may be justifiable when there is no vertical density gradient in the flow.

The other possible case of flow without sediment in suspension occurs when the magnitude of the drag is too small to move the bed material. Then the channel no longer behaves as an alluvial channel. In this case, the bed roughness is an independent variable. For very rough bed, the drag on the bed is essentially due to the presence of a separation zone behind the sand waves, so that the size of material becomes unimportant. Consequently, one may again write

$$k = f_{13}\,(U_m,\ D,\ \rho_w,\ \mu\ ,\ g,\ K)\ ,$$

leading back to Eq 29 and Eq 32. It is thus seen that when little sediment is in suspension the Kármán constant may be governed by the same non-dimensional parameters whether the channel is alluvial or not.

The foregoing reasoning indicates that the observed variation of k (also see Chapter II) with sediment concentration on the one hand, and with the relative roughness on the other hand, is not necessarily contradictory. One may regard Eq 30 as the general expression for the presentation of data. When little sediment is in suspension, Eq 30 may be reduced to Eq 32. When a considerable density gradient exists in the vertical direction, Eq 30 itself should be used. Consideration of the mechanism of exchange reduction due to the density gradient, however, leads to a more convenient form, Eq 28. It will be noted that Eq 28 conforms to the theoretical considerations set forth in the beginning of this chapter.

Total discharge of bed material--From Eqs 21 and 23

$$q_t = f_{17}\,(U_m,\ D,\ \rho_w,\ \mu\ ,\ U_*,\ w).$$

The Pi-theorem then leads to

$$\frac{q_t}{\rho_w g q} = f_{18}\left(\frac{U_m}{U_*}\ ,\ \frac{U_m D}{\nu}\ ,\ \frac{w}{U_m}\right) = f_{18}\left(\frac{C}{\sqrt{g}}\ ,\ \frac{U_m D}{\nu}\ ,\ \frac{w}{U_m}\right)$$

As sediment transport is essentially a function of the tractive force or shear, the parameters $U_m D/\nu$ and w/U_m can influence the transport of sediment in so far as the velocity distribution may vary with these parameters. It is possible that the effects of these parameters are included in the parameter $C/\sqrt{g}$. If this is the case, then

$$\frac{q_t}{\gamma q} = f_{19}\left(\frac{C}{\sqrt{g}}\right) \qquad (34)$$

In view of Eq 34, one may also write

$$\frac{q_t}{\gamma q} = f_{20}\left(\frac{wc}{U_* S}, \frac{w}{U_*}\right) . \qquad (35)$$

Eq 34, if verified by experimental data, should be of considerable interest in practical applications.

Distribution of Sediment in a Vertical

As stated in Chapter II, the distribution of uniform sediment in a vertical was presented by Rouse,

$$\frac{c}{c_a} = \left(\frac{D-y}{y} \quad \frac{a}{D-a}\right)^Z , \qquad (36)$$

where $Z = w/kU_*$, Other factors being the same, when the sediment is not uniform in size, the foregoing equation must be modified. Let the bed material have a distribution of fall velocity as shown in Fig 4. It will be assumed arbitrarily in the present report, that the size distribution of material in suspension at a distance of D/20 above the mean bed is identical with that of the bed material.

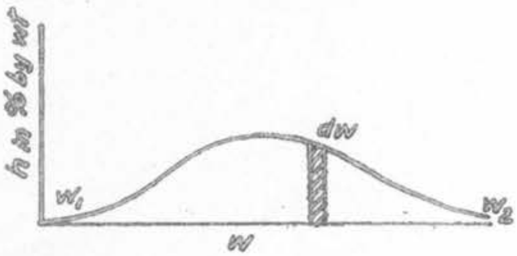

Fig. 4 Schematic fall velocity distribution curve

At a distance of y above the bed, the concentration of that part of sediment having a fall velocity lying between w and w + dw is given by

$$dc = H^Z c_a \, h dw,$$

where

$$H = \frac{D-y}{y} \cdot \frac{a}{D-a} .$$

Since the governing differential equation is linear, the concentration of all sizes of sediment at a distance y above the bed is given by

$$c = c_a \int_{w_1}^{w_2} H^Z \, h dw . \qquad (37)$$

Although Eq 37 is quite general it is not convenient for practical calculations because of the irregular distribution of fall velocity normally encountered in experimental studies. The integral of Eq 37, therefore, is evaluated by the method of finite difference. In this case, it is more convenient to write

$$c = c_a \sum_{i=1}^{n} H_i^z \, (h \, \Delta w)_i \qquad (38)$$

By means of a planimeter, the area under the distribution curve of fall velocity, Fig 4 may be divided into equal parts, so that

$$c = c_a \, h \, \Delta w \sum_{i=1}^{n} H_i^z$$

A graph for the evaluation of H^z was prepared (see Fig A4 in the Appendix). The computation of a sediment distribution curve was then reduced to a process of summing the values of H^z read from Fig A4.

It must be pointed out that both Eqs 37 and 38 only account for the effect of non-uniform distribution of fall velocity. Otherwise, these equations are subject to the same limitations as Eq 36.

CHAPTER IV

EXPERIMENTAL EQUIPMENT AND PROCEDURE

This chapter gives a brief description of the equipment as it was used for gathering the data presented in this report. The flume and its circulation system are treated briefly, after which the various measuring devices are described. A short description of the sediment used in the experiments is included and the operating procedures are summarized at the end of this chapter.

General Description of the Flume

The experiments were performed in a tilting flume which was four feet wide, two feet deep, and seventy feet long. The flume was of wood construction consisting of a two-by-four framework lined with 1/2-in. plywood. The wooden frames rested on two 8-in. I-beams, which ran the entire length of the flume. The I-beams were supported by jacks spaced on 8-ft centers, and by adjusting the jacks the slope of the flume could be set at any desired slope between 0 and 0.015.

Sand was placed in the bottom of the flume to a depth of about three to four inches. The sand was a natural sand taken from a delta formation in Loveland Lake which is a small irrigation storage lake located about thirteen miles from Fort Collins. The sand was passed through a 28-mesh Tyler screen to remove some organic materials from the lake sand. The median size of the sand was approximately 0.18 mm. Size distribution curves for the sand are in the Appendix.

The water and sediment moving in the flume was circulated through a 12-in. low-head centrifugal pump driven by a 35-horsepower motor. The sediment-laden water leaving the flume was collected in a 4-ft trough and then returned to the head of the flume through a 14-in. pipeline. At the head of the flume the water passed through a vertical transition which enabled the water to enter the flume relatively uniformly across the 4-ft width. Five baffles were placed in the flume immediately downstream from the transition. The baffles consisted of two honeycomb type wooden baffles placed 6 in. apart about 1 ft from the transition. The other three baffles consisted of 1/4-in. mesh screen. The first screen was 3 ft downstream from the last wooden baffle, and the last two screens were two inches apart and were located about 1 ft downstream from the first screen. The screens were installed after run 21. Prior to that time the baffling system consisted of 3 honeycomb type wooden baffles, but one of the wooden baffles was replaced by the 3 screens after run 21.

The depth of flow was controlled by a gate at the downstream end of the flume. The gate consisted of vertical notches in which wood slats were moved up and down to control the gate opening. This type of gate worked very nicely since it did not cause any obstruction to the sediment moving near the bed of the flume. A 2 in. by 4 in. wood strip was nailed across the floor of the flume to prevent excessive scour of the bed near the control gate. A schematic drawing of the flume is shown in Fig. 5.

Circulation System

The water flowing in the flume was collected in a 4-ft trough at the end of the flume, thence it flowed into a sump at one end of the trough. The sump was 4-ft square and about 7 ft deep. The water and sediment then flowed from the bottom of the sump through a 14-in. smooth steel pipe to the pump. At the pump a 12-in. discharge pipe rose vertically for about 10 ft. Installed in this vertical line was a 10-in. orifice for measuring the discharge. Sediment sampling tubes were also installed near the orifice to measure the total sediment load being transported in the system. Beyond the 12-in. riser, the pipe diameter increased to 14 in. In the 14-in. line near the head end of the flume a 14-in. valve was installed to control the discharge in the flume. With the valve fully open the pump could deliver slightly over 9 cfs to the flume. At the valve the pipeline was about 5 ft above the floor of the flume so a vertical transition was installed to expand the flow and discharge it as uniformly as possible across the width of the flume. Three vanes in the transition distributed the flow across the width of the flume, but honeycomb type baffles (previously described) were required below the transition to even out the flow and distribute it uniformly across the width of the flume.

Several arrangements of the baffles were tried before arriving at the final arrangement of two wooden honeycomb type baffles followed by three screens as mentioned previously. The honeycomb baffles had openings about 1 1/4 in. square. Three of these were installed initially but, after run 21, analysis of the data indicated that the turbulence generated by these baffles was affecting the values of k. In the case of a smooth sand bed, the turbulence generated at the bed was dominated by the turbulence generated by the baffles, and this condition existed for the entire length of the flume. Therefore, the screens were installed to break up the larger eddies created by the honeycomb baffles. The screens generated a small-scale turbulence which tended to decay more rapidly than the large-scale turbulence created by the honeycomb baffles. With the decay of the eddies generated by the screens, the normal turbulence generated at the bed was able to establish itself about half way down the flume. This condition insured a normal velocity distribution at the point where the velocity and the sediment distribution measurements were made. Measurements of the velocity profile were made at several points along the center line of the flume. These points were generally 8 ft to 10 ft apart.

When the velocity distribution was the same at two successive points along the centerline of the flume, uniform flow was considered to have been established. In the case of a rough bed (due to sand waves), uniform flow was established at the measuring station which was about 2/3 of the length of the flume from the inlet even though the baffles consisted of three honeycomb baffles without the screens. In the case of a plane bed, however, the screens were required to establish uniform flow at the measuring station. The experience with the baffles in these tests emphasized the necessity of adequate baffling to insure normal velocity and sediment distribution patterns in laboratory flume tests.

Just beyond the baffles a 2-in. by 12-in. board was allowed to float on the water surface to smooth out the surface disturbances caused by the baffles. At a point about 2/3 of the distance from the inlet to the end of the flume, the velocity and sediment concentration profiles were measured at the centerline of the flume. Approximately 3 ft upstream from the end of the flume, the slotted gate was installed to control the depth of flow in the flume. This gate enabled fairly delicate adjustments to be effected so that the slope of the water surface could be made to agree as nearly as possible with the slope of the wooden floor of the channel, thereby eliminating any backwater curve. With this condition existing in the flume, measurements indicated that the slope of the sand bed also rapidly approached the slope of the water surface. In fact, the experiments indicated that the slope of the sand bed adjusted itself to the slope of the water surface, even though the water surface slope varied somewhat from the slope of the flume floor; but it sometimes required more time to establish uniform conditions. The 2 in. by 4 in. sill which held the bottom of the control gate prevented excessive scour of the sand bed as the water accelerated through the gate. Beyond the control gate the water and sediment fell about 3 ft into the collecting trough after which the whole cycle was then repeated.

Measuring Devices

Several measuring devices were required in the performance of the experiments. The devices for measuring discharge, slope, velocity, sediment discharge, bed roughness, depth, and temperature are described in the following paragraphs.

Discharge measurements--A 10 in. orifice meter was used to measure the flow. The orifice was calibrated in place by two methods. The first method consisted of filling the flume and timing the period of filling. This volumetric method was good for discharges up to 5 cfs, but the storage volume was too small for larger discharges. The second method consisted of installing a calibrated 10-in. orifice plate in the pipeline and measuring the flow which coincided with the curve established by the volumetric method. Although the calibration was made by using clear water, it was assumed that the small concentrations of sediment would not have appreciable influence on the calibration. This assumption was based on the experiments performed at the Neyrpic Laboratory in Grenoble, France as described in La Houille Blanche (January-February 1953). The head differential across the orifice was measured in feet of water by a differential manometer. For small discharges, which gave a differential head of more than 3 ft, another gage was required and it could be read to the nearest hundredth of a foot.

Slope measurements--Piezometer holes 1/16 in. in diameter were connected to an open manometer board with plastic tubing. Readings on the manometer could be made to the nearest thousandth of a foot. The piezometer holes were 6 in. above the floor of the flume and their longitudinal spacing varied from 2 ft to 5 ft. Another set of piezometer holes was later installed 3 in. above the old set of holes because the lower set clogged with sand when there were sand bars in the flume. Care was taken in making the holes perfectly flush and smooth with the wall, but at times there was some interference caused by boundary irregularities near the holes. The first two and the last two holes were often in zones of non-uniform flow so that little or no weight was given to the readings on these holes. Although the slope measurements were generally satisfactory, the data did scatter somewhat in each of the slope measurements.

Velocity measurements--Velocity measurements were made with the pitot tube pictured in Fig. 6. This pitot tube was carefully calibrated in a 250-ft towing tank used for the calibration of current meters. The results of the pitot tube calibration are quite consistent. The pitot tube had a quick response so that equilibrium was reached without great delay. Because there was not appreciable surging on the gage, very consistent results could be obtained without spending much time on each reading.

Suspended sediment measurements--The suspended sediment was sampled through a brass tube which had a rectangular entrance as shown in Fig. 6. A pitot tube opening was located on each side of the sediment sampler so that sediment intake velocities could be carefully controlled. A small pump with a variable speed motor was connected to the sampler and the samples were pumped into Imhoff cones having a capacity of five liters. The flow through the sampler also went through a small venturi meter so that the intake velocity could be regulated to agree with the natural velocity of flow at the sampling point. The pump generally functioned satisfactorily although at times there was difficulty in maintaining constant discharge. During the last three or four runs the samples were siphoned (instead of pumped) out and the sampling rate then was very steady. Unfortunately, for large velocities, the siphon did not have adequate capacity so that it was necessary to use the pump.

The cones used to gather the sediment samples were calibrated so that the volume of sediment in a 5-liter sample could be read easily. Although volumetric readings were calibrated to give weight measurements, the cone readings were somewhat uncertain; therefore, each of the samples was also dried and weighed on an analytical balance. The weighed samples gave more consistent results than the calibrated cone readings.

Total sediment load measurements--The total sediment load measurements were made in the 12-in. vertical pipe about 7 ft above the discharge side of the 12-in. pump. These measurements were made in a horizontal plane located 1/2-in. downstream from (above) the sharp edge of the orifice plate as shown in Fig. 7. The velocity in the jet at this point was fairly uniform across the entire cross section so all samples for a given test were taken at the same intake velocity. The sampler consisted of a 1/4-in. brass tube with a tapered end. The tapered end projected into the flow in a manner similar to that of a standard pitot tube. There were two sampling tubes placed on horizontal diameters which were normal to each other. Six or eight 5-liter samples were withdrawn along each diameter and the average concentration of all samples was used as the average concentration for the total flow.

Bed roughness measurements--The bed roughness was evaluated by two arbitrary methods. The first method consisted of measuring all of the crests and troughs along the centerline of the flume. Measurements were also made along a line 1 ft from the centerline. All of these measurements were made in the region of the flume where the flow was uniform. Since the measurements were confined to a single line, the maximum and minimum elevations of the dunes were generally not obtained. Therefore, in order to determine more nearly the actual dune heights, a region of the bed was chosen and all of the high points and low points in that region were measured. Normally, the region selected was in the immediate vicinity of the station where the velocity and sediment concentration measurements were made. Generally, the second method gave a greater average dune height than the first method. The average length of the dunes was determined from the first method by recording the flume stations of some of the dune crests. The number of dunes in a given distance could then be determined and the average length could be calculated.

In the case of some runs, the speed at which the dunes migrated downstream was measured. This measurement was time-consuming and so it was not taken for all runs.

Average depth--The average depth of the flow was measured in most cases by the first of two methods. The first method consisted of recording the water surface elevation at the measuring station while the run was in progress. After the water had been shut off, the bed was smoothed out with a trowel and the average elevation of the bed was determined at the measuring station to obtain the average depth.

The second method involved a measurement of the depth of flow at the glass-wall section of the flume. For a rough bed the average elevation of the bed was estimated by making a grease pencil line on the window that represented the average elevation of the bed as far as it could be determined visually. A scale was then used to measure the distance from the bed to the water surface. Depth measurements were made at 3 different points on the window and the measurements were repeated several times during a run. When the bed was plane, the measurements at the window were easily made and the results were generally very consistent.

Temperature measurements--Temperatures were measured by inserting a centigrade thermometer into the flow near the downstream end of the flume. The water temperature increased between the time of the beginning and end of a run. However, by the time velocity and sediment profiles were measured the temperature generally was reasonably constant.

Description of the Sediment

In order to describe some of the physical properties of the sand, a sample was observed under a microscope. Although no extensive study was made, about 50% of the sand particles were determined to be quartz grains, approximately 40% were mica flakes (principally biotite), and the remaining 10% consisted of a variety of minerals dominated by grains of orthoclase. The orthoclase and quartz particles exhibted signs of considerable wear since most of their sharp edges had been fairly well rounded. The mica flakes, which were typically flat particles, had no unusual characteristics. The sand was observed under the microscope after all the runs were completed, and at that time there were only a few of the very fine particles present. Most of the particles seemed to range in size somewhere between 0.1 mm and 0.2 mm in diameter. Although the size distribution of the sediment varied slightly, the mean size remained essentially constant. During the early runs the sediment contained considerable fines, but eventually these were washed out of the sand and pumped out of the system with the waste water. This variation is illustrated by two sediment distribution curves shown in Figs. 1a and 2a in the Appendix. The standard deviation of the bed-material sample taken in March 1954 was 0.045 mm while the standard deviation of the bed-material sample analyzed in July 1954 was 0.037 mm. Since the variation in sediment characteristics appeared to be small, the median size of 0.18 mm was used in the analysis of the data.

Fall velocity measurements were made by the Missouri River Division Laboratory of the Corps of Engineers, and the fall velocity for the median size was 0.0645 ft/sec at a temperature of 24°C as shown in Fig. A-2. This fall velocity was used in the analysis of most of the data since most of the runs were made at temperatures closely approximating 24°C. The fall velocity for the median size of 0.180mm varied essentially as a straight line from 0.0595 ft/sec for 20°C to 0.0720 ft/sec for 30°C.

Operation and Sampling Procedure

Water was first pumped from a storage sump into the tail box of the flume. An 8-in. pump was used for this purpose. As the water began to fill the tail box the 12-in. centrifugal pump was started and the control valve was opened to allow water to flow into the flume. Before the 12-in. pump was started, a line leading from the city water supply and connected to the pump bearing was opened to maintain flow into the pump to prevent sand from entering the bearing. The control valve in the 14-in. supply line was opened until the desired discharge was flowing. The 8-in. pump was shut off when sufficient water had been put in the system. The amount of water in the system was adequate when there was enough to supply the required discharge and to keep the level of the water in the tail box at the desired elevation. The elevation of the water in the tailbox was held at a point such that no sediment was deposited in the tail box. Since the small quantity of water coming into the bearing of the pump entered the system, an overflow into the storage sump was required to maintain the water in the tail box at a constant elevation.

Once the flow had been established in the flume the desired water surface slope was set by adjusting the control gate at the end of the flume. After each gate adjustment, the water was allowed to circulate for fifteen minutes to half an hour. A profile measurement was then made and, if the slope was not the desired one, the gate was adjusted again. This process was repeated until the desired slope had been established and no backwater curve existed. The flume was then allowed to flow for several hours and occasional checks were made on the slope. If the slope remained constant for a period of time, then the measurements of velocity and sediment distribution were made. However, if the slope continued to vary, the gate was readjusted until the slope did remain steady over a period of at least two hours.

After the velocity and sediment measurements were made, the discharge had to be shut off without disturbing the bed. In addition to the sliding gate used to control the depth of flow in the flume, there was an 18-in. end gate hinged at the end of the flume so that it could be raised to act as a weir and increase the depth of flow in the flume. When this gate was raised slowly the depth of water increased until no water was left in the tail box and the 12-in. pump no longer had a supply. In the case of a plane bed, this end gate was raised rapidly to avoid the formation of small ripples during the shut-down process. Although a rather large surface wave was formed when the gate was closed rapidly, the surface wave did not disturb the sand bed. The 12-in. pump was then shut off and a valve was opened to allow water in the tail box to drain back into the supply sump. The end gate on the flume was not sealed so that water slowly leaked around the end gate back into the tail box. When the tail box filled the water then emptied into the storage sump. The water leaked out of the flume so slowly that it did not disturb the roughness pattern. The flume had to drain for 8 to 10 hours before measurements of the channel roughness could be made.

During a run, the discharge, the temperature, the average depth of flow at the window, the water surface slope, and the water surface elevation in the tail box were measured frequently. Generally, measurements of these items were recorded every hour or two during the run.

Sampling Methods

Sampling was started when uniform steady conditions were finally established. Most velocity and sediment concentration profiles were taken at the centerline of the flume and at flume station 73.0. Measurements for runs prior to run 22 were taken at flume station 67.0. The measuring station was moved to station 73.0 because for runs which involved a plane bed, the velocity distribution was better established at station 73.0 than at station 67.0. The last baffle at the head of the flume was located at station 33 (which was 5 ft from the inlet at the upstream end of the flume), and the control gate at the end of the flume was at station 94.

The velocity profiles were generally the first measurements made and at about 12 to 15 points in a vertical section. The pitot tube was carefully bled of all air in the system and then set at a new point approximately every two or three minutes. In this way one profile could be obtained in less than an hour. Near the bed the flow pattern varied with time because, as the dunes moved by the measuring section, the flow pattern at the crest of a dune was not the same as the flow pattern over a trough. However, a few inches above a crest the flow pattern remained essentially constant with time in spite of the shifting bed.

The sediment distribution measurement required considerably more time than the velocity profile. Samples were collected at 12 to 15 points in a vertical, and the rate of withdrawal of the samples was controlled to make the sediment tube entrance velocity equal to the velocity of the flow at the point of measurement. Samples were pumped or siphoned into 5-liter cones with glass bottoms where they were allowed to settle for at least twenty minutes before a reading of the volume of sediment was taken. The bottoms of the cones were calibrated in milliliters and the cones were tapped vigorously with a piece of plastic tubing before each reading. The volume of sediment was recorded and then the sediment was decanted into a pyrex drying cup to be placed in the oven for drying. When the samples were thoroughly dried they were weighed on an analytical balance. The weights obtained represented the weight of sediment in five liters of water.

The total load samples were gathered in the 12-in. riser 7 ft above the pump at the section containing the orifice plate. Eight 5-liter samples were gathered along each of two sampling diameters. The diameters were 90° to each other and generally the average concentration along one diameter was essentially the same as that along the other diameter. The average concentration for the total flow was taken as the average of the 16 measurements taken on the two diameters. The time required for sampling was calculated and the time required to collect the 5-liter sample was timed with a stop watch. By trial and error the corrected sampling time was established so that the entrance velocity into the 1/4-in. diameter sediment sampler was equal to the velocity of the surrounding flow. The required sampling velocity was determined by dividing the discharge by the area of the orifice. By hooking up one of the sampler tubes as a pitot tube, it was found that the velocity across a diameter of the orifice was practically constant. After these measurements were finished the water was shut off and the bed roughness measurements were taken as described previously.

All data were dated, tabulated, and filed into folders so that the information for each run was kept together.

Pictures of the flume and various measuring devices are shown in Figs. 8, 9, and 10.

CHAPTER V

DISCUSSION AND ANALYSIS OF DATA

The experimental data collected in the present study will be analyzed in the light of the theoretical considerations presented in Chapter III. Before the main topics are discussed, however, certain terms used for describing the bed conditions in this report will be defined.

Terms Used to Describe the Bed Conditions

The term sand wave, as used in the present report, will denote any disturbance on the bed of a stream caused by the movement of the bed material such as dunes, sandbars, and anti-dunes explained below. This usage of the term sand wave is derived from a definition given by E. W. Lane (19), who defines a sand wave as "a ridge on the bed of a stream formed by the movement of the bed material, which is usually approximately normal to the direction of flow, and has a shape somewhat resembling a water wave." In this report, the term is extended to include sandbars of which the fronts are usually not normal to the direction of flow. In the order of increasing mean velocity of flow, dunes, sandbars, plane bed, and anti-dunes may form.

A dune as mentioned in this report is one of a group of sand waves which are more or less triangular in profile and which appear somewhat like fish scales or a shingled roof when looked upon from above (Fig. 11). The dunes observed in the course of the present study were generally about one inch high (ranging from one-sixth to one-sixteenth of the depth of flow) with a length always less than twice the depth of flow. The authors consider it a significant fact that when dunes prevailed on the bed, the surface fluctuations were comparable in magnitude to those normally encountered in flow involving fixed boundaries.

A sandbar as referred to herein is a large sand wave, which is, in profile, distinctly higher and many times longer than the dunes in the neighborhood, and which, in plan, has a general wave front that is not normal to the direction of flow (Fig. 12). In the present series of experiments, the profile of a sandbar was observed to be four or five inches high and in general between six and ten feet long. It was also observed to have a markedly greater wave velocity than the dunes. When a sandbar occurred on the bed, it was accompanied by one or more standing waves on the water surface which, although not always discernible to the naked eye, were definitely detectable with a point gage. The water surface under such conditons was so erratic that uniform flow no longer existed.

When a bed is even and free of sand waves, it is called a plane bed (Fig. 13). The roughness of a plane bed depends primarily on the grain-size of the bed material.

The term anti-dune has been defined by E. W. Lane (19) as "a sand wave, indicated on the water surface by a regular undulating wave, in appearance like that formed behind a stern wheel steamboat. These ridges move, usually upstream. The surface waves become gradually steeper on their upstream sides until they break like surf and disappear. These waves are usually in series and often reform after disappearing." This definition will be adopted in the present report.

Variation of Bed Conditions with Mean Velocity of Flow

Although other factors have an influence in governing the variation of bed configuration, there does appear to be a general relationship between the mean velocity of flow and the bed conditions.

In the present study, the flow was always turbulent. It was observed that as soon as the drag on the bed was sufficient to move the materials, dunes began to form. Under the conditions of uniform flow at a given slope, there was a general tendency for the average length of dunes to increase with the velocity of flow, although the change in length was so small that it was not plainly noticeable (see Appendix). No definite trend of the variation in dune heights with velocity could be observed. When dunes were prevailing on the bed, introduction of an object close to the bed gave rise not only to active scour under the object but also to a train of sand waves of decreasing sizes downstream from the object. Even after the object was removed, disturbances caused originally by the object would grow in size, eventually becoming dunes as large as those prevailing on the bed nearby. Thus, in the stage of dune formation, the bed is unstable to any perturbation in the sense that a disturbance will be magnified.

When the velocity was increased, a point was soon reached at which it was noted that some of the dunes tended to grow more rapidly than others. These larger waves were traveling at a higher speed than the small ones and hence were able to accelerate their growth by overtaking smaller dunes. Eventually one or more long sand waves, or sandbars was formed (Fig. 12). As stated in the previous section, the general front of a sandbar was not normal to the direction of flow and the wave velocity was markedly higher than that of the dunes. Sandbars often had rather steep fronts but only slightly inclined backs. It was quite common that the back of a sandbar was covered with small dunes. In some cases, the entire sandbar was covered with dunes, so that, when looked upon from above, the bed would appear to consist of dunes riding on a gently rolling base of which the ridge traveled in an oblique direction across the flume alternately from one side wall to the other as if it were reflected by the walls.

When the velocity of flow was further increased, the sandbars would rapidly disappear leaving behind a plane bed (Fig. 13). In some cases, small dunes were found in the narrow strips along the side walls. The central part of the bed, however, was free of dunes, as was easily ascertained by a rather swift sweep of the hand over the bed surface. Under the conditions of a plane bed, introduction of an object near the bed brought about active scour under the object, but no other disturbance was observed downstream. As soon as the object was removed, refilling of the scour hole took place. In time a plane bed was restored. Thus a plane bed is stable in the sense that any small disturbance will eventually disappear.

If one continues to increase the velocity of flow, after a plane bed has come into being, anti-dunes accompanied by high surface waves will eventually appear. Under such circumstances, uniform flow again does not exist. In this study laboratory data were collected for plane beds and beds with dunes. Some approximate information was gathered also when sandbars occurred. Anti-dunes were observed visually without any data being taken.

Resistance of an Alluvial Channel

As far as hydraulics is concerned, an alluvial channel differs from an ordinary channel in that even in a given material the condition of the bed of an alluvial channel is a function of various flow and fluid properties. However, a theoretical solution for the problem of evaluating the resistance of an alluvial channel is impossible to obtain before the mechanics of dune formation and destruction by the flow is understood.

The experimental data may be presented in two different ways indicated by Eqs 25 and 27 in Chapter III. Eq 25 is similar to an expression first proposed by Ali and Albertson (1). By reasoning that the Froude number may be neglected in a uniform flow and by using d/D instead of w/U_* in Eq 25, Ali and Albertson proposed that

$$\frac{C}{\sqrt{g}} = f_{21}\left(\frac{U_m D}{\nu}, \frac{d}{D}\right) \qquad (39)$$

Fig. 14, taken from a thesis by Ali (1), is the result of analyzing a multitude of data from various sources on the basis of Eq 39. Although there is considerable scatter, it appears that general trends of curves can be established.

On the other hand, in the present study in which an appreciable density gradient always existed in the vertical direction, experimental data may also be presented according to Eq 27. The result is Fig.15. In this figure, two trends of data are obvious. All data pertaining to a plane bed fall on the upper curve, whereas those obtained for a bed covered with dunes fall on the lower curve. The existence of two trends need not be surprising, if one recalls that, when dunes exist on the bed, the vortex in the separation zone downstream from a dune tends to throw more sediment into suspension by larger-scale circulation, so that the mechanism of sediment entrainment and distribution in the case of a bed with dunes is not the same as that in the case of a plane bed. If the resistance of an alluvial channel is governed by the influence of density gradients--that is, to some extent by the distribution of sediment--then it is only logical that there should be two curves relating the dimensionless Chezy coefficient and the Richardson number.

For the data presented in Fig. 15, w/U_* varies from 0.15 to 0.55. It is of interest to note that no systematic variation of $C/\sqrt{g}$ with w/U_* can be observed. Thus when data are presented according to Eq 27, two significant observations may be made:

(1) The relative fall velocity w/U_* of the material composing an alluvial channel is not a factor of primary importance in determining the resistance of an alluvial channel. In other words, the influence of w/U_* on $C/\sqrt{g}$ is adequately determined by the abscissa parameter wc/U_*S,

(2) Over a fairly wide range of fall velocity distributions, such as that of the material used in the present study, the characteristics of the distribution have no appreciable effect on the resistance of an alluvial channel.

Both curves of Fig. 15 indicate an increase in Chezy's C or a decrease in the Darcy-Weisbach resistance coefficient with the increase in the

Richardson number. Thus the contention in this report that density gradients reduce the intensity of momentum transfer and hence, for the same discharge, reduce the resistance of the channel is supported by experimental data (see the section entitled "Kármán Constant," Chapter III).

At very large Richardson numbers, the resistance coefficient could theoretically approach that for turbulent flow in a hydrodynamically smooth channel, although the range of present data is not sufficient to check this statement. As the Richardson number approaches zero, the flow may either be free of any sediment in suspension or contain relatively very fine sediment that is uniformly distributed in the vertical direction. In either case, since the density gradient is either non-existent or negligible, the Froude number is of little importance.

Another expression which is applicable when the sediment gradient is small may be obtained by leaving the Froude number out of Eq 26. The result is:

$$\frac{C}{\sqrt{g}} = f_{22}\ (c\ ,\ w/U_*) \tag{40}$$

As mentioned previously, the experimental data may be presented in accordance with two basic ways of grouping the variables as indicated by the general Eqs 25 and 26. In practical applications, both ways of presentation are desirable. A plot prepared on the basis of Eq 25 (Fig. 14) will be useful to a designer for the estimation of channel resistance from his data of channel characteristics, water discharge required, and the type of sediment encountered. A plot prepared on the basis of Eq 26 (Fig. 15) will then enable him to estimate the capacity of the channel for transporting sediment, and thereby to determine whether his design is satisfactory in so far as sediment is concerned. Eq 39 is a particular form of Eq 25 whereas Eqs 27 and 40 are particular forms of Eq 26.

To be more specific, the main steps to be taken in the hydraulic computations for an unlined channel will be outlined. Let it be assumed that the capacity and the cross-sectional shape of the channel have been specified. Soil samples taken along the proposed route of the channel will then furnish the size distribution of the material composing the channel. Hydraulic computations may be started with a trial value of D. On the basis of this trial value, and the specified shape and capacity of the channel, the mean velocity of low U as well as the hydraulic radius R may be computed. Knowing the prevailing temperature at which the channel will be operated and with a proper choice of effective size for the bed material[1], one can compute the Reynolds number and d/R as well as the fall velocity w. A plot such as Fig. 14 will then enable one to find $C/\sqrt{g}$, from which the slope of the channel may be computed. Knowing the value of $C/\sqrt{g}$, one may also make use of a plot such as Fig. 15 and obtain the value of wc_{10}/U_*S.

---

1 It should be noted that the mean size of the bed material would be greater than that of the land nearby.

Since $U_* = \sqrt{gRS}$, c_{10} can be computed. The total and suspended sediment discharges may then be estimated by various methods reviewed in Chapter II. (It may be pointed out that Fig. 20, which is to be discussed later in this report, is particularly suitable for the purpose of computing the total bed-material discharge.) With all these values computed, the design engineer may consider various practical requirements and determine whether the assumed value of D is desirable. Another interesting plot concerning channel roughness is Fig. 16, in which it is shown that $C/\sqrt{g}$ is approximately an exponential function of K/D , the relative height of roughness. In the case of a plane bed, K is set equal to the grain-size at 65% finer. In the case of dunes, K is taken as the average height of the dunes.

The following table shows some values of the Manning coefficient obtained by keeping the discharge constant while varying the slope and depth. The table shows clearly that for a given discharge, the roughness of an alluvial channel decreases with a decrease in the mean depth or with an increase in the average velocity. It is significant that for a given discharge a bed with sandbars has smaller effective roughness than a bed with dunes. The plane bed would be expected to have the smallest effective roughness. Needless to say, the values of the different variables pertaining to the conditions of sandbars are only approximate, owing to the fact that uniform flow does not exist when sandbars occur. Nevertheless, the general order of mannitudes should be correct.

Discharge Q (cfs)	Mean Depth D (ft)	Average Velocity $U_m = Q/A$ (ft/sec)	Manning "n"	Bed Condition
5.8	0.94	1.54	0.0216	Dunes
5.8	0.85	1.70	0.0204	Dunes
5.8	0.79	1.84	0.0183	Sandbars
5.8	0.66	2.20	0.0154	Sandbars
5.8	0.61	2.38	0.0137	Plane

Kármán Constant

In Fig. 17, the experimental values of the Kármán constant are plotted against the Richardson number wc_{10}/U_*S . The quantity c_{10} in the Richardson number stands for the concentration at $(D-y)/y = 10$. Fig. 17 shows clearly that the Kármán constant decreases with increasing Richardson number. As explained in Cahpter III, this variation is due to the fact that, in overcoming the density gradient, part of the turbulent energy is converted to potential energy when the heavier mixture is being carried up and the lighter mixture forced down. The turbulent energy available for mixing or exchange in a vertical section is thereby reduced, resulting in a reduction in the Kármán constant.

Thus Richardson number is a parameter indicating the relative amount of turbulent energy being converted into potential energy. It is not concerned with the total amount of turbulent energy available or the characteristics of turbulence in the flow. Since, for two-dimensional flow, the bed is the main source of turbulence, it appears reasonable for the experimental data to follow two curves corresponding to the case of a plane bed and the case of a bed with dunes. It should be noted that Fig. 17 also contains some of the field data collected on the Missouri River by the Corps of Engineers. The laboratory and field data seem to corroborate well.

Sediment Distribution in a Vertical Section

For sediment having a narrow size range, the equation

$$\frac{c}{c_a} = \left(\frac{D - y}{y} \cdot \frac{a}{D - a}\right)^{Z}$$

is qualitatively correct in describing the distribution of sediment in a vertical section; although in order to be quantitatively correct, the exponent Z must be modified.

In the case of non-uniform material such as the sediment used in the present experiment, the following equation has been proposed in Chapter III for the distribution of sediment in a vertical section:

$$\frac{c}{c_a} = \int_{w_1}^{w_2} \left(\frac{D - y}{y} \cdot \frac{a}{D - a}\right)^{Z} h dw \qquad (37)$$

This equation also is, at best, only qualitatively correct. By determining the size distribution of the bed material, the integral in this equation can be evaluated numerically, so that a theoretical curve of sediment distribution may be computed (see Chapter III). In this manner, theoretical curves have been computed for several runs.

It was found that in the case of a plane bed, the theoretical curve of distribution followed the experimental data quite well. In the case of a bed covered with dunes, however, the actual distribution of sediment was invariably more uniform than that indicated by the theoretical curve. In order to obtain a theoretical curve that will approach the experimental distribution of sediment, the value of Z must be modified. Let the modified value of Z be Z_1. As yet there is no well established relationship between Z and Z_1. The limited analysis carried out for the present study, however, hints strongly that the ratio Z_1/Z depends on the bed configuration. Unfortunately, the computation of Z_1 by trial is so laborious and time-consuming that at the present time it is impossible to complete the calculation of Z_1 values for all the runs. Consequently, more extensive study of the relationship between Z and Z_1 must be deferred for the time being.

Figs. 18 and 19 show the velocity and sediment distribution curves for several runs. It can be seen that the velocities in a vertical lie close to a straight line on the "semi-log" plot, thus indicating that the velocity follows the Kármán-Prandtl distribution. In the case of a plane bed, the theoretical curve of sediment distribution can be seen to come close to the experimental distribution; whereas, when dunes prevail on the bed, a definite and sizeable divergence between the theoretical and experimental curves exists. The ratio of Z_1/Z for one run for a bed with dunes is of the order of 0.2 !

Total Bed-Material Discharge

In Chapter III, it was suggested that the average concentration computed on the basis of total sediment discharge depended solely on the dimensionless Chezy coefficient (or any other forms of resistance coefficients such as the Darcy-Weisbach f). Fig. 20 shows that the data collected in the present study do indicate a single trend, when $q_t/\gamma q$ is plotted against $C/\sqrt{g}$. It is of interest to note that a slight minimum in the curve can be seen at a small value of $q_t/\gamma q$. Unfortunately, relatively few points have been determined in this region, so that the present trend of reaching a minimum value of $C/\sqrt{g}$ is not regarded as completely established. In the determination of the experimental trend, little weight is given to the point corresponding to a value of $C/\sqrt{g}$ equal to 6.8, because this run was considered a poor one. If more weight were given to this point, the dip in the left portion of the experimental curve would have been even more pronounced.

That a signle trend exists in Fig. 20 is considered by the authors to be highly significant. The value of w/U_m for the data used in Fig. 20 varies from 0.017 to 0.07. Therefore, since no systematic variation of the points with w/U_m can be observed in Fig. 20, one may conclude that w/U_m is at best of secondary importance. This fact suggests the possibility of establishing the relationship between $q_t/\gamma q$ and $C/\sqrt{g}$ over the entire practical range of w/U_m by a relatively small number of experimental curves.

Fig. 20 will enable one to compute the total bed-material discharge by determining the discharge, the depth, the slope, and the approximate median fall velocity. A small variation of w/U_m will not have appreciable effect on the computed value of $q_t/\gamma q$.

Sediment Sampling Efficiency

In the field, usually only a part of the suspended load is sampled. Sediment discharge computed on the bases of the sampled load obviously does not represent the total discharge of sediment which consists of bed load as well as suspended load. The ratio of the sampled average concentration to the average concentration computed on the basis of total bed-material discharge has been termed the sampling efficiency.

Sadar (29) has made a preliminary analysis of the data collected in the present study and presented a series of plots of which some are reproduced in Fig. 21. According to this figure, the sampling efficiency is definitely influenced by the bed condition. For a given depth sampled, when dunes prevail on the bed, the sampling efficiency is primarily a function of only the Reynolds number in terms of shear velocity and the sedimentation diameter. In the case of a plane bed, the sampling efficiency depends also on the slope of the energy gradient in addition to the Reynolds number and the depth sampled. In general, the sampling efficiency is higher in the case of a bed covered with dunes than in the case of a plane bed. The existence of two types of functions as well as of high sampling efficiency in the case of a bed with dunes is understandable, if it is again remembered that (other factors being the same) the large vortex in the separation zone behind a dune tends to throw more material into suspension and the increased intensity of mixing resulting from the action of the vortex tends to bring about more uniform distribution of sediment in a vertical (see the section: "Resistance of an alluvial channel"). Fig. 21 shows that the sampling efficiency increases with the Reynolds number, and that in the case of a plane bed the sampling efficiency at a given Reynolds number decreases with the slope. Quantitatively, the increase in sampling efficiency with the Reynolds number is small in the case of a bed covered with dunes, but is quite sizeable in the case of a plane bed. Thus when the bed of a river does not have dunes, sampling efficiency is an important factor to consider in the estimation of total sediment discharge.

It is significant that, according to Sadar, the variable d/R within the range of the present study has no sensible effect on the sampling efficiency. Two important deductions can be made immediately. Firstly, there is the possibility of covering the practical range of sediment size by a relatively small amount of test data. Secondly, the characteristics of size distribution probably have only secondary effect on the sampling efficiency.

CHAPTER VI

SUMMARY AND SUGGESTIONS FOR FUTURE STUDY

The principal findings of the present study will be summarized along with some suggestions for future study.

Summary

(1) In addition to the three well-known regimes of dunes, plane bed, and anti-dunes (see Chapter II), a regime of sandbars was also observed in the course of the present study. This regime is the transition between the regimes of dune formation and a plane bed without dunes. Starting with a bed of dunes, and maintaining a given surface slope, it was observed that increasing the discharge would in time bring about a rapid deterioration of the regular pattern of dunes to an irregular pattern of sandbars amid dunes. In general, these sandbars travelled at a considerably higher speed than the dunes, and the general orientation of the front of a sandbar is usually at a considerable angle with the normal to the channel walls. When sandbars are present, the water surface is often so irregular and erratic that uniform flow no longer exists (see Chapter V). The regime of sandbars would exist for a certain range of discharge. As the discharge was increased beyond this range, sandbars as well as dunes would rather abruptly disappear. A plane bed thus came into being.

(2) For a given bed configuration, the dimensionless Chezy coefficient $C/\sqrt{g}$ increases with the Richardson number (see Fig. 15). Two experimental trends are apparent, one for points obtained with a plane bed and the other for a bed covered with dunes. The variation of the resistance coefficient with the Richardson number in the case of a bed covered with dunes is less than in the case of a plane bed. Over a range of w/U_* from 0.15 to 0.55, no systematic deviation from the trends can be observed. A plot of this type will be useful for estimating the suspended load, when $C/\sqrt{g}$ is known or vice versa (see Chapter V).

(3) The data follow reasonably well the trends on the plot of $C/\sqrt{g}$ against Re suggested by Ali and Albertson. A plot of this type will be useful for a designer to estimate $C/\sqrt{g}$ when the water discharge, channel characteristics and the mean size of bed material are known (see Fig. 14).

(4) The resistance coefficient of an alluvial channel can also be considered a function of the total bed-material discharge per unit weight of the water discharge, $q_t/\gamma q$ (see Fig. 20). Over a range of w/U_m from 0.017 to 0.07 no systematic variation of $C/\sqrt{g}$ exists in Fig. 20. Such a plot is highly interesting, because knowing w, q, D, and S, one would be able to estimate the total bed-material discharge.

(5) The Kármán constant is not a constant for flow in alluvial channels (see Fig. 17). Its value depends on the Richardson number wc_{10}/U_*S. The decrease of the Kármán constant with increasing Richardson number supports the theory that a large sediment concentration gradient in a vertical section decreases the rate of mixing of the flow. For the same Richardson number, the two values of Kármán constant exist, one for the case of a plane bed and the other for the case of a bed with dunes.

(6) Intuitive reasoning indicates that the Kármán constant for flow of clean water over a rough bed may depend only on the relative roughness

(see Chapter III). This is not contradictory to statement number 4 because a density gradient exists in the case of statement number 4. Under such conditions, it is more convenient and significant to use the Richardson number as a parameter in presenting the data of the Kármán constant.

(7) In the case of flow over a plane bed, the proposed equation for the distribution of non-uniform sediment follows the experimental distribution quite well. However, for flow over a bed with dunes, the actual sediment distribution is always more uniform than that predicted by the equation. It appears certain that the relationship between Z and Z_1 depends to a great extent upon the bed conditions. For a plane bed, Z is approximately equal to Z_1. For a bed with dunes, Z_1 is smaller than Z.

(8) In the case of a bed covered with dunes, the sampling efficiency is essentially a function of the relative sampled depth and Reynolds number in terms of the shear velocity and sedimentation diameter. In the case of a plane bed, the sampling efficiency also depends on the energy gradient in addition to the two parameters just mentioned. Since, in general, sampling efficiency in the case of a plane bed is not only considerably lower than that in the case of a bed covered with dunes, but also varies rapidly with the Reynolds number, sampling efficiency is an important factor to consider when sampling suspended load in a river with a plane bed.

Future Study

(1) The present study covers a range of w/U_* from 0.15 to 0.55. When the data are presented in the manner described in this report, the parameters indicating the relative size of sediment, such as w/U_*, w/U_m, and d/R, are found to have little or negligible effect on the resistance coefficient, the Kármán constant, the bed-material discharge per unit water discharge, and the sampling efficiency. It would be of interest to see if this is the case when the size range is extended. In any case, there is at least the great possibility of covering the entire practical size range with relatively few sizes of sediment, even if the size parameters were found not to be negligible in the future.

(2) The data of sediment distribution obtained in the present study should be analyzed to establish the relationship between Z and Z_1.

(3) The effect of secondary circulation on the distribution of velocity and sediment should be investigated. In the case of a plane bed, this proposed investigation is particularly of interest.

(4) Measurement of the velocity distribution over the top of a dune and the turbulent characteristics in the wake of a dune would be desirable as a first step toward understanding the mechanics of dune formation.

BIBLIOGRAPHY

1. Ali, S. and Albertson, M. L. Some aspects of roughness of alluvial channels. Research Report, Civil Engineering Department, Colorado Agricultural and Mechanical College, Fort Collins, Colorado. Publication pending.

2. Anderson, A. G. The characteristics of sediment waves formed by flow in open channels. Proceedings of the Third Midwestern Conference on Fluid Mechanics. The University of Minnesota, 1953.

3. Boussinesq, M. J. Essai sur la theorie des eaux courantes. Memoires, Presente par divers savants. L'Academie de l'Institut de France. Vol. 23, 1877.

4. Chien, N. The efficiency of depth -integrating suspended -sediment sampling. Trans., AGU, Vol. 33, No. 5, 1952.

5. Craven, J. P. The transportation of sand in pipes. Proceedings of the Fifth Hydraulics Conference, 1952.

6. Danel, P., Durand, R., and Condolios, E. Introduction a l'etude de la saltation. La Houille Blanche. December 1953.

7. Durand, R. Basic relationships of the transportation of solids in pipes--experimental research. Proceedings, Minnesota International Hydraulics Convention, 1953.

8. Einstein, H. A. The bed-load function for sediment transportation in open channel flows. Soil Conservation Service, Technical Bulletin No. 1026, 1950.

9. Einstein, H. A. and Barbarossa, N. L. River channel roughness. Trans., ASCE, Vol. 117, 1952.

10. Einstein, H. A. and Banks, R. B. Linearity of friction in open channels. Rapports et comptes rendus des Seances de la Commission des Eaux de Surface. Association Internationale d'Hydrologie Scientifique. Assemblee Generale de Bruxelles. Tom III, 1951.

11. Einstein, H. A. and Banks, R. B. Fluid resistance of composite roughness. Trans., AGU, Vol. 31, No. 4, 1950.

12. Einstein, H. A. and Chien, N. Second approximations to the solution of the suspended load theory. The Missouri River Division Sediment Series, No. 3.

13. Gilbert, G. K. The transport of debris by running water. USGS Professional Paper No. 86, 1914, pp 26-33.

14. Goldstein, S. Modern developments in fluid dynamics. Clar Press, 1938.

15. Hooker, E. H. Suspension of solids in flowing water. Trans., ASCE, Vol. 36, 1896.

16. Ismail, H. M. Turbulent transfer mechanism and suspended sediment in closed channels. Trans., ASCE, Vol. 117, 1952.

17. Kalinske, A. A. and Hsia, C. H. Study of transportation of fine sediments by flowing water. University of Iowa Studies in Engineering, Bulletin No. 29, 1945.

18. v. Kármán, T. Sand ripples in the desert. Technion Year Book, 1947.

19. Lane, E. W. Hydraulic engineering aspects of sediment transportation and deposition. Lecture Notes, Department of Civil Engineering, Colorado Agricultural and Mechanical College, Fort Collins, Colorado, 1946.

20. Lane, E. W. and Kalinske, A. A. The relation of suspended to bed-materials in rivers. Trans., AGU, 1939.

21. Lane, W. E. and Kalinske, A. A. Engineering calculations of suspended sediment. Trans., AGU, 1941.

22. Menard, H. W. Deep ripple marks in the sea. Journal of Sedimentary Petrology, Vol. 22, No. 1.

23. Laursen and Ran d. Discussion of item 34.

24. O'Brien, M. P. Review of the theory of turbulent flow and its relation to sediment--transportations. Trans., AGU, Vol. 14, 1933.

25. Prandtl, L. Einfluss stabilisierender Krafte auf die Turbulenz. Vortrage aus d. Geb. d. Aerodyn. u. verwandter Gebiete, Aachen, 1929, 1.

26. Rouse, H. Modern conceptions of the mechanics of fluid turbulence. Trans., ASCE, Vol. 102, Pt. II, 1937 (author's closure).

27. Rouse, H. An analysis of sediment transportation in the light of fluid turbulence. Soil Conservation Service. Cooperative Laboratory, California Institute of Technology, SCS-TP-25, 1939.

28. Rouse, H. Laws of transportation of sediment by streams, suspended load. Report prepared for round-table discussion of the role of hydraulic laboratories in Geophysical research at the National Bureau of Standards, 1939.

29. Sadar, D. J. Preliminary study of sampling efficiency. M. S. thesis, Department of Civil Engineering, Colorado Agricultural and Mechanical College, Fort Collins, Colorado, 1954.

30. Schmidt, W. Der Massenaustausch in freier Luft, und verwandte Erscheinungen. Probleme der Komischer Physik, Vol. 7, Hamburg, 1925.

31. Sheppard, P. A. The aerodynamic drag of the earth's surface and the value of von Kármán's constant in the lower atmosphere. Proc. Roy. Soc. of London, A 188, p 208, 1947.

32. Shields, A. Anwendung der Änlichkeitsmechanik und der Turbulenzforschung auf die Geschiebewegung. Mitteilungen der Prussischen Versuchsanstalt für Wasserbau und Schiffbau, Berlin, 1936.

33. Tison, L. J. Origine des ondes de sable (ripplemarks) et des bancs de sable sous l'action des courants. International Association for Hydraulic Structures Research, Third Meeting, Grenoble, France, September 1949.

34. Vanoni, V. A. Some effects of suspended sediment on flow characteristics. Proceedings of the Fifth Hydraulic Conference. Bulletin 34, State University of Iowa Studies in Engineering, 1953.

35. Vanoni, V. A. Transportation of suspended sediment by water. Trans., ASCE, Vol. 111, 1946.

36. Vanoni, V. A. A summary of sediment transportation mechanics. Proceedings of the Third Midwestern Conference on Fluid Mechanics. The University of Minnesota, 1953.

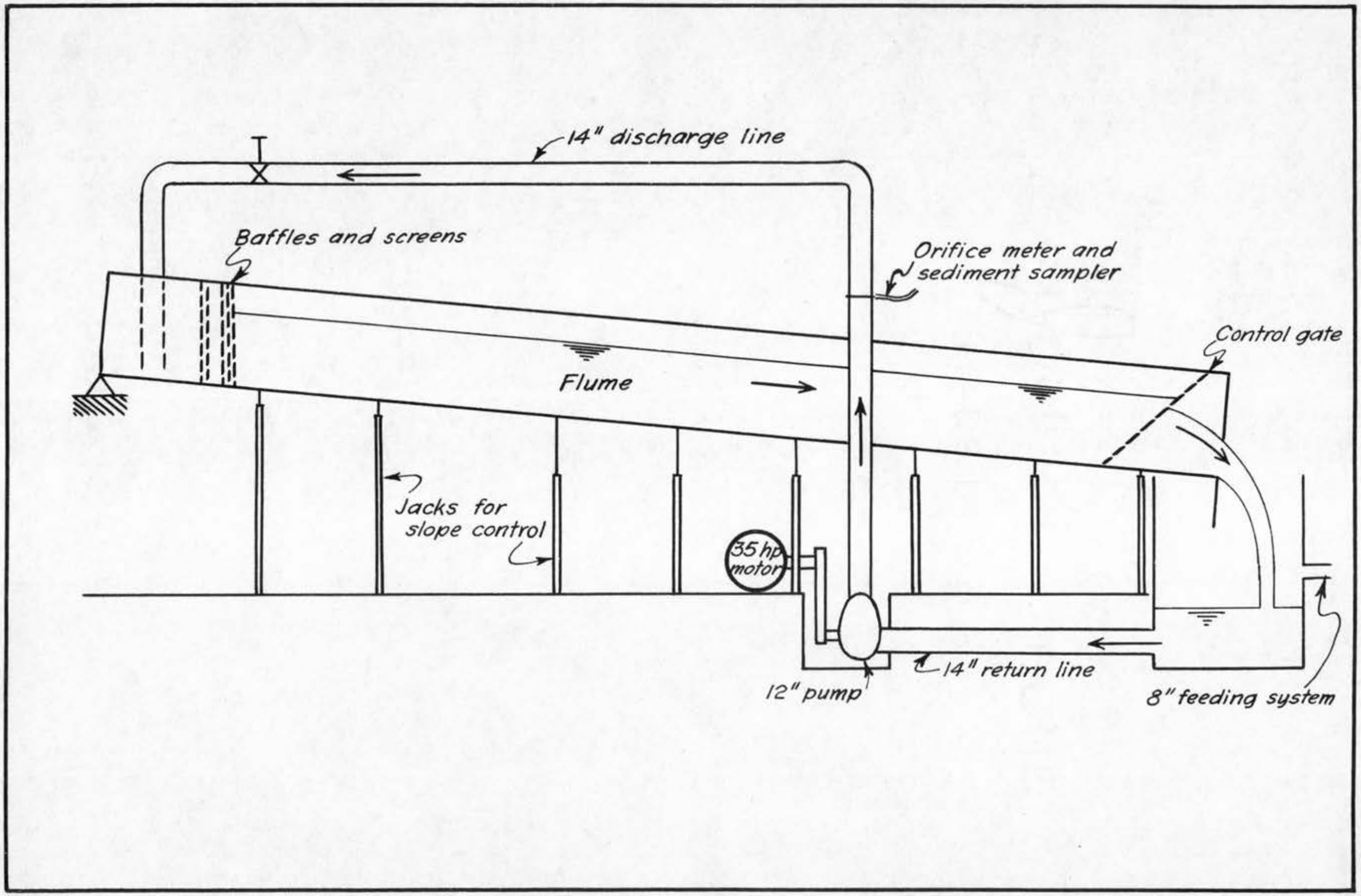

Fig. 5 Schematic diagram of the flume

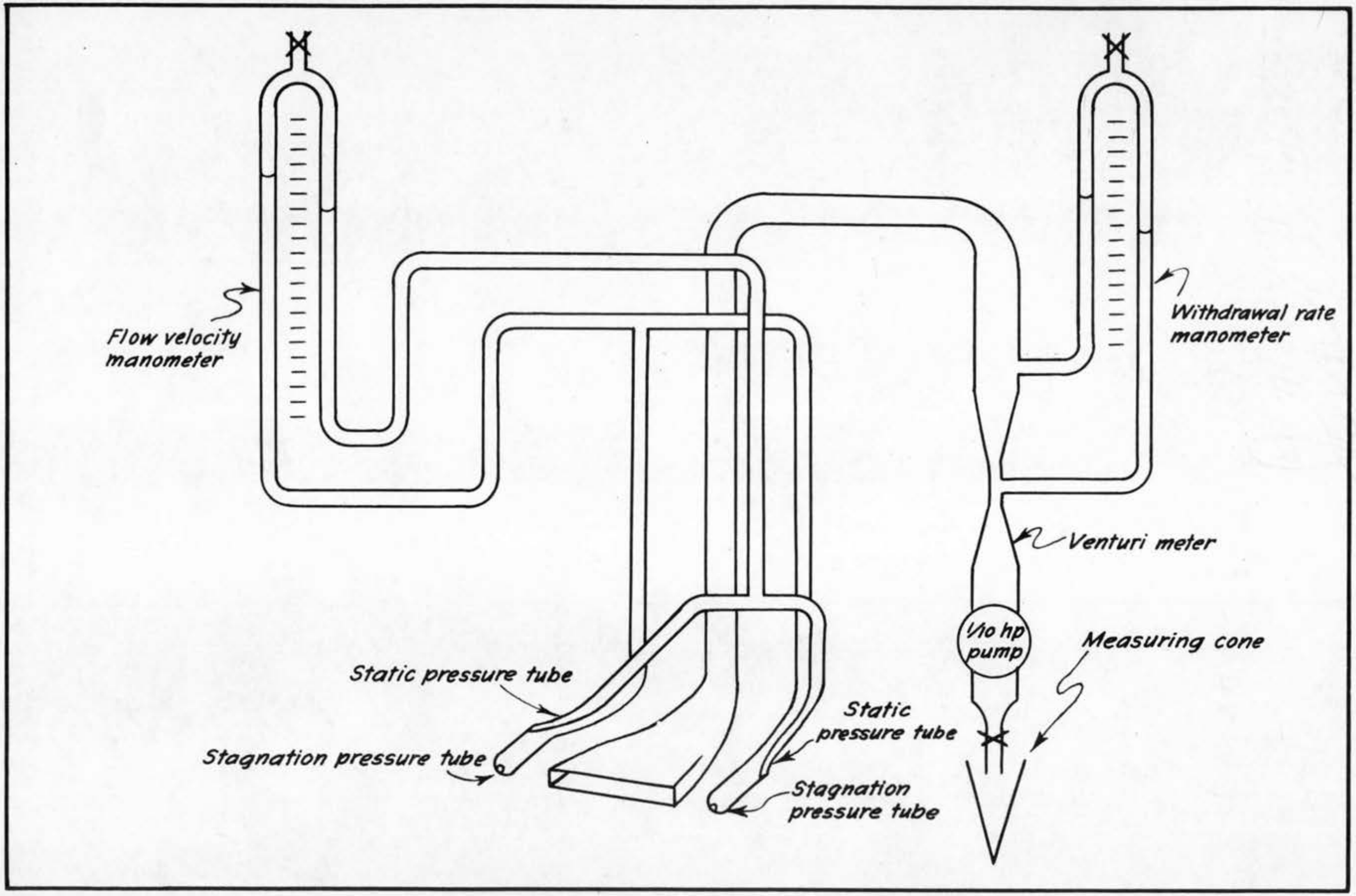

Fig. 6 Schematic diagram of pitot tube and sediment sampler.

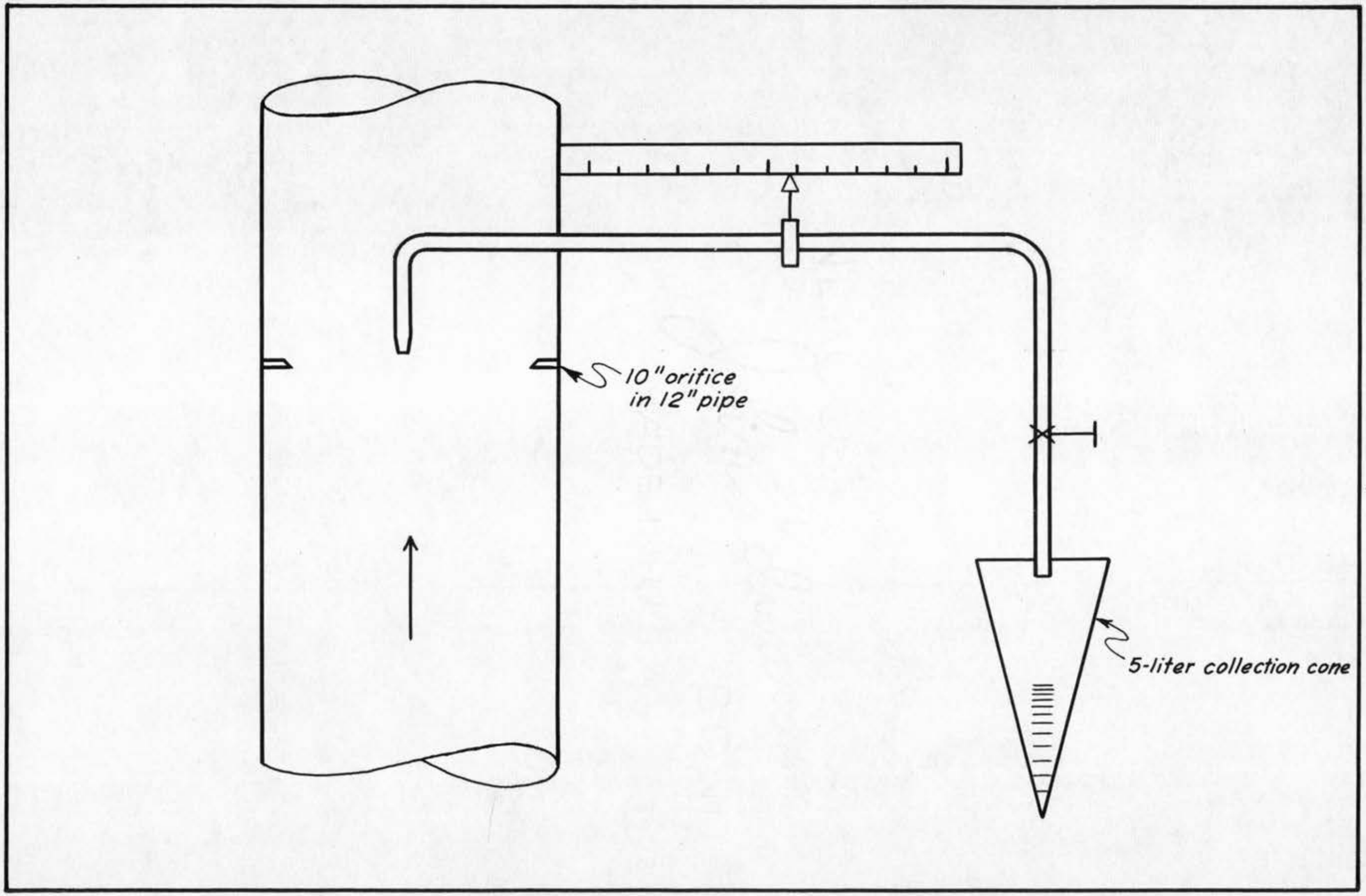

Fig. 7 Schematic diagram of sampler for total sediment load

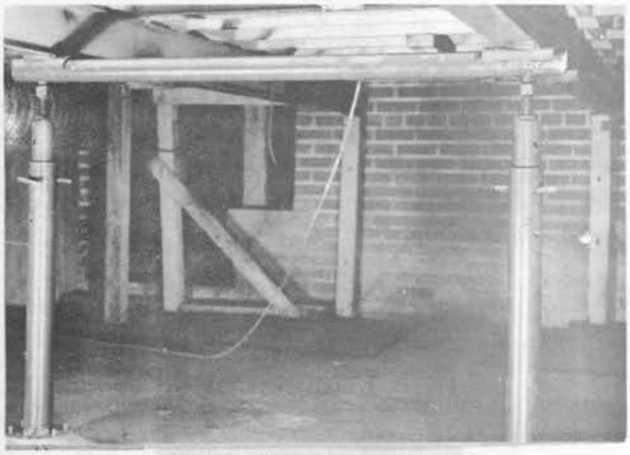

Jacks for adjusting
slope of flume

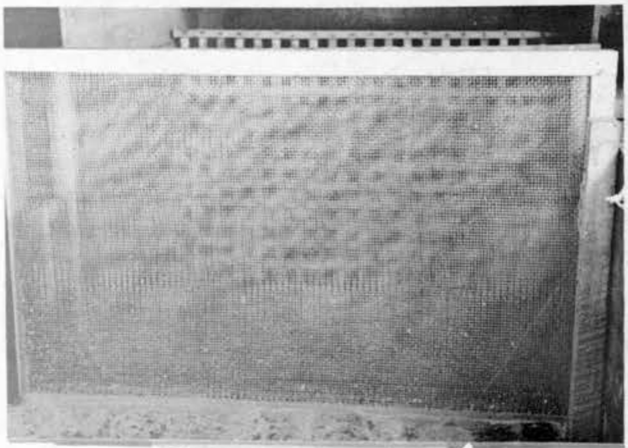

Upstream baffles
with screens

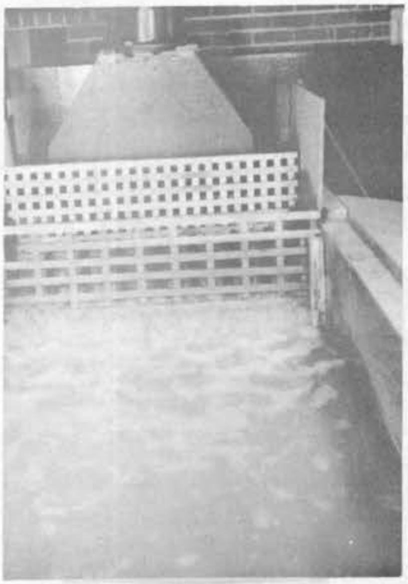

Upstream baffles
without screens

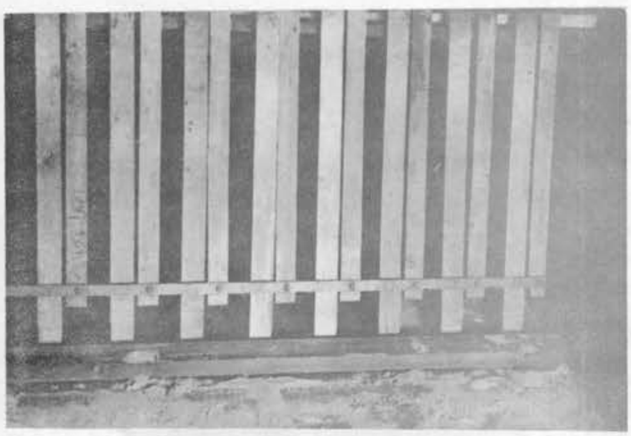

Downstream control gate

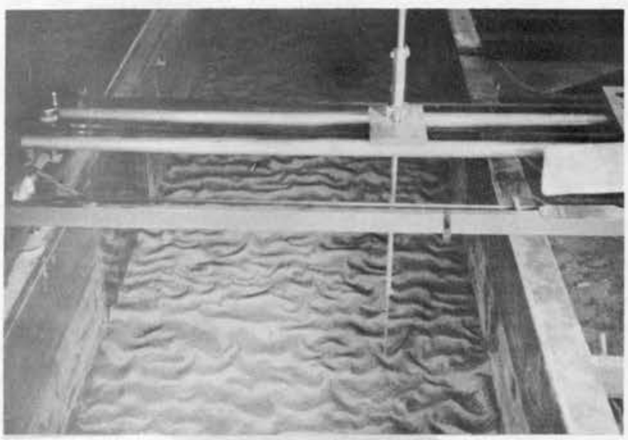

Point gage on
sampling carriage

Fig. 8 Views of flume equipment

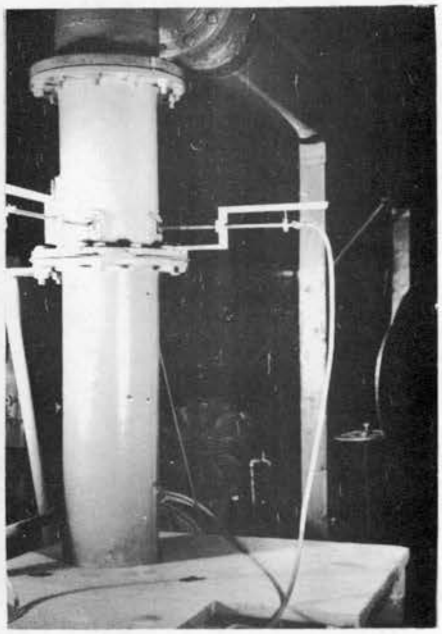

Total load sampler

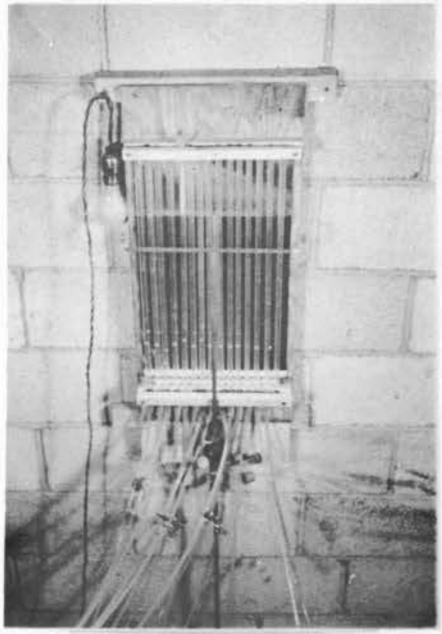

Manometer bank for
slope measurements

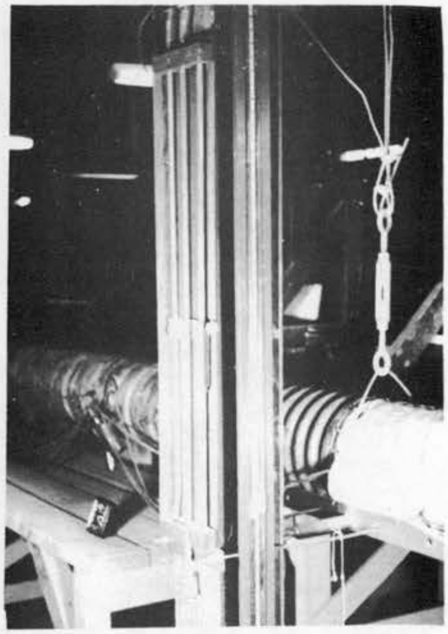

Differential water manometer
for discharge measurements

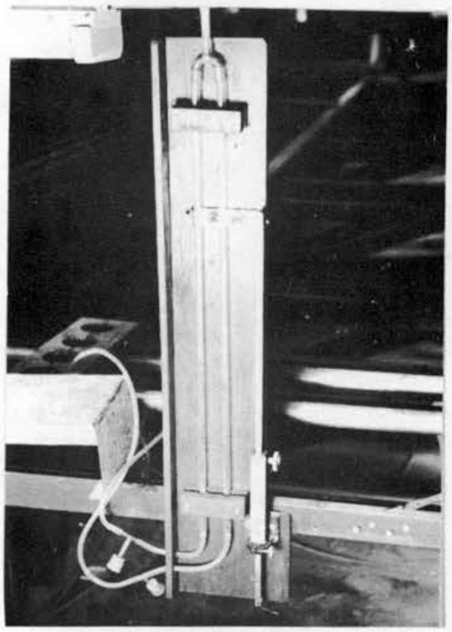

Gage for pitot tube

Fig. 9 Views of measuring equipment

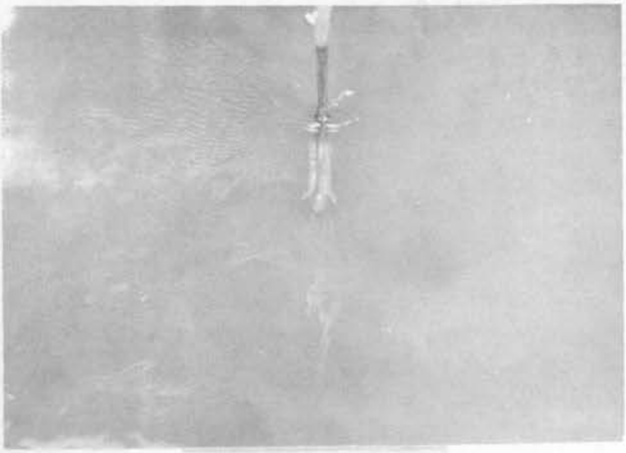

Sediment sampler
front view

Sediment sampler
side view

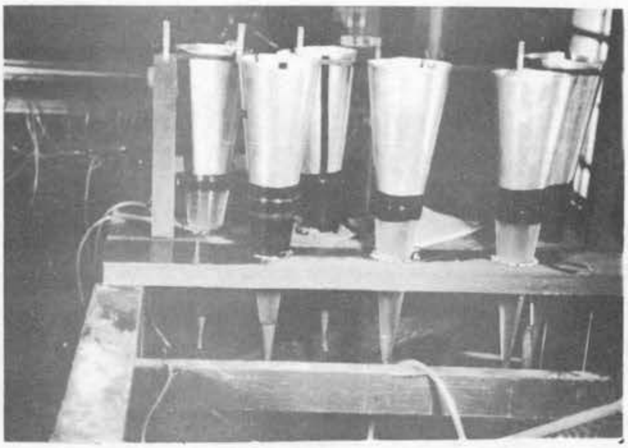

Sediment measuring cones
capacity 5 liters

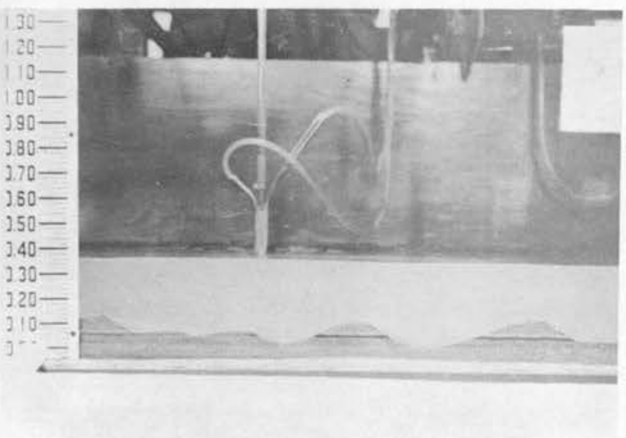

Sediment sampler
in operation

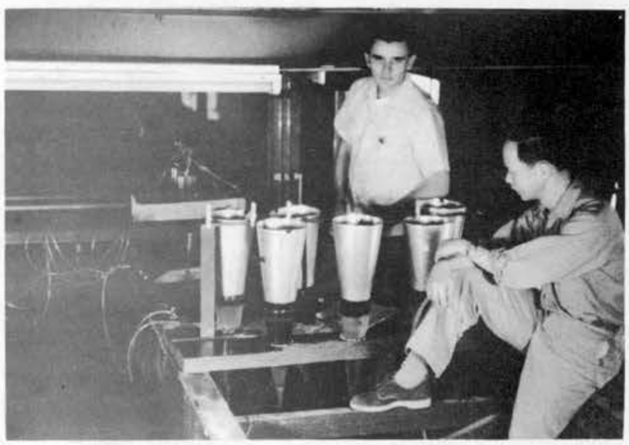

Sampling carriage and
sediment measuring cones

Fig. 10 Views of sampling equipment

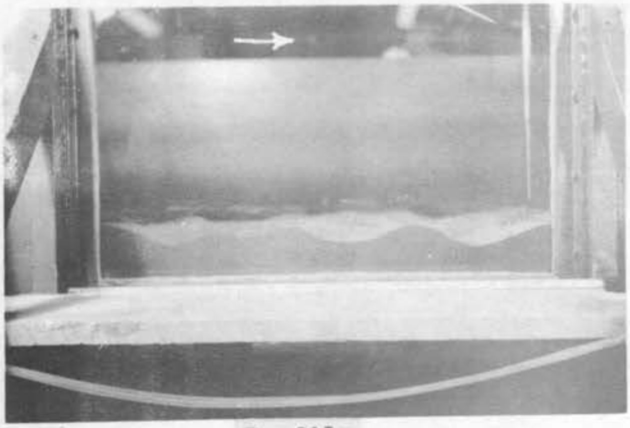

Profile

Run 21

Run 27

Run 28

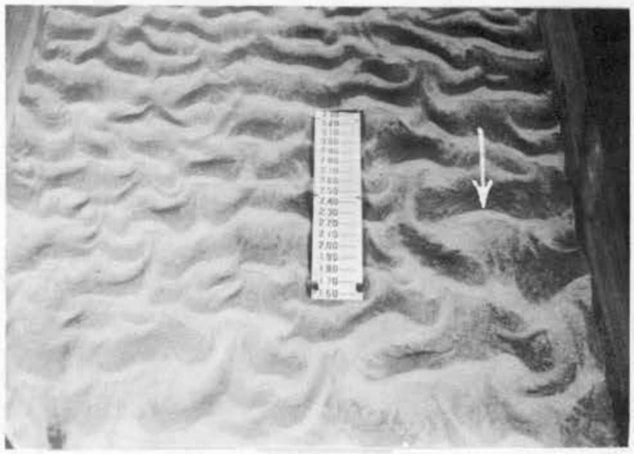

Run 37

Fig. 11 Views of typical dune patterns

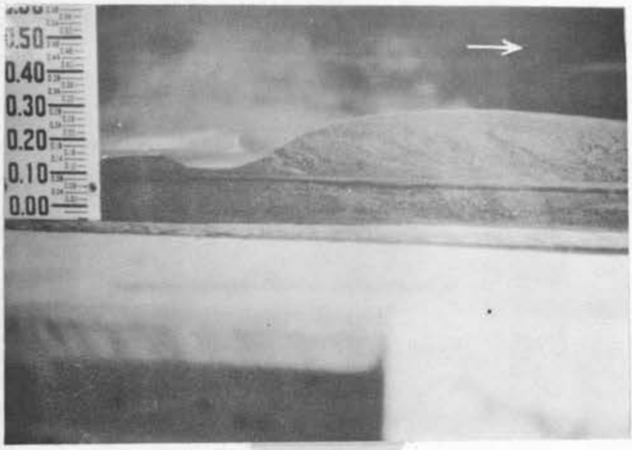

Profile

Run 15

Run 15

Run 30

Fig. 12 Views of typical sandbar patterns

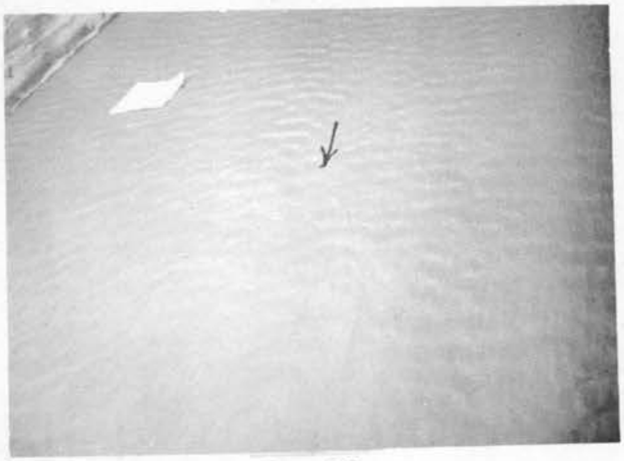

Run 18

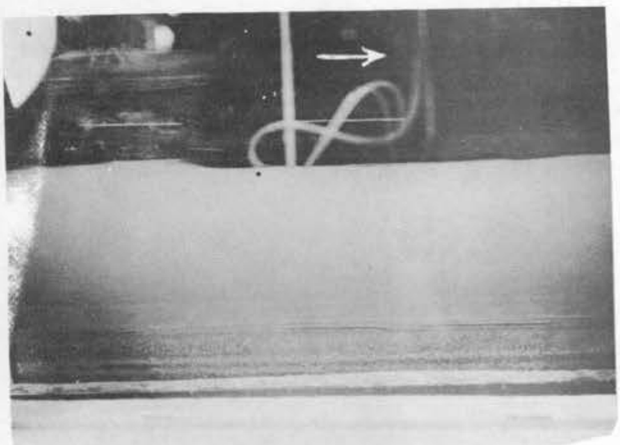

Profile

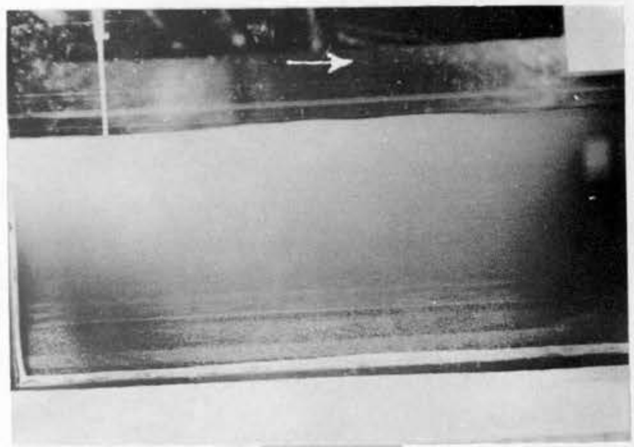

Profile

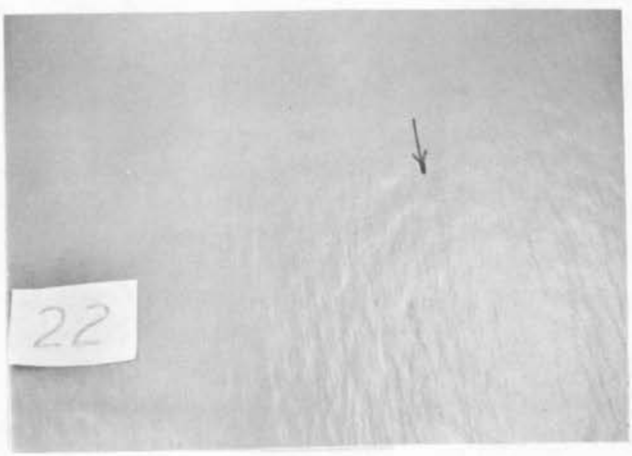

Run 22

Fig. 13 Views of a typical plane bed

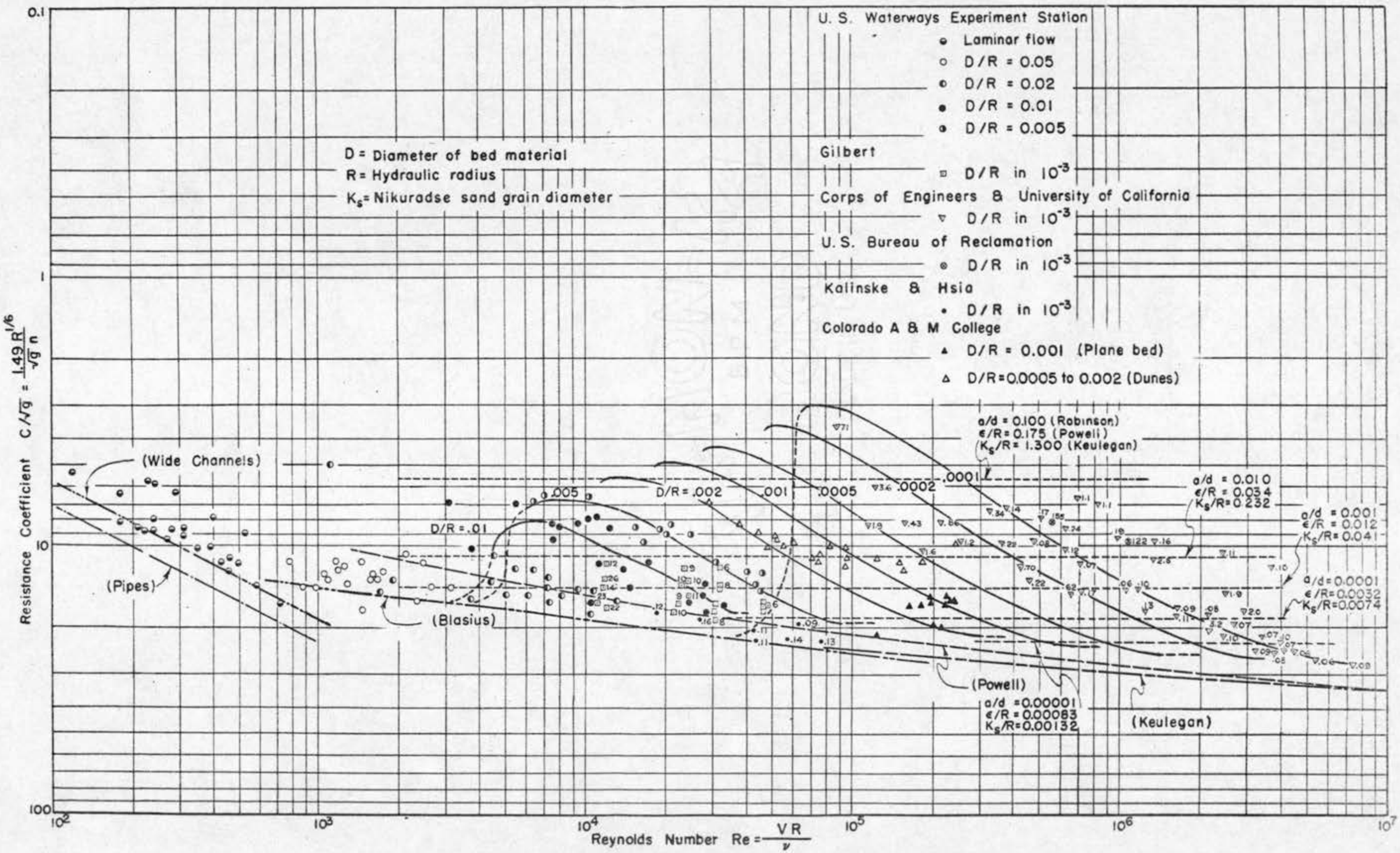

Fig. 14 Variation of Resistance Coefficient with Reynolds Number — — Relative Roughness as Third Variable

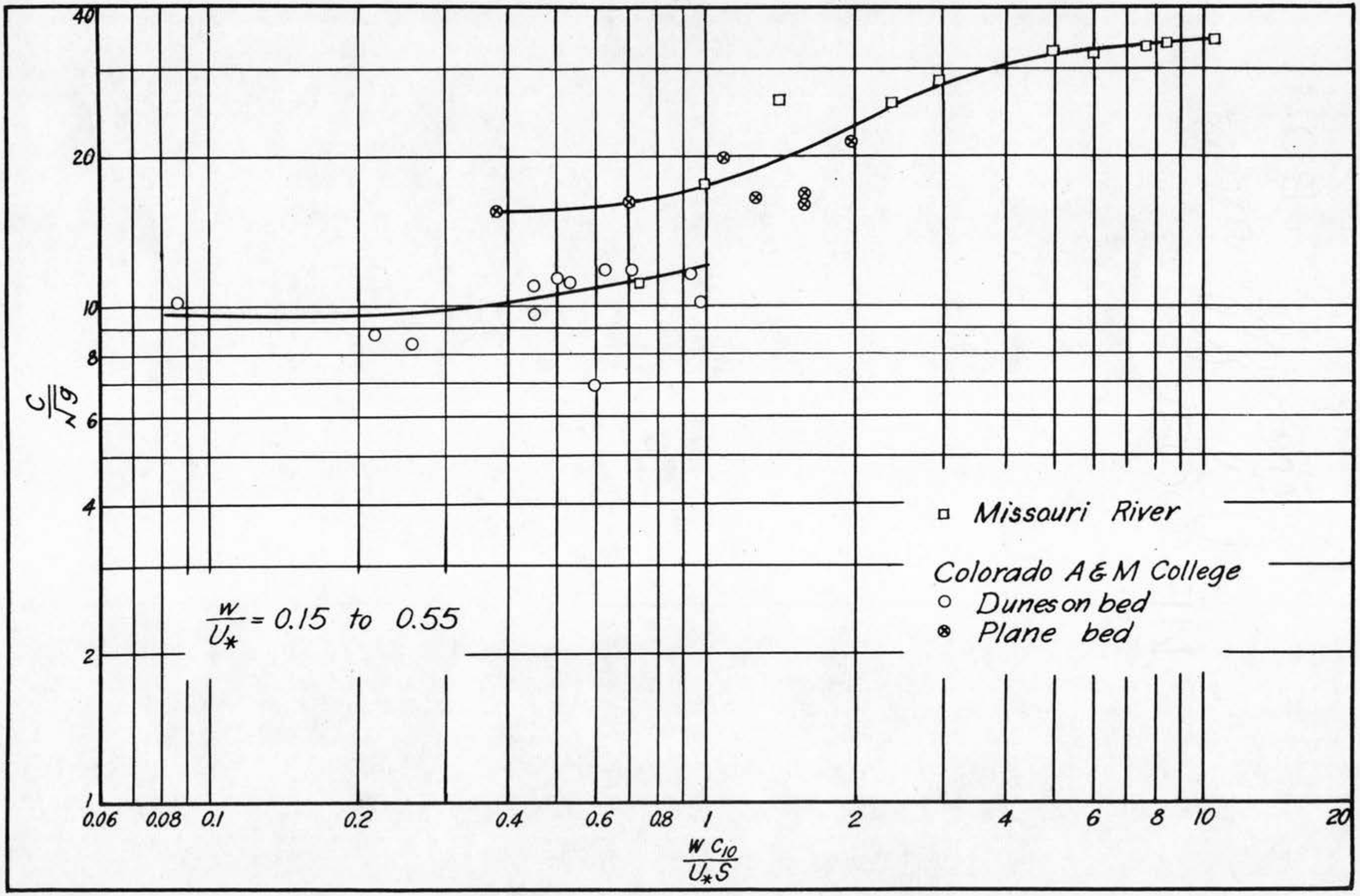

Fig. 15 Variation of resistance coefficient with Richardson number and bed conditions

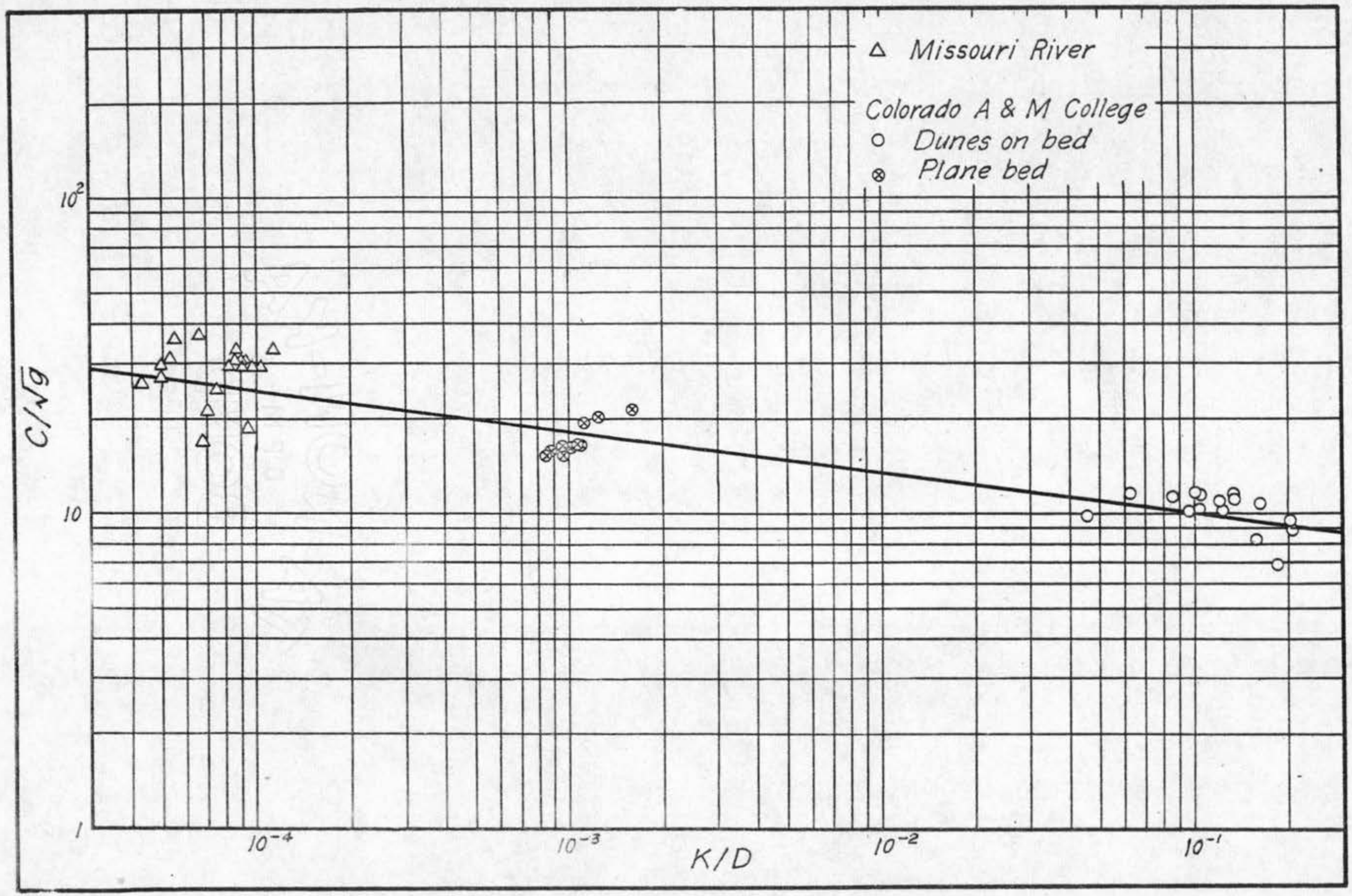

Fig. 16 Variation of resistance with relative roughness

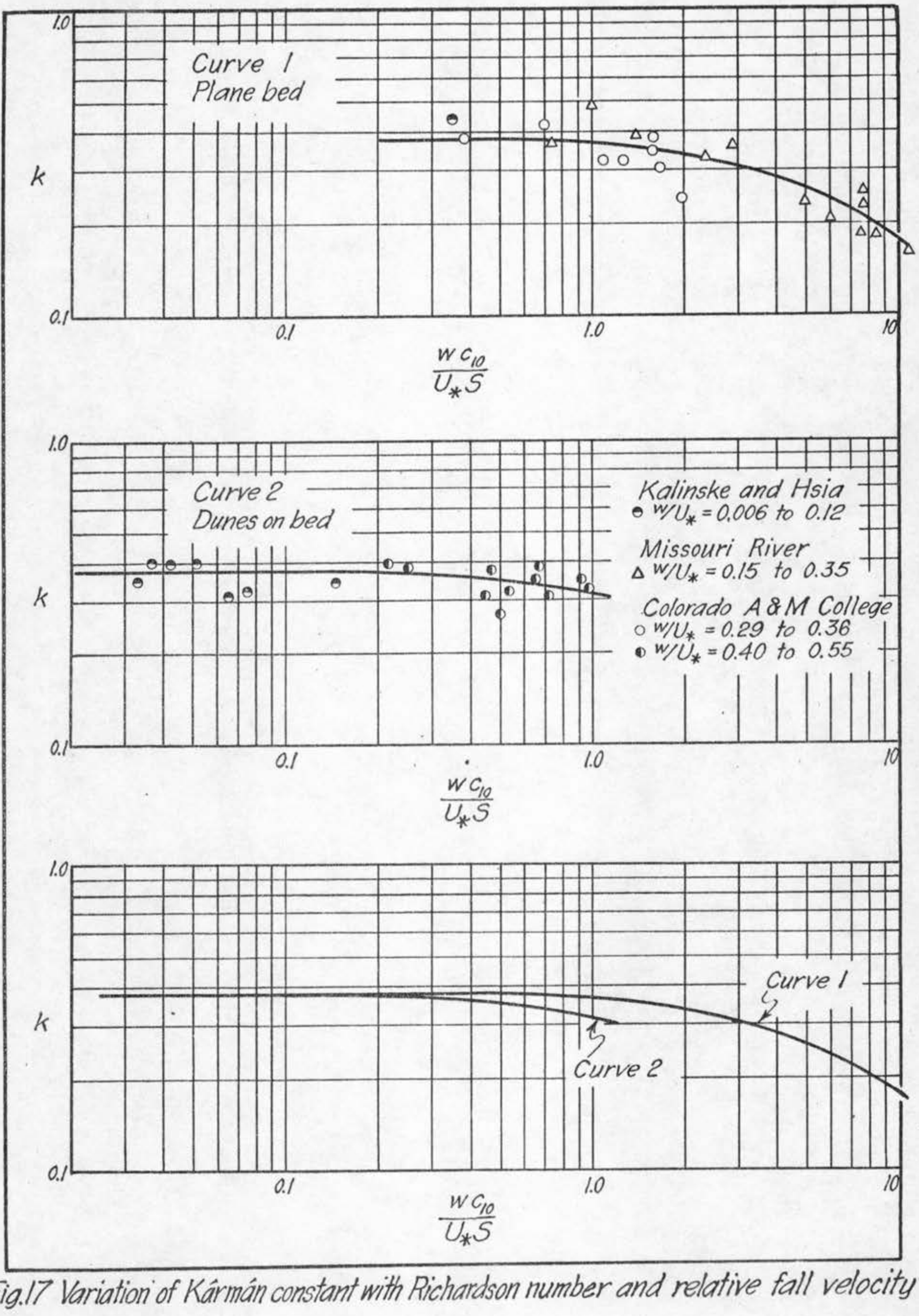

Fig.17 Variation of Kármán constant with Richardson number and relative fall velocity

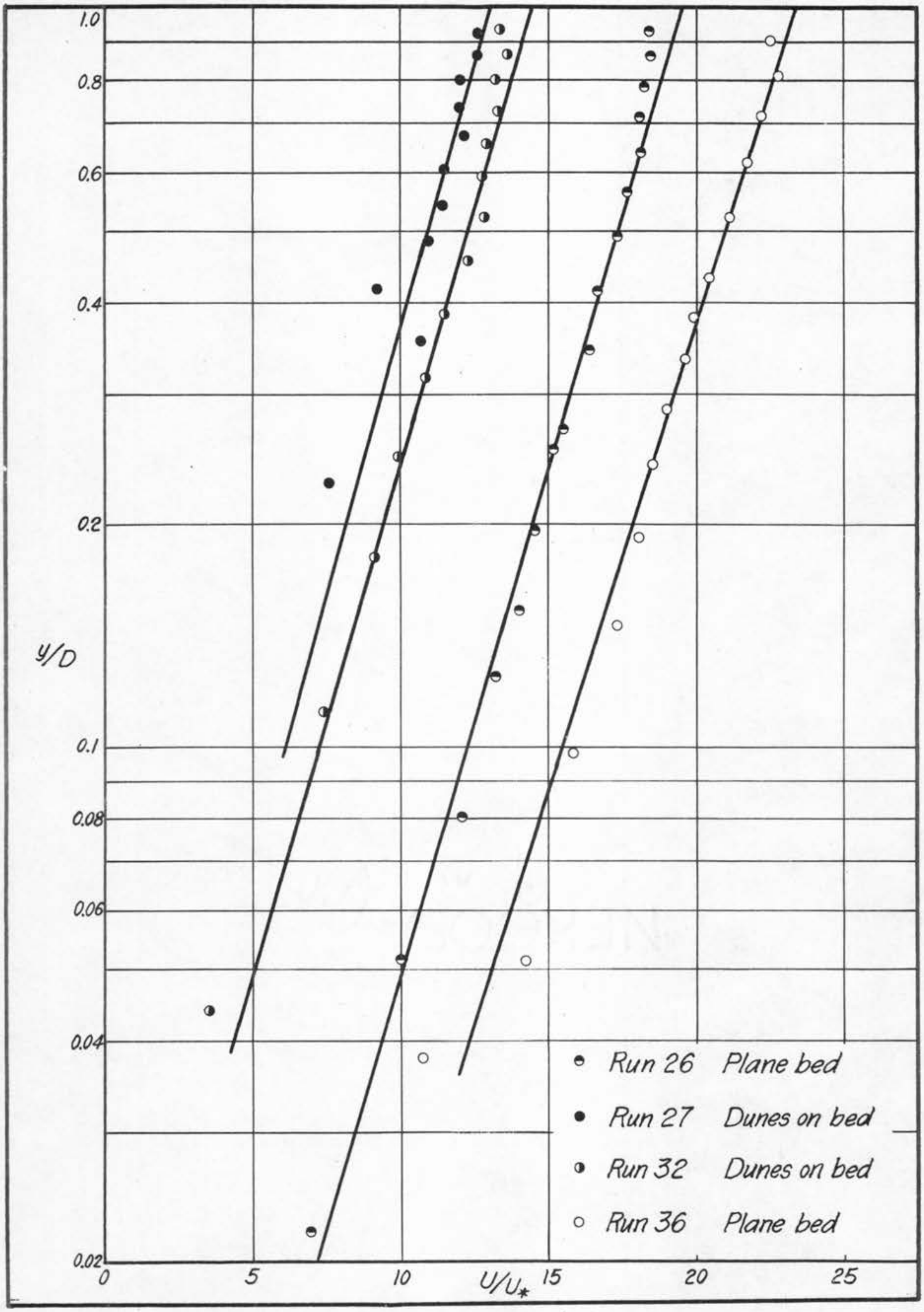

Fig. 18 Typical velocity distribution curves

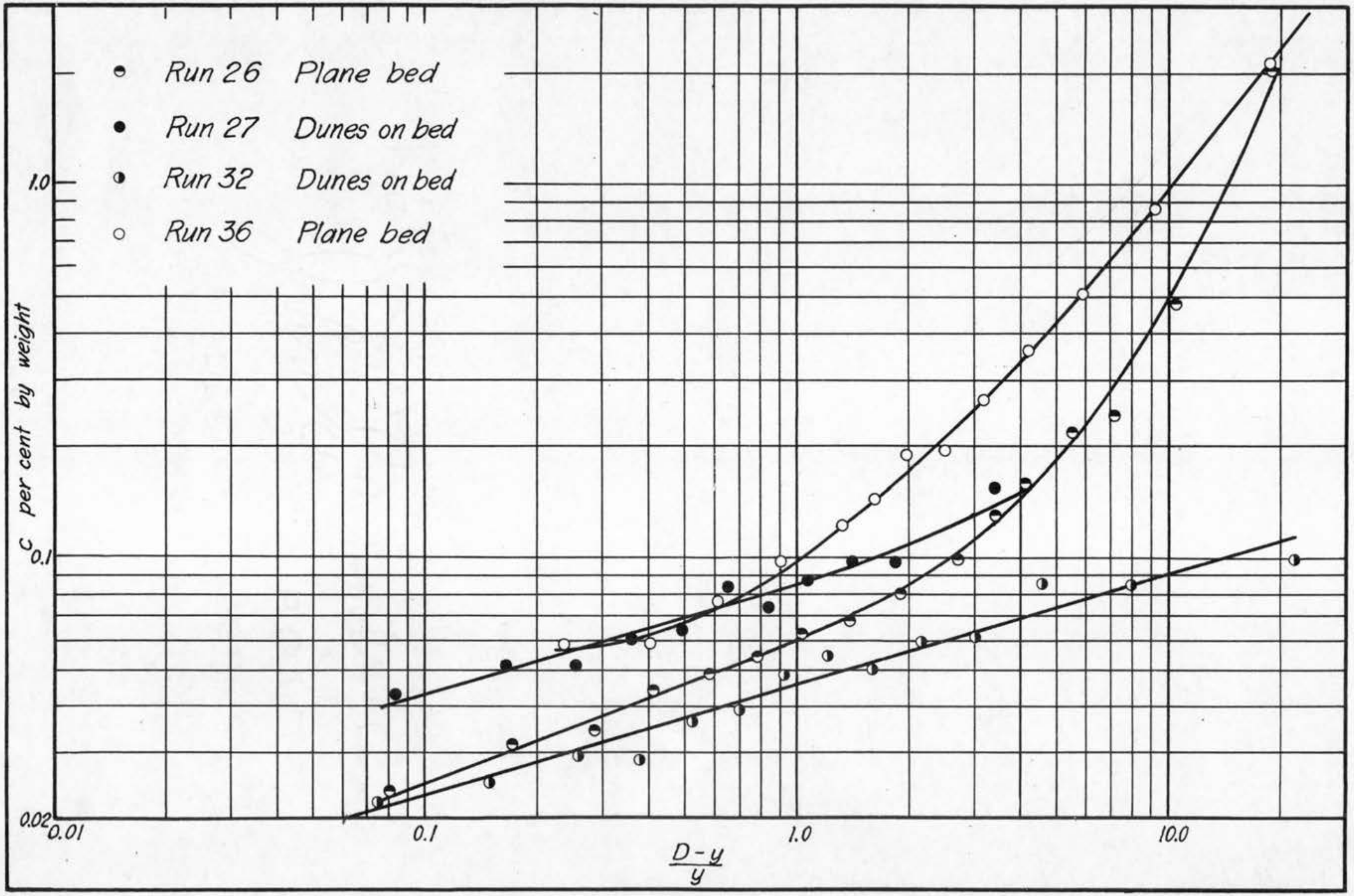

Fig. 19 Typical sediment distribution curves

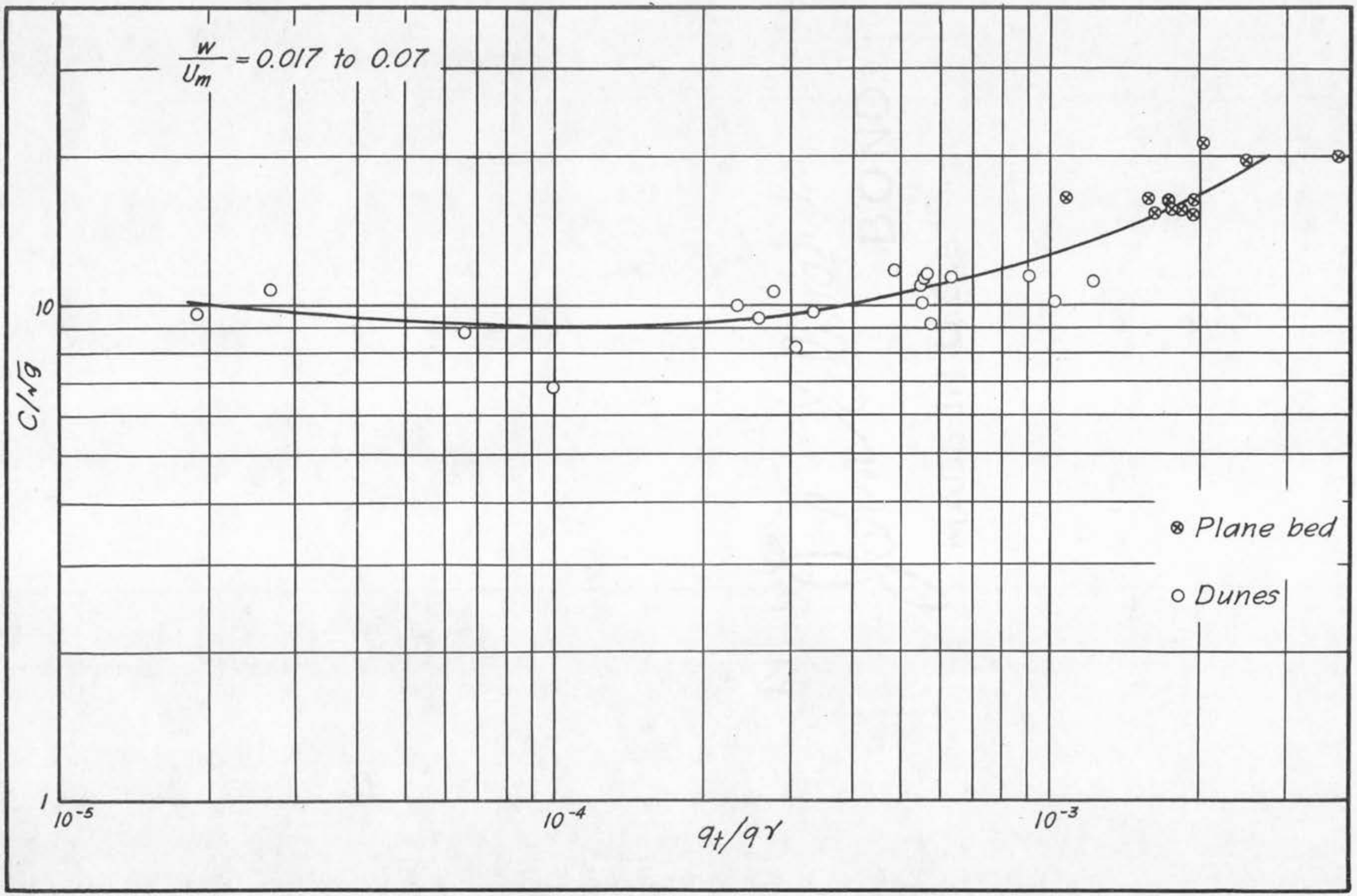

Fig. 20 Variation of resistance coefficient with concentration of total sediment load

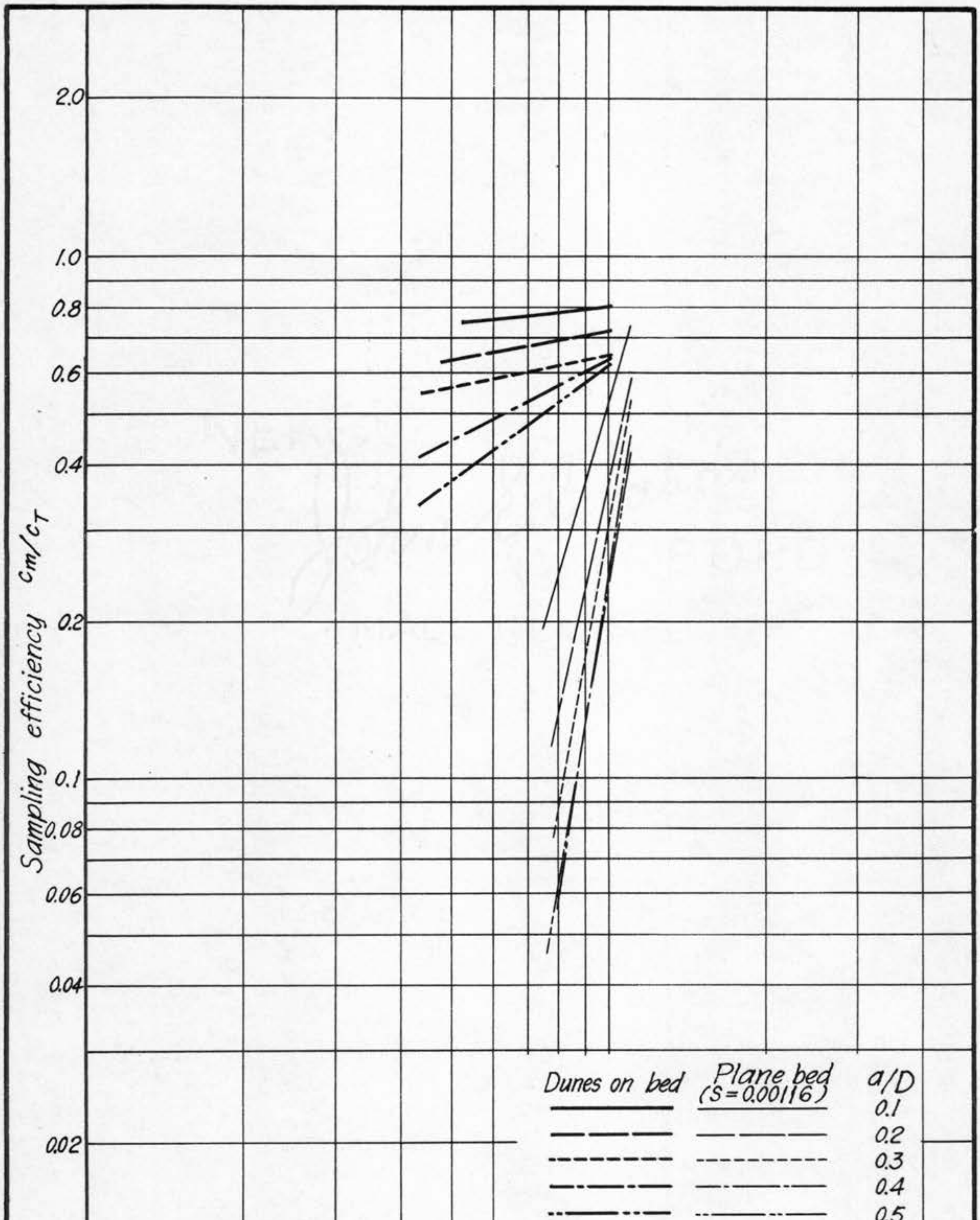

Fig. 21 Variation of sampling efficiency with Reynolds number

A P P E N D I X

Summary of Data and Results

Run	n_o	K_c	L_c	K_s	L_s	K_m	G	$\frac{Re}{10^{-5}}$	F	$\frac{R_*}{10^{-4}}$	Remarks
1	.027	.074	.64	.077	.83	.061	0.153	0.951	.300	0.945	Fair - Cone
3	.022	.092	.59	.091	.57		0.005	0.756	.320	0.695	Calibration
4	Included in Run 8										
5	.023	.061	.64	.067	.66		0.105	0.936	.347	0.798	Fair
6	.024	.072	.68	.095	.55		0.136	0.959	.327	0.871	Good
7	.024	.085	.67	.091	.57		0.216	1.500	.344	1.290	Fair
8	.027	.116	.68				0.045	0.825	.291	0.825	Fair
10	.029	.100	.53	.106	.49		0.032	0.524	.282	0.551	Good
11	.032	.096	.45	.095	.45		0.0061	0.427	.257	0.483	Good
12	.032	.063	.43	.064	.49		0.0023	0.601	.202	0.621	Fair
13	.028	.053	.44	.060	.44		0.0266	0.478	.216	0.473	Fair
15	.022	.065	.74	.057	.85	.079	0.206	0.705	.430	0.632	Fair
16	.028	.070	.69	.062	.61	.095	0.068	0.522	.365	0.570	Good
17	.032	.055	.49	.060	.51	.088	0.0254	0.373	.335	0.451	Good
18	.017	Smooth			Bed		0.897	1.950	.603	1.263	Baffles were
19	.016	Smooth			Bed		1.027	2.300	.644	1.460	affecting the
20	.016	Smooth			Bed		0.805	1.780	.670	1.080	velocity
21	.037	.051	.48	.062	.49	.090	0.0063	0.286	.277	0.412	distribution Fair
22	.018	Smooth			Bed		0.990	2.360	.661	1.500	Good
23	.017	Smooth			Bed		0.788	2.200	.695	1.355	Fair
24	No velocity or sediment data										
25	.017	Smooth			Bed		0.813	2.220	.553	1.450	Good
26	.016	Smooth			Bed		0.625	1.940	.575	1.200	Good
27	.023	.050	.50	.050	.55	.100	0.132	0.547	.367	0.544	Fair
28	.022	.070	.70	.060	.70	.090	0.149	0.747	.390	0.645	Fair
29	.015	Smooth			Bed		0.384	1.610	.573	0.969	Good
30	.022	Dunes but no measurement						1.540	.290	1.250	Good
31	.012	Smooth			Bed		0.430	1.220	.738	0.573	Good
32	.024	.070	.70	.055	.50	.090	0.145	1.210	.323	1.080	Fair
33	.021	.065	.60	.065	.60	.090	0.252	1.800	.283	1.570	Good
34	.029	.070	.67	.058	.59	.091	0.184	2.400	.249	2.490	Fair
35	.013	Smooth			Bed		1.113	1.970	.786	1.000	Good
36	.012	Smooth			Bed		1.790	2.120	.915	1.070	Good

Note: Screens were added to the upstream baffles after Run 22.

The following are additional symbols not previously listed in Definition of Symbols.

ν	ft^2/sec	Kinematic viscosity.
U_m	ft/sec	Mean velocity in a vertical at centerline of the flume.
U_a	ft/sec	Q/A
n	$ft^{1/6}$	Manning n at centerline of flume.
n_o	$ft^{1/6}$	Manning n based on U_a
K_c	ft	Average height of dunes along centerline of flume.
L_c	ft	Average length of dunes along centerline.
K_s	ft	Average dune height 1 ft. South of centerline.
L_s	ft	Average dune length 1 ft. South of centerline.
K_m	ft	Average dune height based on a given area of the bed rather than along a line traverse.
R_*	U_*D/ν	Reynolds number based on shear velocity.

Summary of Data and Results

Run	S %	Q	D	ν	Flume Sta.	U_m	U_s	U_*	k	$C/\sqrt{g}$	n
1	.088	4.45	0.78	1.230	74	1.50	1.43	.149	.38	10.1	.026
3	.086	3.9	0.56	1.008	67	1.36	1.34	.125	.46	10.9	.022
4	Included in Run 8										
5	.0866	3.5	0.63	1.050	67	1.56	1.39	.133	.35	11.8	.021
6	.088	4.0	0.69	1.110	67	1.54	1.45	.140	.31	11.0	.022
7	.088	5.5	0.84	1.005	67	1.79	1.64	.154	.37	11.6	.022
8	.081	3.1	0.65	1.025	67	1.30	1.19	.130	.37	10.0	.024
10	.088	2.0	0.51	1.110	67	1.14	0.98	.120	.25	9.5	.025
11	.087	1.5	0.46	1.065	67	0.99	0.815	.112	.40	8.9	.027
12	.044	1.96	0.66	1.020	67	0.93	0.740	.096	.55	9.7	.025
13	.045	1.53	0.54	1.015	67	0.90	0.710	.089	.58	10.2	.023
15	.150	2.70	0.45	1.047	67	1.64	1.500	.147	.39	11.1	.021
16	.158	1.90	0.40	1.005	67	1.31	1.190	.143	.40	9.2	.025
17	.161	1.34	0.36	1.100	67	1.14	0.930	.138	.38	8.25	.027
18	.156	7.40	0.69	1.005	67	2.84	2.680	.184	.72	15.4	.016
19	.167	9.0	0.75	1.030	67	3.17	3.000	.201	.61	15.8	.016
20	.166	6.7	0.61	1.020	67	2.97	2.740	.180	.53	16.5	.015
21	.160	0.90	0.30	0.902	67	0.86	0.750	.124	.36	6.9	.031
22	.170	9.1	0.76	1.053	75	3.27	2.990	.208	.38	15.8	.016
23	.183	7.4	0.65	0.940	67	3.18	2.840	.196	.42	16.2	.015
24	No velocity or sediment data										
25	.124	8.1	0.78	0.945	67	2.69	2.600	.176	.38	15.3	.016
26	.125	7.1	0.69	0.965	73	2.71	2.580	.168	.34	16.3	.015
27	.135	2.1	0.40	0.965	73	1.32	1.310	.131	.33	10.1	.023
28	.116	2.64	0.48	0.990	73	1.54	1.390	.133	.31	11.6	.020
29	.121	5.8	0.60	0.945	73	2.54	2.410	.153	.32	16.6	.014
30	.0555	5.8	0.94	0.976	73	1.60	1.540	.130	.28	12.3	.021
31	.129	4.2	0.41	0.930	73	2.77	2.560	.130	.24	21.3	.011
32	.082	4.15	0.73	0.942	73	1.56	1.420	.139	.32	11.2	.022
33	.061	7.2	1.03	0.935	73	1.63	1.750	.142	.35	11.5	.023
34	.065	8.85	1.38	0.954	73	1.66	1.600	.170	.38	9.75	.028
35	.160	7.2	0.56	0.950	73	3.34	3.220	.170	.32	19.7	.012
36	.210	7.6	0.53	0.935	73	3.74	3.600	.189	.30	20.0	.012

Note: Beds referred to as Smooth Beds in this summary are referred to as plane beds in the main report.

Definition of Symbols

The data recorded in the following pages of the appendix were gathered in a tilting flume which was 4 feet wide, 70 feet long, and about 2 feet deep. Most of the data were gathered at either station 73 or station 67. The last screen on the upstream baffle was at station 33, and the downstream control gate was at station 94 so station 73 was almost exactly two-thirds of the working length of the flume from the upstream baffle. Data indicated that uniform flow conditions generally existed in the middle third of the working length of the flume. The following symbols were the ones used in the tabulation of the flume data. All measurements involving velocity and sediment distribution data were made on the centerline of the flume.

Symbol	Dimensions	Definition
Q	cfs	Quantity of water flowing in the flume.
G	lb/sec	Sediment discharge in the flume includes suspended and bed loads.
D	ft	Depth of water flowing in the flume. In case of dunes D was measured from the mean elevation of the sand bed.
U_m	ft/sec	Mean velocity determined from the velocity distribution curve.
U	ft/sec	Velocity at depth y above the mean bed elevation.
U_*	ft/sec	Shear velocity - $U_* = \sqrt{gDS}$
S		Slope of the water surface.
k		The mixing coefficient - Kappa.
$C/\sqrt{g}$		Chezy's resistance coefficient divided by the square root of the gravitational constant, g.
n	$(ft)^{1/6}$	Manning's roughness coefficient - n.
Re		Reynolds number.
F		Froude number.
c	% by weight	Sediment concentration at a given elevation y.
y	ft	Depth of flow to some point above the bed-measured from the mean elevation at the bed.

Symbol	Dimensions	Definition
E_p	ft	Average elevation of the peaks of the dunes measured along the center-line or a line parallel to the center-line of the flume.
E_t	ft	Average elevation at the troughs of the dunes.
$E_p - E_t$	ft	Average height of dunes.
L	ft	Average length of dunes.
N		Number of measurements used to evaluate E_p, E_t , and L.

Time: To conserve space, time was designated as 0 to 12 for a.m. and 12 to 24 for p.m. For example, 1720 is 5:20 p.m. or 0640 is 6:40 a.m.

Slope: The piezometers were numbered from 1 to 14. They consisted of small 1/16 inch holes drilled in the side of the flume, and they had the following spacing:

Piezometer Number	Spacing along flume in feet
1	
	5.0
2	
	2.5
3	
	2.5
4	
	2.5
5	
	2.5
6	
	2.0
7	
	3.0
8	

Piezometer Number	Spacing along flume in feet
8	
	2.0
9	
	3.0
10	
	2.5
11	
	2.5
12	
	5.0
13	
	5.0
14	

RUN 1

General Data

				Temperature	
				Time	Temp. °C
Q (cfs)	4.45	k	0.384	0830	12.0
G (lb/sec)	0.153	$C/\sqrt{g}$	10.1	0915	12.5
D (ft)	0.78	n (ft) $^{1/6}$	0.026	1030	13.5
U_m (ft/sec)	1.50	Re x 10^{-5}	0.951	1530	15.8
U_* (ft/sec)	0.1485	F	0.30	1720	17.5
S (%)	0.088				

Dune Characteristics

	E_p	E_t	L	N
Profile along C	1.180	1.108	0.64	47
Profile 1 ft. from C	1.198	1.121	0.83	36
Area near Sta. 67	1.173	1.112		52
Description of bed	Dunes			

Velocity and Concentration Profiles

$\frac{D-y}{y}$	c Sta. 66	$\frac{D-y}{y}$	c Sta. 74	y/D	U/U_* Sta. 66	y/D	U/U_* Sta. 74
0.147	0.0188	0.147	0.0240	0.872	12.87	0.872	12.26
0.310	0.0268	0.310	0.0320	0.743	13.33	0.743	11.99
0.625	0.0320	0.625	0.0410	0.615	12.80	0.615	11.91
0.815	0.0345	0.815	0.0430	0.551	12.51	0.551	10.98
1.050	0.0740	1.050	0.0335	0.487	11.91	0.487	10.63
1.36	0.0820	1.360	0.0550	0.423	11.39	0.423	10.30
1.79	0.1120	1.790	0.0650	0.359	10.99	0.359	9.57
2.39	0.0910		0.1240	0.295	10.11	0.231	9.24
	0.1500			0.231	9.18		
	0.1810			0.167	8.41		

Slope of Water Surface

Piezometer Readings in ft.

Time	1	2	4	6	8	10	12	13	Slope %
					July 15, 1954				
1035	.970	.968	.964	.958	.954	.952	.950	.944	.080
1530	.969	.968	.963	.957	.953	.950	.948	.942	.886
1720	.972	.969	.965	.958	.955		.947	.944	.845
					July 16, 1954				
0830	.976	.973	.965	.957	.956	.952	.945	.942	.103
0945	.972	.971	.965	.959	.956	.954	.952	.942	.886
1215	.974	.972	.967	.960	.957	.955	.952	.947	.829

Note: General data based on Sta. 74.

RUN 3

General Data				Temperature	
				Time	Temp. °C
Q (cfs)	3.0	k	0.46	1200	22.7
G (lb/sec)	0.005	$C/\sqrt{g}$	10.9	1110	23.2
D (ft)	0.56	n (ft) $^{1/6}$	0.022	1520	24.0
U_m (ft/sec)	1.36	Re x 10^{-5}	0.756		
U_* (ft/sec)	0.125	F	0.32		
S (%)	0.086				

Dune Characteristics

	E_p	E_t	L	N
Profile along C	1.178	1.086	0.59	53
Profile 1 ft. from C	1.191	1.100	0.57	56
Profile 1 ft. from C	1.167	1.073	0.61	51
Description of bed	Dunes			

Velocity and Concentration Profiles

$\frac{D-y}{y}$	c	y/D	
0.218	0.00143	0.911	12.53
0.368	0.00182	0.821	12.30
1.155	0.00173	0.732	12.30
1.667	0.00310	0.643	11.81
2.496	0.00305	0.554	11.73
4.050	0.00305	0.464	11.73
8.346	0.00370	0.375	11.33
55.000	0.00510	0.286	10.37
		0.196	9.48
		0.107	8.68
		0.178	8.43

Slope of Water Surface

Piezometer Readings in ft.
January 30, 1954

Time	1	2	3	4	5	6	7	8	9	Slope%
1130	.932	.927	.926	.920	.916	.912	.907	.903	.895	.0898
1140	.931	.925	.923	.918	.914	.910	.907	.903	.897	.085
1315	.919	.914	.910	.907	.903	.899	.897	.888	.886	.0825

RUN 5

General Data

Temperature

Q (cfs) 3.5	k 0.346	Time	Temp. °C
G (lb/sec) 0.1045	$C/\sqrt{g}$ 11.8	0725	19.0
D (ft) 0.63	n (ft) $^{1/6}$ 0.021	0845	19.4
U_m (ft/sec) 1.56	Re x 10^{-5} 0.936	1315	21.0
U_* (ft/sec) 0.133	F 0.347	1545	22.0
S (%) 0.086			

Dune Characteristics

	E_p	E_t	L	N
Profile along C	1.192	1.131	0.64	50
Profile 1 ft. from C	1.181	1.117	0.65	57
Profile 1 ft. from C	1.187	1.118	0.67	52
Description of bed . . . . . . Dunes				

Velocity and Concentration Profiles

$\frac{D-y}{y}$	c	y/D	U/U_* Sta. 67
0.0995	0.022	0.910	14.92
0.2045	0.028	0.830	14.18
0.3320	0.023	0.750	13.58
0.4890	0.023	0.671	13.58
0.6890	0.034	0.582	13.10
0.9500	0.038	0.512	12.82
1.3080	0.037	0.413	11.91
1.8270	0.041	0.354	11.05
2.6400	0.050	0.274	10.78
4.1200	0.083	0.195	10.19
		0.116	8.30

Slope of Water Surface

Piezometer Readings in ft.
February 20, 1954

Time	2	3	4	5	6	7	8	9	10	11	12	13	Slope %
0715	1.125	1.124	1.118	1.118	1.115	1.114	1.114	1.112	1.108	1.108	1.105	1.100	.0853
0830	1.123	1.117	1.114	1.111	1.110	1.108	1.107	1.105	1.106	1.103	1.104	1.097	.085
1305	1.116	1.113	1.107	1.107	1.105	1.103	1.103	1.101	1.100	1.096	1.092	1.087	.0866
1705	1.116	1.113	1.109	1.107	1.105	1.103	1.102	1.100	1.098	1.096	1.095	1.089	.0866

RUN 6

General Data

Q (cfs)	4.0	k	0.31
G (lb/sec)	0.1360	$C/\sqrt{g}$	11.0
D (ft)	0.69	n (ft) $^{1/6}$	0.022
U_m (ft/sec)	1.54	Re x 10^{-5}	0.959
U_* (ft/sec)	0.140	F	0.327
S (%)	0.088		

Temperature

Time	Temp. °C
0850	15.0
1120	16.9
1320	18.0
1620	19.3
1950	20.1

Dune Characteristics

	E_p	E_t	L	N
Profile along C	1.194	1.123	0.68	48
Profile 1 ft. from C	1.212	1.119	0.55	60

Description of bed . . . . Dunes

Velocity and Concentration Profiles

$\frac{D-y}{y}$	c	y/D	U/U_* Sta. 67
0.0787	0.024	0.927	14.3
0.1690	0.022	0.855	14.2
0.2770	0.029	0.783	14.0
0.4040	0.030	0.712	13.7
0.5620	0.033	0.640	13.0
0.7640	0.035	0.567	11.9
1.0200	0.038	0.495	11.8
1.3600	0.041	0.424	11.7
1.8200	0.050	0.355	10.8
2.5700	0.067	0.280	9.7
3.8100	0.075	0.208	9.2
0.1220	0.022	0.891	14.0
0.4810	0.034	0.675	13.1
0.8800	0.044	0.532	11.9

Slope of Water Surface

Piezometer Readings in ft.
February 23, 1954

Time	2	3	4	5	6	7	8	9	10	11	12	13	Slope%
1125	1.167	1.163	1.158	1.158	1.159	1.155	1.152	1.151	1.149	1.150	1.143	1.142	.0873
1315	1.168	1.165	1.160	1.159	1.157	1.157	1.155	1.153	1.152	1.149	1.149	1.143	.084
1630	1.169	1.167	1.166	1.163	1.159	1.158	1.157	1.152	1.153	1.151	1.151	1.147	.080
1650	1.165	1.160	1.158	1.155	1.155	1.154	1.153	1.149	1.146	1.144	1.141	1.142	.0833
1835	1.163	1.160	1.158	1.155	1.155	1.154	1.148	1.147	1.146	1.143	1.143	1.140	.088
1955	1.162	1.159	1.158	1.154	1.154	1.153	1.151	1.147	1.148	1.145	1.139	1.139	.085

RUN 7

General Data

Q (cfs)	5.5	k	0.37
G (lb/sec)	0.2160	$C/\sqrt{g}$	11.6
D (ft)	0.84	n (ft) $^{1/6}$	0.022
U_m (ft/sec)	1.79	Re x 10^{-5}	1.50
U_* (ft/sec)	0.154	F	0.344
S (%)	0.088		

Temperature

Time	Temp. °C
0500	23.0
0805	22.8
1030	23.0

Dune Characteristics

	E_p	E_t	L	N
Profile along C	1.220	1.134	0.67	43
Profile 1 ft. from C	1.230	1.140	0.57	53

Description of bed . . . . Dunes

Velocity and Concentration Profiles

$\frac{D-y}{y}$	c	y/D	U/U_* Sta. 67
0.312	0.0225	0.94	13.2
0.423	0.0249	0.881	13.2
0.555	0.0269	0.822	13.0
0.715	0.0260	0.762	13.0
0.908	0.0410	0.703	12.9
1.155	0.0351	0.643	12.8
1.470	0.0402	0.583	12.7
1.899	0.0511	0.524	12.2
2.496	0.0551	0.464	12.1
3.425	0.0582	0.405	11.5
4.989	0.0773	0.345	11.0
8.346	0.1088	0.286	10.8
		0.226	10.0
		0.167	9.4
		0.107	8.3

Slope of Water Surface

Piezometer Readings in ft.

Time	2	3	4	5	6	7	8	9	10	11	12	13	Slope %
February 25, 1954													
	1.329	1.327	1.325	1.321	1.318	1.312	1.313	1.312	1.310	1.307	1.304	1.302	.0870
0920	1.332	1.326	1.322	1.321	1.316	1.316	1.315	1.308	1.310	1.306	1.302		.0938
1255	1.335	1.331	1.325	1.323	1.324	1.321	1.317	1.317	1.314	1.314	1.308	1.306	.088
1623	1.335	1.331	1.329	1.324	1.320	1.322	1.320	1.316	1.317	1.313	1.312	1.312	.090
2330	1.330	1.327	1.324	1.319	1.317	1.316	1.317	1.314	1.311	1.310	1.306	1.307	.085
February 26, 1954													
0610	1.332	1.327	1.324	1.322	1.320	1.318	1.315	1.313	1.310	1.309	1.308	1.304	.0858
1040	1.338	1.332	1.330	1.328	1.325	1.323	1.321	1.320	1.317	1.316	1.315	1.315	.0863

RUN 8

General Data				Temperature	
				Time	Temp. °C
Q (cfs)	3.1	k	0.37	0005	21.0
G (lb/sec)	0.0452	$C/\sqrt{g}$	10.0	0800	21.0
D (ft)	0.65	n (ft) $^{1/6}$	0.024	1310	21.8
U_m (ft/sec)	1.33	Re x 10^{-5}	0.825		
U_* (ft/sec)	0.133	F	0.291		
S (%)	0.084				

Dune Characteristics

	E_p	E_t	L	N
Profile along C	1.220	1.104	0.68	51
Description of bed	Dunes			

Velocity and Concentration Profiles

$\frac{D-y}{y}$	U/U_* Sta. 67	y/D	U/U_* Sta. 67
0.923	13.3	0.923	12.4
0.846	13.4	0.846	12.2
0.769	13.1	0.769	12.0
0.692	12.7	0.692	11.6
0.615	12.5	0.615	11.2
0.538	11.7	0.538	10.8
0.462	11.9	0.462	10.5
0.385	11.3	0.385	10.0
0.308	10.5	0.308	9.3
0.231	10.0	0.231	8.8
0.154	8.0	0.154	7.8

Slope of Water Surface

Piezometer Readings in ft.

Time	2	3	4	5	6	7	8	9	10	11	12	13	Slope %
						February 17, 1954							
1325	1.116	1.113	1.111	1.109	1.109	1.107	1.107	1.104	1.100	1.099	1.097	1.094	.079
1450	1.091	1.088	1.082	1.082	1.080	1.080	1.077	1.077	1.075	1.070	1.069	1.064	.085
1535	1.086	1.086	1.085	1.080	1.077	1.078	1.077	1.076	1.076	1.068	1.067	1.065	.085
1715	1.087	1.085	1.081	1.080	1.079	1.079	1.079	1.077	1.074	1.071	1.070	1.066	.086
						February 27, 1954							
0805	1.089	1.091	1.088	1.086	1.084	1.081	1.079	1.078	1.076	1.073	1.071	1.067	.086
1205	1.093	1.090	1.088	1.087	1.086	1.086	1.083	1.081	1.079	1.078	1.075	1.070	.076
1300	1.075	1.070	1.070	1.069	1.069	1.069	1.066	1.063	1.062	1.058	1.057	1.052	.082
1325	1.070	1.067	1.066	1.064	1.062	1.060	1.060	1.058	1.056	1.053	1.051	1.047	.092

RUN 10

General Data

Q (cfs)	2.0	k	0.25
G (lb/sec)	0.0322	$C/\sqrt{g}$	9.5
D (ft)	0.51	n (ft) $^{1/6}$	0.025
U_m (ft/sec)	1.14	Re x 10^{-4}	5.24
U_* (ft/sec)	0.120	F	0.282
S (%)	0.088		

Temperature

Time	Temp. °C
1845	18.4
2210	19.2
2330	19.3

Dune Characteristics

	E_p	E_t	L	N
Profile along C ± 0.3 ft.	1.194	1.094	0.53	69
Profile 1 ft. from C ± 0.3 ft	1.193	1.087	0.49	73

Description of bed . . . . . . Dunes

Velocity and Concentration Profiles

$\frac{D-y}{y}$	c	y/D	U/U_* Sta. 67
0.063	0.95	0.941	12.1
0.134	1.20	0.882	12.5
0.215	1.25	0.823	12.7
0.307	1.35	0.765	12.4
0.419	1.35	0.705	12.0
0.548	1.50	0.646	11.6
0.701	1.45	0.588	11.0
0.891	1.50	0.529	10.7
1.130	1.75	0.470	10.5
1.430	1.80	0.411	9.75
1.840	1.60	0.352	9.75
2.400	1.70	0.294	9.15
3.260	2.00	0.235	7.75
4.670		0.176	8.00

Slope of Water Surface

Piezometer Readings in ft,
March 11, 1954

Time	1	2	3	4	5	6	7	8	9	10	11	12	13	14	Slope %
1655	.947	.944	.942	.939	.937	.934	.933	.931	.929	.927	.925	.922	.917	.910	.099
1850	.948	.945	.942	.941	.940	.938	.936	.933	.930	.927	.927	.923	.918	.914	.089
2230	.954	.950	.947	.944	.944	.941	.939	.937	.934	.933	.930	.928	.923	.920	.087
2335	.955	.951	.948	.945	.942	.942	.940	.937	.934	.933	.928	.928	.923	.919	.091

RUN 11

General Data / Temperature

General Data				Time	Temp. °C
Q (cfs)	1.50	k	0.40	0745	19.0
G (lb/sec)	0.0061	$C/\sqrt{g}$	8.9	1405	21.5
D (ft)	0.46	n (ft) $^{1/6}$	0.031		
U_m (ft/sec)	0.99	Re x 10^{-4}	4.27		
U_* (ft/sec)	0.112	F	0.257		
S (%)	0.087				

Dune Characteristics

	E_p	E_t	L	N
Profile along C ± 0.3 ft.	1.177	1.081	0.45	78
Profile 1 ft. from C ± .3 ft.	1.171	1.076	0.45	78
Description of bed	Dunes			

Velocity and Concentration Profiles

$\frac{D-y}{y}$	c	y/D	U/U* Sta. 67
0.072		0.933	11.5
0.156	0.0048	0.865	10.9
0.250	0.0058	0.800	10.3
0.364	0.0061	0.733	10.3
0.503	0.0054	0.665	10.4
0.667	0.0054	0.600	10.4
0.877	0.0066	0.533	9.6
1.145	0.0072	0.466	9.6
1.500	0.0098	0.400	9.0
2.000	0.0088	0.333	8.6
2.760	0.014	0.266	8.0
4.00	0.011	0.200	6.0

Slope of Water Surface

Piezometer Readings in ft.

Slope %	Time	1	2	3	4	5	6	7	8	9	10	11	12	13	14
March 12, 1954															
0.085	1645	.886	.881	.880	.877	.875	.874	.871	.867	.867	.866	.862	.859	.856	.851
0.087	1905	.893	.887	.885	.880	.881	.879	.876	.877	.872	.870	.870	.866	.863	.856
March 13, 1954															
0.0888	0805	.891	.887	.885	.882	.882	.880	.875	.873	.871	.870	.866	.864	.863	.859
0.084	1400	.892	.887	.886	.882	.881	.880	.879	.878	.876	.873	.869	.868	.864	.860

RUN 12

General Data				Temperature	
				Time	Temp. °C
Q (cfs)	1.96	k	0.55	1315	21.3
G (lb/sec)	0.00227	$C/\sqrt{g}$	9.7	1720	22.3
D (ft)	0.66	n $(ft)^{1/6}$	0.032	1850	22.5
U_m (ft/sec)	0.93	Re x 10^{-4}	6.01	2040	22.5
U_* (ft/sec)	0.096	F	0.202	2130	22.5
S (%)	0.044				

Dune Characteristics

	E_p	E_t	L	N
Profile along C ± 0.3 ft.	1.052	0.989	0.43	64
Profile 1 ft. from C + .3	1.148	1.090	0.48	56
Profile 1 ft. from C ∓ .3 ft.	1.183	1.013	0.51	29

Description of bed . . . . . . Dunes

Velocity and Concentration Profiles

$\frac{D-y}{y}$	c	y/D	U/U_* Sta. 67
0.083		0.923	11.6
0.182	0.0030	0.847	11.0
0.297		0.771	10.27
0.460	0.0026	0.685	10.68
0.617		0.618	10.27
0.845	0.0028	0.542	10.27
1.150	0.0041	0.465	9.85
1.570	0.0025	0.389	9.65
2.195	0.0054	0.313	9.44
3.235	0.0053	0.236	9.13
5.250	0.0066	0.160	7.88
10.910		0.084	7.46

Slope of Water Surface

Piezometer Readings in ft.
March 17, 1954

Time	2	3	4	5	6	7	8	9	10	11	12	13	Slope %
1325	1.098	1.096	1.097	1.095	1.093	1.092	1.092	1.089	1.087	1.086	1.083	1.083	.054
1600	1.098	1.095	1.096	1.093	1.092	1.092	1.092	1.091	1.090	1.089	1.086	1.085	.042
1710	1.098	1.095	1.095	1.094	1.092	1.093	1.093	1.091	1.090	1.088	1.087	1.085	.049
1850	1.097	1.096	1.097	1.094	1.094	1.094	1.094	1.092	1.091	1.090	1.086	1.087	.039
2100	1.097	1.096	1.097	1.095	1.094	1.095	1.095	1.092	1.089	1.089	1.088	1.085	.035
2125	1.098	1.096	1.097	1.095	1.095	1.096	1.096	1.091	1.090	1.090	1.088	1.087	.039

Remarks: Data appears to be good, but Kappa is too large.

RUN 13

General Data				Temperature	
				Time	Temp. °C
Q (cfs)	1.53	k	0.58	1050	21.4
G (lb/sec)	0.0266	$C/\sqrt{g}$	10.2	1310	22.2
D (ft)	0.54	n (ft) $^{1/6}$	0.023	1500	22.8
U_m (ft/sec)	0.90	Re x 10^{-4}	4.78	1730	23.0
U_* (ft/sec)	0.089	F	0.216		
S (%)	0.045				

Dune Characteristics

	E_p	E_t	L	N
Profile along Ċ ± 0.3 ft.	1.161	1.108	0.44	80
Profile 1 ft. from C ± .3 ft.	1.175	1.115	0.44	69
Profile 1 ft. from C ∓ .3 ft.	1.162	1.102	0.47	73
Description of bed	Dunes			

Velocity and Concentration Profiles

$\frac{D-y}{y}$	c	y/D	U/U_* Sta. 67
0.175	.00138	0.925	11.7
0.424	.00274	0.851	11.7
0.806	.00294	0.777	11.4
1.087	.0038	0.702	11.5
1.470	.0034	0.628	11.4
2.020	.0034	0.554	11.0
2.900	.0045	0.479	11.0
4.490	.0039	0.405	11.0
8.25	.0053	0.331	10.5
29.3	.0049	0.256	10.1
		0.182	8.2
		0.108	7.8
		0.033	7.3

Slope of Water Surface

Piezometer Readings in ft.
March 19, 1954

Time	1	2	3	4	5	6	7	8	9	10	11	12	13	14	Slope %
1050	.995	.991	.990	.990	.989	.988	.987	.987	.985	.984	.982	.980	.979	.975	.047
1135	.994	.991	.990	.990	.989	.988	.987	.987	.985	.984	.982	.980	.978	.975	.047
1300	.995	.990	.990	.990	.989	.988	.987	.987	.986	.984	.982	.981	.978	.976	.045
1505	.995	.992	.990	.990	.989	.988	.988	.988	.986	.984	.982	.981	.978	.976	.046
1730	.997	.994	.993	.993	.992	.991	.989	.989	.989	.987	.986	.985	.981	.979	.044

RUN 15

General Data

Q (cfs)	2.7	k	0.39
G (lb/sec)	0.206	$C/\sqrt{g}$	11.1
D (ft)	0.45	n (ft)$^{1/6}$	0.021
U_m (ft/sec)	1.64	Re x 10^{-4}	7.05
U_* (ft/sec)	0.147	F	0.43
S (%)	0.150		

Temperature

Time	Temp. °C
1140	19.2
1400	20.8
1720	22.4

Dune Characteristics

	E_p	E_t	L	N
Profile along C	1.104	1.039	0.74	46
Profile 1 ft. from C	1.095	1.038	0.85	41
Area near Sta. 67	1.104	1.025		50

Description of bed . . . . Dunes

Velocity and Concentration Profiles

$\frac{D-y}{y}$	c	y/D	U/U_* Sta. 67
0.126	0.050	0.941	13.6
0.290	0.067	0.888	12.9
0.541	0.063	0.775	12.6
0.814	0.086	0.662	12.2
1.28	0.137	0.551	12.2
2.06	0.147	0.439	12.0
3.65	0.142	0.327	11.2
8.72	0.256	0.215	8.97
		0.103	8.3

Slope of Water Surface

Piezometer Readings in ft.
April 10, 1954

Time	1	2	3	4	5	6	7	8	9	10	11	12	13	14	Slope %
1145	.844	.836	.831	.827	.824	.821	.810	.809	.802	.801	.798	.783	.787	.779	0.16
1345	.841	.829	.827	.823	.820	.816	.814	.812	.808	.807	.802	.800	.794	.780	0.145
1600	.835	.829	.825	.818	.819	.810	.807	.808	.809	.807	.800	.796	.790	.783	0.132
1715	.835	.825	.821	.819	.815	.814	.817	.809	.807	.801	.796	.796	.794	.785	0.125
1755	.836	.829	.828	.820	.820	.813	.813	.810	.806	.804	.797	.794	.790	.784	0.136

RUN 16

General Data				Temperature	
				Time	Temp. °C
Q (cfs)	1.9	k	0.40	1000	18.9
G (lb/sec)	0.0675	$C/\sqrt{g}$	9.2	1310	21.0
D (ft)	0.40	n (ft) $^{1/6}$	0.025	1735	23.0
U_m (ft/sec)	1.31	Re x 10^{-4}	5.22	2005	23.4
U_* (ft/sec)	0.143	F	0.365		
S (%)	0.158				

Dune Characteristics

	E_p	E_t	L	N
Profile along C	1.085	1.015	0.69	47
Profile 1 ft. from C	1.074	1.012	0.61	55
Area near Sta. 67	1.090	0.995		62
Description of bed . . . . Dunes				

Velocity and Concentration Profiles

$\frac{D-y}{y}$	c	y/D	U/U_* Sta. 67
0.189	0.02	0.921	11.0
0.311	0.0247	0.841	11.2
0.461	0.0237	0.763	11.1
1.240	0.0525	0.684	10.2
1.720	0.0504	0.605	10.2
2.460	0.0655	0.525	9.8
3.760	0.0757	0.446	9.4
6.630	0.1700	0.368	9.0
17.800	0.1580	0.289	8.5
		0.210	8.3
		0.131	8.0
		0.053	7.2

Slope of Water Surface

Piezometer Readings in ft.
April 12, 1954

Time	1	2	3	4	5	6	7	8	9	10	11	12	13	14	Slope %
1000	.774	.770	.763	.761	.756	.752	.750	.743	.742	.737	.732	.730	.722	.713	.160
1120	.772	.764	.763	.753	.752	.749	.747	.743	.740	.734	.733	.729	.719	.710	.148
1310	.771	.765	.761	.757	.752	.748	.745	.742	.737	.733	.730	.726	.719	.710	.154
1410	.768	.760	.758	.752	.750	.748	.743	.740	.737	.734	.729	.725	.716	.710	.148
1535	.766	.760	.754	.752	.750	.744	.741	.735	.733	.727	.724	.721	.714	.705	.156
1720	.764	.756	.754	.746	.747	.744	.738	.736	.730	.726	.722	.720	.709	.700	.160
2025	.764	.756	.756	.752	.747	.742	.740	.738	.733	.728	.723	.721	.715	.703	.158

RUN 17

General Data

Q (cfs)	1.34	k	0.38
G (lb/sec)	0.0254	$C/\sqrt{g}$	8.25
D (ft)	0.36	$n\ (ft)^{1/6}$	0.027
U_m (ft/sec)	1.14	Re x 10^{-4}	3.73
U_* (ft/sec)	0.138	F	0.335
S (%)	0.161		

Temperature

Time	Temp. °C
0730	18.5
1700	20.0

Dune Characteristics

	E_p	E_t	L	N
Profile along C	1.062	1.007	0.49	66
Profile 1 ft. from C	1.069	1.009	0.51	61
Area near Sta. 70	1.077	0.989		124

Description of bed . . . . Dunes

Velocity and Concentration Profiles

$\frac{D-y}{y}$	c	y/D	U/U_* Sta. 67
0.090	0.0180	0.918	10.7
0.193	0.0172	0.835	10.7
0.324	0.0194	0.755	10.2
0.484	0.0226	0.674	9.4
0.692	0.0236	0.591	9.0
0.961	0.0276	0.510	8.8
1.333	0.0390	0.429	8.5
1.875	0.0528	0.348	8.1
2.760	0.0544	0.266	7.2
		0.184	6.7

Slope of Water Surface

Piezometer Readings in ft.
April 14, 1954

Time	1	2	4	6	7	8	9	10	11	12	13	14	Slope %
0835	.702	.696	.691	.684	.680	.677	.673	.670	.665	.659	.651	.644	.157
1105	.701	.695	.687	.682	.677	.673	.670	.665	.660	.655	.648	.640	.161
1305	.706	.700	.696	.690	.686	.681	.677	.672	.668	.664	.655	.648	.168
1500	.706	.703	.696	.690	.685	.682	.679	.674	.670	.665	.656	.648	.163
1700	.707	.705	.698	.693	.690	.687	.683	.678	.675	.671	.664	.654	.153

RUN 18

General Data

Q (cfs)	7.4	k	0.72
G (lb/sec)	0.897	$C/\sqrt{g}$	15.4
D (ft)	0.69	n (ft) $^{1/6}$	0.016
U_m (ft/sec)	2.84	Re x 10^{-4}	1.95
U_* (ft/sec)	0.184	F	0.603
S (%)	0.156		

Temperature

Time	Temp. °C
1540	22.1
1615	22.5
1720	22.7
1915	23.2
2035	23.5

Dune Characteristics

Description of bed . . . . Smooth bed

Velocity and Concentration Profiles

$\frac{D-y}{y}$	c x%	y/D	U/U_* Sta. 67
0.080	0.0602	0.926	16.57
0.174	0.0730	0.852	16.67
0.286	0.0828	0.778	16.51
0.421	0.0936	0.704	16.40
0.588	0.0988	0.630	16.24
0.800	0.1068	0.556	16.14
1.077	0.1224	0.482	16.03
1.454	0.1342	0.408	15.82
2.000	0.1492	0.334	15.55
2.375	0.1604	0.297	15.38
2.857	0.1620	0.260	15.07
3.500	0.1796	0.222	14.85
4.400	0.2070	0.185	14.37
5.750	0.2374	0.148	14.00
8.000	0.2382	0.111	13.56

actual → x10⁶ ppm
0.000602 602

Slope of Water Surface

Piezometer Readings in ft.
April 26, 1954

Time	2	3	4	5	6	7	8	9	10	11	12	13	Slope%
1540	1.103	1.099	1.093	1.090	1.086	1.080	1.079	1.075	1.069	1.065	1.063	1.057	.160
1615	1.101	1.098	1.092	1.090	1.084	1.080	1.078	1.074	1.069	1.067	1.062	1.056	.151
1710	1.102	1.098	1.092	1.089	1.084	1.080	1.078	1.074	1.069	1.066	1.062	1.057	.158
1920	1.105	1.102	1.096	1.091	1.088	1.083	1.082	1.078	1.072	1.069	1.067	1.061	.152
2020	1.106	1.102	1.096	1.092	1.089	1.085	1.083	1.078	1.072	1.070	1.067	1.061	.155
2040	1.105	1.099	1.092	1.091	1.086	1.082	1.080	1.077	1.070	1.066	1.063	1.058	.161
2235	1.101	1.095	1.088	1.087	1.081	1.076	1.076		1.067	1.065	1.060	1.055	.155

Note: Kappa affected by upstream baffles.

RUN 19

General Data

Q (cfs)	9.0	k	0.61
G (lb/sec).	1.027	$C/\sqrt{g}$	15.8
D (ft).	0.75	n (ft) $^{1/6}$	0.016
U_m (ft/sec)	3.17	Re x 10^{-5}	2.3
U_* (ft/sec)	0.201	F	0.644
S (%)	0.167		

Temperature

Time	Temp. °C
1345	21.3
1425	21.5
1900	22.5

Dune Characteristics

Description of bed . . . . Smooth bed

Velocity and Concentration Profiles

$\frac{D-y}{y}$	c		y/D	U/U_* Sta. 67
0.072	0.0332	1	0.934	16.77
0.155	0.0450	2	0.867	16.87
0.251	0.0486	3	0.800	16.81
0.366	0.0562	4	0.733	16.67
0.503	0.0616	5	0.666	16.61
0.671	0.0692	6	0.599	16.51
0.881	0.0748	7	0.532	16.41
1.154	0.0852	8	0.465	16.16
1.517	0.0944	9	0.398	15.86
2.365	0.1052	10	0.298	15.40
3.343	0.1272	11	0.230	15.10
5.123	0.1554	12	0.163	14.25
9.375	0.2410	13	0.096	13.29
14.894	0.2972	14	0.064	12.59
32.955	0.5436	15	0.031	11.68
73.700	0.7292	16	0.015	10.83

Slope of Water Surface

Piezometer Readings in ft.
April 27, 1954

Time	2	3	4	5	6	7	8	9	10	11	12	13	Slope %
0930	1.174	1.168	1.161	1.159	1.153	1.150	1.148	1.143	1.137	1.136	1.130	1.124	.159
1138	1.171	1.165	1.158	1.154	1.150	1.146	1.144	1.40	1.133	1.133	1.128	1.122	.170
1306	1.175	1.169	1.163	1.158	1.154	1.149	1.147	1.143	1.139	1.135	1.132	1.125	.173
1431	1.175	1.169	1.163	1.158	1.154	1.149	1.147	1.143	1.138	1.136	1.132	1.125	.163
1900	1.176	1.170	1.164	1.158	1.155	1.150	1.149	1.145	1.140	1.137	1.133	1.127	.165

Note: High Kappa value caused by upstream baffles.

RUN 20

General Data

Q (cfs)	6.7	k	0.53
G (lb/sec)	0.805	$C/\sqrt{g}$	16.5
D (ft)	0.61	n (ft) $^{1/6}$	0.015
U_m (ft/sec)	2.97	Re x 10^{-5}	1.78
U_* (ft/sec)	0.180	F	0.67
S (%)	0.166		

Temperature

Time	Temp. °C
1130	22.5
1305	22.6
1505	22.5
1600	22.5
1700	22.5

Dune Characteristics

Description of bed . . . . Smooth bed

Velocity and Concentration Profiles

$\frac{D-y}{y}$	c	y/D	
0.090	0.0366	0.918	18.0
0.198	0.0456	0.835	18.2
0.330	0.0560	0.753	17.9
0.494	0.0620	0.670	17.7
0.704	0.0680	0.587	17.5
0.984	0.0816	0.504	17.2
1.373	0.0836	0.422	16.9
1.951	0.1020	0.339	16.4
2.903	0.1250	0.256	15.9
3.654	0.2440	0.215	15.5
4.762	0.1750	0.174	15.2
6.562	0.2140	0.132	14.8
10.000	0.2820	0.091	14.0
19.167	0.4740	0.050	13.0
120.000	1.1700	0.008	11.2

Slope of Water Surface

Piezometer Readings in ft.
April 29, 1954

Time	2	3	4	5	6	7	8	9	10	11	12	13	14	Slope %
0903	1.015	1.009	1.003	.998	.995	.990	.987	.982	.978	.975	.972	.966	.958	.167
0935	1.013	1.008	1.002	.998	.993	.990	.986	.983	.978	.974	.971	.965	.957	.165
1135	1.016	1.010	1.002	.998	.993	.990	.987	.983	.979	.975	.972	.966	.960	.165
1320	1.016	1.009	1.003	.998	.995	.990	.988	.984	.979	.976	.972	.966	.959	.167
1500	1.016	1.010	1.003	1.000	.995	.991	.988	.984	.980	.976	.972	.966	.958	.167
1603	1.016	1.010	1.003	.999	.995	.991	.989	.984	.979	.977	.975	.967	.958	.167

Note: High Kappa Value caused by upstream baffles.

RUN 21

General Data

Q (cfs)	0.90	k	0.36
G (lb/sec)	0.0063	$C/\sqrt{g}$	6.9
D (ft)	0.30	n (ft) 1/6	0.031
U_m (ft/sec)	0.86	Re x 10^{-4}	2.86
U_* (ft/sec)	0.124	F	0.277
S (%)	0.160		

Temperature

Time	Temp. °C
0835	23.0
1520	23.0
1755	22.7

Dune Characteristics

	E_p	E_t	L	N
Profile along C	1.049	0.998	0.48	79
Profile 1 ft. from C	1.058	0.996	0.49	64
Area near Sta. 67	1.067	0.977		77

Description of bed . . . . Dunes

Velocity and Concentration Profiles

$\frac{D-y}{y}$	c	y/D	U/U_* Sta. 67
0.108	.00408	0.902	9.81
0.243	.00456	0.804	9.25
0.416	.00876	0.706	8.35
0.642	.00798	0.608	7.44
0.785	.01250	0.560	7.85
0.955	.00917	0.511	7.27
1.162	.01320	0.462	7.11
1.417	.00928	0.413	6.79
1.741	.02320	0.365	6.79
2.165	.03140	0.316	6.54
2.744	.03740	0.267	6.21
		0.218	5.56
		0.170	5.56

Slope of Water Surface

Piezometer Readings in ft.
April 29, 1954

Time	1	2	4	6	8	10	12	13	14	Slope %
0715	.641	.636	.627	.621	.614	.605	.596	.587	.579	.162
0840	.639	.635	.625	.621	.614	.605	.596	.587	.581	.157
1315	.633	.626	.620	.612	.604	.595	.585	.587	.567	.155
1330	.630	.625	.617	.611	.602	.597	.587		.567	.164
1345	.629	.626	.617	.609	.601	.593	.585		.564	.160
1517	.630	.624	.617	.610	.602	.594	.584		.568	.163
1750	.628	.621	.614	.608	.598	.590	.581		.566	.162

Run 22

General Data

				Time	Temp. °C
Q (cfs)	9.1	k	0.38	0930	18.1
G (lb/sec)	0.990	$C/\sqrt{g}$	15.8	1240	20.2
D (ft)	0.76	n (ft)$^{1/6}$	0.016	1800	22.3
U_m (ft/sec)	3.27	Re x 10^{-5}	2.36		
U_* (ft/sec)	0.208	F	0.661		
S (%)	0.170				

Temperature

Dune Characteristics

Description of bed . . . . Smooth bed.

Velocity and Concentration Profiles

$\frac{D-y}{y}$	c	y/D	
0.071	0.0305	0.935	16.84
0.154	0.0359	0.870	16.93
0.250	0.0399	0.805	17.00
0.364		0.740	17.00
0.500	0.0479	0.674	17.10
0.666	0.0511	0.609	17.00
0.875	0.0492	0.543	16.90
1.150	0.0551	0.478	16.50
1.500	0.0599	0.412	16.21
2.000	0.0690	0.346	15.78
2.750	0.0820	0.282	15.15
4.000	0.0955	0.216	14.52
6.500	0.1420	0.190	14.09
8.370		0.151	13.50
14.000	0.3060	0.111	13.59
36.500	0.9370	0.085	12.10
		0.046	10.60
		0.020	7.60

Slope of Water Surface

Piezometer Readings in ft.
June 3, 1954

Time	2	3	4	5	6	7	8	9	10	11	12	13	Slope %
0845	1.135	1.128	1.121	1.115	1.110	1.107	1.102	1.098	1.094	1.089	1.086	1.080	.170
0930	1.135	1.130	1.122	1.116	1.109	1.107	1.101	1.098	1.094	1.089	1.086	1.080	.160
1020	1.133	1.127	1.122	1.115	1.109		1.102	1.099	1.095	1.090	1.086	1.079	.163
1230	1.133	1.127	1.121	1.115	1.108	1.106	1.101	1.098	1.093	1.089	1.085	1.080	.173
1510	1.134	1.128	1.121	1.114	1.108	1.106	1.100	1.097	1.092	1.088	1.084	1.079	.173
1645	1.133	1.128	1.121	1.114	1.108	1.106	1.101	1.099	1.093	1.090	1.087	1.080	.173

RUN 23

General Data		Temperature	
		Time	Temp. °C
Q (cfs) 7.4	k 0.42		
G (lb/sec) 0.778	$C/\sqrt{g}$ 16.2	0855	26.3
D (ft) 0.65	n (ft) $^{1/6}$ 0.015	1140	26.0
U_m (ft/sec) 3.18	Re x 10^{-5} 2.2	1615	26.2
U_* (ft/sec) 0.196	F 0.695		
S (%) 0.183			

Dune Characteristics

Description of bed . . . . Smooth bed

Velocity and Concentration Profiles

$\frac{D-y}{y}$	c	y/D	
0.083	0.022	0.923	17.09
0.181	0.029	0.846	17.09
0.300	0.034	0.769	17.35
0.444	0.038	0.692	17.24
0.625	0.044	0.615	17.09
0.857	0.039	0.538	16.94
1.166	0.055	0.461	16.86
1.600	0.071	0.384	16.43
2.250	0.065	0.307	15.95
3.333	0.089	0.230	15.18
5.500	0.105	0.153	14.16
12.000	0.175	0.076	12.60
25.000	0.440	0.038	9.85
	1.250		

Slope of Water Surface

Piezometer Readings in ft.
June 5, 1954

Time	1	2	3	4	5	6	7	8	9	10	11	12	13	Slope %
0915	1.038	1.026	1.018	1.010	1.005	1.000	.997	.992	.989	.983	.979	.977	.972	.170
1000	1.035	1.022	1.013	1.005	1.000	.994	.992	.990	.986	.981	.978	.977	.971	.152
1145	1.037	1.026	1.019	1.012	1.007	1.002	.999	.993	.989	.979	.978	.975	.970	.193
1330	1.047	1.034	1.027	1.018	1.014	1.008	1.003	.998	.990	.984	.980	.978	.971	.270
1405	1.033	1.018	1.013	1.005	1.000	.994	.994	.985	.980	.973	.972	.972	.963	.183

RUN 25

General Data

Q (cfs)	8.1	k	0.38
G (lb/sec)	0.813	$C/\sqrt{g}$	15.8
D (ft)	0.78	n (ft)$^{1/6}$	0.016
U_m (ft/sec)	2.77	Re x 10^{-5}	2.22
U_* (ft/sec)	0.176	F	0.553
S (%)	0.124		

Temperature

Time	Temp. °C
0805	24.5
0915	24.3
0950	24.3
1310	25.0
1420	25.0

Dune Characteristics

Description of bed . . . . Smooth bed

Velocity and Concentration Profiles

$\frac{D-y}{y}$	c	y/D	
0.147	0.0480	0.872	17.3
0.238	0.0535	0.808	17.3
0.345	0.0590	0.744	17.1
0.472	0.0650	0.680	17.2
0.625	0.0720	0.616	16.9
0.813	0.0810	0.552	16.7
1.050	0.0890	0.488	16.6
1.360	0.0940	0.424	16.1
1.790	0.1100	0.360	15.7
2.390	0.1300	0.296	15.3
3.340	0.1770	0.232	14.3
4.030	0.2000	0.192	14.2
4.880	0.2230	0.168	13.6
6.430	0.2150	0.134	12.8
8.750	0.5840	0.104	11.4
13.200	0.6250	0.071	10.1
		0.038	5.8
		0.006	4.6

Slope of Water Surface

Piezometer Readings in ft.
June 10, 1954

Time	2	3	4	5	6	7	8	9	10	11	12	13	Slope %
1025	1.152	1.150	1.145	1.137	1.136	1.133	1.132	1.131	1.130	1.124	1.122	1.117	.120
1040	1.154	1.148	1.144	1.136	1.140	1.137	1.133	1.129	1.126	1.123	1.121	1.118	.123
1123	1.157	1.150	1.148	1.141	1.138	1.136	1.133	1.130	1.128	1.123	1.121	1.116	.128
1305	1.160	1.153	1.146	1.143	1.142	1.139	1.137	1.135	1.131	1.126	1.123	1.122	.125
1500	1.156	1.150	1.146	1.140	1.140	1.142	1.135	1.130	1.126	1.124	1.123	1.119	.124

RUN 26

General Data / Temperature

General Data				Temperature	
				Time	Temp. °C
Q (cfs)	7.0	k	0.32	1000	24.2
G (lb/sec)	0.625	$C/\sqrt{g}$	16.4	1055	24.2
D (ft)	0.69	n (ft) $^{1/6}$	0.016	1335	25.0
U_m (ft/sec)	2.71	Re x 10^{-5}	1.94	1450	25.4
U_* (ft/sec)	0.166	F	0.575		
S (%)	0.125				

Dune Characteristics

Description of bed . . . . Smooth bed

Velocity and Concentration Profiles

$\frac{D-y}{y}$	c	y/D	U/U_* Sta. 73
0.0799	0.023	0.926	18.4
0.1696	0.031	0.855	18.4
0.2810	0.034	0.781	18.2
0.4110	0.043	0.709	18.1
0.5750	0.048	0.635	18.1
0.7770	0.054	0.563	17.6
1.0400	0.062	0.490	17.3
1.4000	0.067	0.416	16.6
1.9100	0.080	0.344	16.3
2.7100	0.098	0.270	15.5
3.4200	0.130	0.226	15.1
4.0800	0.158	0.197	14.5
5.5400	0.217	0.153	13.9
7.0700	0.238	0.124	13.2
11.4000	0.481	0.0805	12.1
18.7000	2.044	0.0514	10.0
		0.022	6.87

Slope of Water Surface

Piezometer Readings in ft.
June 11, 1954

Time	2	3	4	5	6	7	8	9	10	11	12	13	Slope %
0530	1.059	1.053	1.049	1.045	1.042	1.037	1.034	1.031		1.027	1.023	1.020	.125
0800	1.058	1.052	1.047	1.044	1.042	1.039	1.035	1.031		1.025	1.022	1.018	.129
1000	1.057	1.052	1.047	1.042	1.040	1.036	1.033	1.029	1.026	1.026	1.020	1.016	.141
1100	1.055	1.050	1.047	1.043	1.040	1.037	1.035	1.032	1.027	1.026	1.022	1.018	.125
1335	1.054	1.050	1.044	1.040	1.038	1.034	1.030	1.028	1.022	1.024	1.020	1.016	.125
1500	1.052	1.048	1.041	1.038	1.037	1.034	1.031	1.029	1.024	1.023	1.020	1.017	.123

RUN 27

General Data				Temperature	
				Time	Temp. °C
Q (cfs)	2.1	k	0.31	0820	23.5
G (lb/sec)	0.1316	$C/\sqrt{g}$	10.0	1310	24.5
D (ft)	0.40	n (ft) $^{1/6}$	0.023	1630	25.0
U_m (ft/sec)	1.33	Re x 10^{-4}	5.47		
U_* (ft/sec)	0.133	F	0.37		
S (%)	0.140				

Dune Characteristics

	E_p	E_t	L	N
Profile along C	1.046	0.994	0.52	64
Profile 1 ft. from C	1.050	0.999	0.55	63
Area near Sta. 75	1.055	0.955		64
Description of bed	Dunes			

Velocity and Concentration Profiles

$\frac{D-y}{y}$	c	y/D	U/U_* Sta. 75
0.0823	0.043	0.874	13.6
0.1630	0.051	0.810	13.55
0.2550	0.051	0.746	13.65
0.3630	0.060	0.684	12.8
0.4920	0.064	0.620	12.2
0.6470	0.084	0.494	12.3
0.8390	0.073	0.430	12.4
1.0800	0.087	0.367	11.7
1.4000	0.098	0.304	11.4
1.8300	0.097	0.240	11.2
3.3900	0.152	0.177	10.2
		0.557	12.0

Slope of Water Surface

Piezometer Readings in ft.
June 15, 1954

Time	2	4	6	7	8	9	10	11	12	13	14	Slope %	1
1100	.735	.726	.717	.715	.711	.706	.699	.698	.692	.690	.681	.150	
1300	.734	.730	.724	.721	.715	.711	.707	.702	.700	.644	.683	.147	
1310	.745	.738	.728	.731	.727	.723	.716	.711	.707	.701	.691	.147	.754
1330	.747	.739	.736	.729	.725	.720	.718	.713	.711	.704	.694	.141	.751
1350	.752	.746	.742	.736	.737	.734	.726	.724	.716	.711	.700	.136	.763
1525	.751	.748	.741	.743	.738	.733	.729	.727	.721	.717	.705	.130	.
1620	.756	.746	.742	.739	.737	.730	.728	.722	.719	.715	.702	.140	.760

RUN 28

General Data

Q (cfs)	2.63	k	0.31
G (lb/sec)	0.149	$C/\sqrt{g}$	11.5
D (ft)	0.48	n (ft) $^{1/6}$	0.020
U_m (ft/sec)	1.53	Re x 10^{-4}	7.47
U_* (ft/sec)	0.133	F	0.39
S (%)	0.116		

Temperature

Time	Temp. °C
1405	21.5
1840	23.6
2105	24.2
2145	24.2

Dune Characteristics

	E_p	E_t	L	N
Profile along C	1.055	0.984	0.67	51
Profile 1 ft. from C	1.047	0.988	0.71	49
Area near Sta 73	1.062	0.969		64

Description of bed . . . . Dune Pattern

Velocity and Concentration Profiles

$\frac{D-y}{y}$	c	y/D	U/U_* Sta. 73	y/D	
0.130	0.036	0.885	13.9	0.895	13.6
0.268	0.0425	0.789	13.9	0.789	13.5
0.463	0.048	0.684	13.6	0.684	13.4
0.725	0.054	0.579	13.1	0.579	12.9
0.944	0.062	0.515	12.6	0.474	12.3
1.110	0.067	0.473	12.3	0.368	12.0
1.440	0.091	0.410	12.0	0.305	11.3
1.720	0.081	0.368	11.6	0.263	10.4
2.280	0.118	0.305	10.8	0.200	8.9
2.800	0.094	0.263	10.6	0.158	8.6
4.000	0.101	0.200	9.85	0.095	7.2
5.310	0.111	0.158	8.65		
9.520	0.202	0.095	7.75		
17.900	0.181	0.053	6.92		

Slope of Water Surface

Piezometer Readings in ft.
June 16, 1954

Time	1	2	3	4	5	6	7	8	9	10	11	12	13	14	Slope %
1500	.834	.830	.826	.824	.822	.813	.816	.815	.811	.807	.806	.802	.795	.788	.113
1535	.835	.828	.826	.823	.820	.820	.816	.813	.812	.805	.803	.802	.794	.786	.115
1620	.836	.831	.824	.821	.820	.818	.816	.813	.809	.807	.803	.800	.795	.786	.119
1840	.838	.832	.830	.825	.825	.821	.818	.816	.813	.805	.805	.802	.794	.788	.130
2000	.836	.831	.830	.827	.825	.820	.817	.815	.813	.810	.808	.801	.799	.789	.107
2105	.837	.831	.830	.827	.824	.822	.821	.816	.814	.810	.806	.804	.799	.789	.115
2135	.838	.832	.828	.826	.824	.821	.820	.817	.813	.811	.808	.805	.800	.790	.115
2300	.835	.830	.831	.825	.821	.820	.819	.816	.814	.810	.806	.803	.799	.788	.116

RUN 29

General Data

General Data				Temperature	
				Time	Temp. °C
Q (cfs)	5.8	k	0.32	0630	25.6
G (lb/sec)	0.384	$C/\sqrt{g}$	16.5	0950	25.2
D (ft)	0.60	n $(ft)^{1/6}$	0.014	1305	25.0
U_m (ft/sec)	2.54	Re x 10^{-5}	1.61		
U_* (ft/sec)	0.153	F	0.573		
S (%)	0.121				

Dune Characteristics

Description of bed . . . . Smooth bed.

Velocity and Concentration Profiles

$\frac{D-y}{y}$	c	y/D	U/U_* Sta. 73
0.0893	0.016	0.918	19.0
0.198	0.021	0.835	18.9
0.330	0.027	0.752	18.9
0.493	0.031	0.670	18.4
0.704	0.035	0.587	17.9
0.981	0.045	0.505	17.4
1.370	0.0545	0.422	17.0
1.950	0.059	0.339	16.3
2.950	0.087	0.256	15.6
3.830	0.103	0.207	15.0
4.750	0.143	0.174	14.5
7.070	0.232	0.124	13.0
10.000	0.482	0.091	11.6
23.400	1.074	0.041	6.9
		0.025	5.0

Slope of Water Surface

Piezometer Readings in ft.

Time	1	2	3	4	5	6	7	8	9	10	11	12	13	14	Slope %
June 17, 1954															
0625		.961	.957	.952	.949	.946	.943	.941	.938	.936	.935	.933	.926	.920	.10
0805	.971	.957	.954	.950	.946	.943	.940	.938	.934	.933	.931	.928	.920	.915	.124
0915	.972	.959	.956	.950	.947	.945	.941	.939	.936	.935	.934	.930	.924	.919	.118
June 18, 1954															
0925	.969	.957	.954	.950	.945	.943	.940	.938	.933	.932	.931	.930	.924	.918	.138
1045	.969	.957	.954	.950	.945	.944	.939	.940	.935	.933	.931	.928	.923	.919	.114
1200		.961	.957	.953	.948	.947	.944	.943	.937	.936	.935	.934	.928	.924	.118
1310		.963	.959	.955	.951	.948	.945	.943	.939	.937	.937	.935	.929	.925	.113

RUN 31

General Data | Temperature

				Time	Temp. °C
Q (cfs)	4.2	k	0.25	0650	26.0
G (lb/sec)	0.430	$C/\sqrt{g}$	21.0	0830	26.2
D (ft)	0.42	n (ft) $^{1/6}$	0.011	0955	26.5
U_m (ft/sec)	2.71	Re x 10^{-5}	1.22	1120	27.0
U_* (ft/sec)	0.129	F	0.738		
S (%)	0.123				

Dune Characteristics

Description of bed . . . . Smooth bed.

Velocity and Concentration Profiles

$\frac{D-y}{y}$	c	y/D	U/U_* Sta. 73
0.136	0.0066	0.88	24.4
0.235	0.0084	0.81	24.2
0.351	0.0096	0.74	24.0
0.492	0.0120	0.67	23.4
0.667	0.0149	0.60	22.7
0.924	0.0204	0.52	22.1
1.222	0.0266	0.45	21.8
1.632	0.0338	0.38	20.9
2.230	0.0461	0.31	20.2
3.170	0.0797	0.24	19.4
4.880	0.1490	0.17	18.2
9.530	0.4190	0.095	15.9
19.800		0.048	12.8

Slope of Water Surface

Piezometer Readings in ft.
June 22, 1954

Time	2	4	6	7	8	9	10	11	12	13	14	Slope %
0645	.746	.737	.730	.729	.726	.722	.718	.715	.711	.707	.697	.137
0820	.747	.737	.731	.730	.727	.723	.720	.717	.713	.708	.698	.120
0935	.747	.738	.731	.729	.727	.722	.719	.717	.714	.708	.697	.123
1050	.747	.738	.730	.729	.726	.722	.720	.717	.713	.709	.699	.112
1120	.749	.738	.731	.729	.726	.723	.720	.716	.713	.708	.698	.123

RUN 32

General Data / Temperature

General Data				Time	Temp. °C
Q (cfs)	4.2	k	0.32		
G (lb/sec)	0.145	$C/\sqrt{g}$	11.3	1300	25.2
D (ft)	0.73	n (ft) $^{1/6}$	0.022	1415	26.0
U_m (ft/sec)	1.57	Re x 10^{-5}	1.21	1630	26.7
U_* (ft/sec)	0.139	F	0.323		
S (%)	0.082				

Dune Characteristics

	E_p	E_t	L	N
Profile along C	1.106	1.037	0.66	38
Profile 1 ft. from C	1.124	1.071	0.50	53
Profile 1 ft. from C	1.099	1.044	0.51	48
Area near Sta. 73	1.116	1.024		64
Description of bed	Dune Pattern			

Velocity and Concentration Profiles

$\frac{D-y}{y}$	c	y/D	U/U_* Sta. 73
0.0742	0.022	0.931	13.3
0.159	0.025	0.863	13.6
0.258	0.029	0.795	13.2
0.377	0.029	0.726	13.3
0.520	0.036	0.658	12.9
0.695	0.039	0.590	12.7
0.919	0.048	0.521	12.8
1.209	0.054	0.453	12.2
1.600	0.050	0.385	11.4
2.140	0.059	0.318	10.8
3.030	0.061	0.248	9.85
4.550	0.086	0.180	9.06
7.920	0.085	0.112	7.35
21.70	0.099	0.044	3.52

Slope of Water Surface

Piezometer Readings in ft.
June 23, 1954

Time	2	3	4	5	6	7	8	9	10	11	12	13	Slope %
1145	1.114	1.112	1.110	1.107	1.105	1.103	1.100	1.097	1.096	1.094	1.092	1.091	.088
1300	1.113	1.112	1.110	1.106	1.104	1.103	1.100	1.099	1.096	1.095	1.093	1.091	.080
1410	1.114	1.112	1.111	1.108	1.104	1.104	1.103	1.101	1.098	1.097	1.095	1.091	.078
1530	1.116	1.115	1.111	1.109	1.108	1.105	1.104	1.101	1.099	1.099	1.097	1.093	.081
1625	1.115	1.115	1.112	1.108	1.107	1.106	1.103	1.103	1.100	1.098	1.097	1.092	.081

RUN 33

General Data

				Time	Temp. °C
Q (cfs)	7.2	k	0.35		
G (lb/sec)	0.252	$C/\sqrt{g}$	11.5	1345	26.1
D (ft)	1.03	n (ft) $^{1/6}$	0.023	1520	26.5
U_m (ft/sec)	1.63	Re x 10^{-5}	1.80	1650	27.0
U_* (ft/sec)	0.142	F	0.283		
S (%)	0.061				

Dune Characteristics

	E_p	E_t	L	N
Profile along C	1.111	1.046	0.59	42
Profile 1 ft. from C	1.118	1.063	0.59	45
Profile 1 ft. from C	1.102	1.047	0.58	46
Area near Sta. 73	1.133	1.043		64

Description of bed . . . . Dunes with possible sandbars.

Velocity and Concentration Profiles

$\frac{D-y}{y}$	c	y/D	Sta. 73
0.0515		0.951	14.1
0.106	0.0261	0.904	14.1
0.241	0.0332	0.806	13.9
0.411	0.0414	0.709	13.4
0.636	0.0457	0.611	12.8
0.942	0.0519	0.515	12.2
1.400	0.0579	0.417	11.7
1.710	0.0609	0.369	11.3
2.130	0.0668	0.320	11.2
2.680	0.0802	0.272	10.8
3.490	0.0877	0.223	10.2
4.710	0.1040	0.175	9.15
6.930	0.1090	0.126	8.38
11.900	0.1120	0.0776	8.03
		0.0291	7.31

Slope of Water Surface

Piezometer Readings in ft.
June 24, 1954

Time	2	3	4	5	6	7	8	9	10	11	12	13	Slope%
1310	1.433	1.432	1.426	1.423	1.427	1.427	1.425	1.423	1.418	1.423	1.420	1.412	.058
1345	1.434	1.434	1.428	1.426	1.425	1.428	1.425	1.424	1.422	1.419	1.421	1.416	.060
1515	1.435	1.433	1.432	1.431	1.428	1.424	1.427	1.424	1.422	1.425	1.419	1.420	.060
1610	1.438	1.435	1.434	1.432	1.428	1.430	1.426	1.426	1.425	1.423	1.424	1.421	.0530
1640	1.444	1.440	1.436	1.437	1.432	1.433	1.430	1.427	1.429	1.428	1.424	1.421	.068
1655	1.442	1.439	1.435	1.435	1.432	1.430	1.428	1.426	1.429	1.428	1.424	1.420	.065

RUN 34

General Data

Q (cfs)	8.85	k	0.47
G (lb/sec)	0.184	$C/\sqrt{g}$	9.75
D (ft)	1.38	n (ft) $^{1/6}$	0.028
U_m (ft/sec)	1.66	Re x 10^{-5}	2.40
U_* (ft/sec)	0.170	F	0.249
S (%)	0.065		

Temperature

Time	Temp. °C
1300	25.1
1410	25.3
1500	25.5
1600	25.6
1645	25.6

Dune Characteristics

	E_p	E_t	L	N
Profile along C	1.084	1.014	0.67	41
Profile 1 ft. from C	1.091	1.033	0.59	47
Profile 1 ft. from C	1.090	1.028	0.52	53
Area near Sta. 73	1.106	1.015		96

Description of bed . . . . . . Dunes

Velocity and Concentration Profiles

$\frac{D-y}{y}$	c	y/D	U/U_* Sta. 73	U/U_* Sta. 73
0.0787	0.0145	0.927	10.7	10.95
0.170	0.0163	0.855	10.8	11.0
0.278	0.0185	0.783	10.6	10.8
0.408	0.0201	0.710	10.5	10.8
0.567	0.0215	0.638	10.5	10.6
0.770	0.0244	0.565	10.4	10.52
1.030	0.0269	0.493	10.2	10.3
1.380	0.0291	0.420	9.88	10.0
1.600	0.0289	0.384	9.70	
1.870	0.0317	0.348	9.81	9.54
2.200	0.0332	0.312	9.53	9.54
2.620	0.0376	0.276	9.41	8.77
3.180	0.0401	0.239	8.81	8.47
3.930	0.0432	0.203	8.11	8.53
4.990	0.0418	0.167	7.41	8.01
6.700	0.0621	0.130	7.17	7.24
9.650	0.0742	0.094	7.17	

Slope of Water Surface

Piezometer Readings in ft.
June 27, 1954

Time	2	3	4	5	6	7	8	9	10	11	12	13	Slope %
1300	1.729	1.728	1.726	1.725	1.723	1.722	1.721	1.719	1.717	1.716	1.712	1.708	.070
1400	1.730	1.730	1.729	1.727	1.726	1.726	1.722	1.720	1.718	1.718	1.713	1.707	.060
1430	1.726	1.726	1.724	1.724	1.720	1.721	1.719	1.716	1.714	1.713	1.712	1.706	.068
1535	1.727	1.727	1.726	1.725	1.723	1.721	1.721	1.720	1.716	1.718	1.713	1.710	.065
1630	1.739	1.740	1.737	1.738	1.734	1.736	1.732	1.733	1.728	1.729	1.725	1.722	.061

RUN 35

General Data

Q (cfs) 7.2	k 0.32		
G (lb/sec) 1.113	$C/\sqrt{g}$ 19.7		
D (ft) 0.56	n (ft)$^{1/6}$ 0.012		
U_m (ft/sec) 3.34	Re x 10^{-5} 1.97		
U_* (ft/sec) 0.170	F 0.786		
S (%) 0.160			

Temperature

Time	Temp. °C
0825	25.5
1000	25.5
1055	25.6
1215	26.0

Dune Characteristics

Description of bed . . . . Smooth bed

Velocity and Concentration Profiles

$\frac{D-y}{y}$	c	y/D	U/U_* Sta. 73	U/U_* Sta. 73
0.099	0.027	0.91	22.4	
0.218	0.039	0.82	22.3	22.4
0.368	0.050	0.73	22.1	21.8
0.558	0.063	0.64	21.4	21.6
0.809	0.081	0.55	20.9	21.1
1.160	0.089	0.464	20.5	20.6
1.670	0.108	0.375	19.7	19.8
2.030	0.118	0.330	19.4	19.4
2.500	0.131	0.286	19.1	18.9
3.150	0.150	0.241	18.7	18.7
4.100	0.172	0.196	17.8	18.1
5.580	0.235	0.152	17.1	17.0
8.340	0.343	0.107	16.3	16.5
15.000	0.721	0.063	15.3	15.1
54.500	2.570	0.018	13.0	13.0

Slope of Water Surface

Piezometer Readings in ft.
June 29, 1954

Time	2	3	4	5	6	7	8	9	10	11	12	13	14	Slope %
0815	.950	.942	.933	.926	.922	.917	.914	.908	.908	.903	.897	.892	.885	.168
0930	.946	.939	.931	.926	.920	.915	.913	.910	.907	.904	.896	.893	.886	.150
1010	.950	.939	.935	.927	.921	.917	.915	.910	.907	.905	.900	.894	.886	.150
1055	.957	.947	.940	.931	.926	.921	.916	.911	.909	.904	.899	.893	.882	.180
1150	.947	.940	.933	.927	.922	.917	.915	.910	.908	.905	.900	.895	.887	.150
1210	.947	.938	.932	.927	.921	.916	.915	.910	.907	.905	.899	.892	.883	.157

RUN 36

Q (cfs)	7.6	k	0.30	Time	Temp. °C
G (lb/sec)	1.790	$C/\sqrt{g}$	20.0	0820	25.2
D (ft)	0.53	n (ft) $^{1/6}$	0.012	1320	27.0
U_m (ft/sec)	3.78	Re x 10^{-5}	2.12		
U_* (ft/sec)	0.189	F	0.915		
S (%)	0.21				

Dune Characteristics

Description of bed . . . . Smooth bed

Velocity and Concentration Profiles

$\frac{D-y}{y}$	c	y/D	U/U_* Sta. 73
0.105	0.0258	0.905	22.5
0.235	0.0588	0.810	22.8
0.399	0.0584	0.715	22.2
0.613	0.0764	0.620	21.7
0.905	0.0974	0.525	21.2
1.321	0.1220	0.431	20.4
1.612	0.1440	0.383	19.9
1.975	0.1890	0.336	19.6
2.470	0.1930	0.288	19.0
3.150	0.2660	0.241	18.5
4.180	0.3600	0.193	18.0
5.850	0.5020	0.146	17.3
9.160	0.8560	0.0986	15.8
18.500	2.1180	0.0512	14.2
		0.038	10.7

Slope of Water Surface

Piezometer Readings in ft.

July 1, 1954

Time	1	2	3	4	5	6	7	8	9	10	11	12	13	14	Slope %
0820	.937	.915	.900	.893	.883	.875	.871	.867	.863	.854	.848	.843	.837	.827	.230
1010	.930	.910	.898	.891	.880	.874	.870	.866	.860	.857	.851	.844	.836	.827	.210
1110	.928	.908	.898	.890	.878	.874	.870	.866	.857	.856	.850	.843	.833	.823	.248
1200	.926	.908	.897	.889	.877	.873	.869	.866	.856	.856	.851	.845	.835	.826	.200
1320		.904	.894	.887	.876	.871	.866	.863	.856	.854	.848	.843	.834	.823	.203

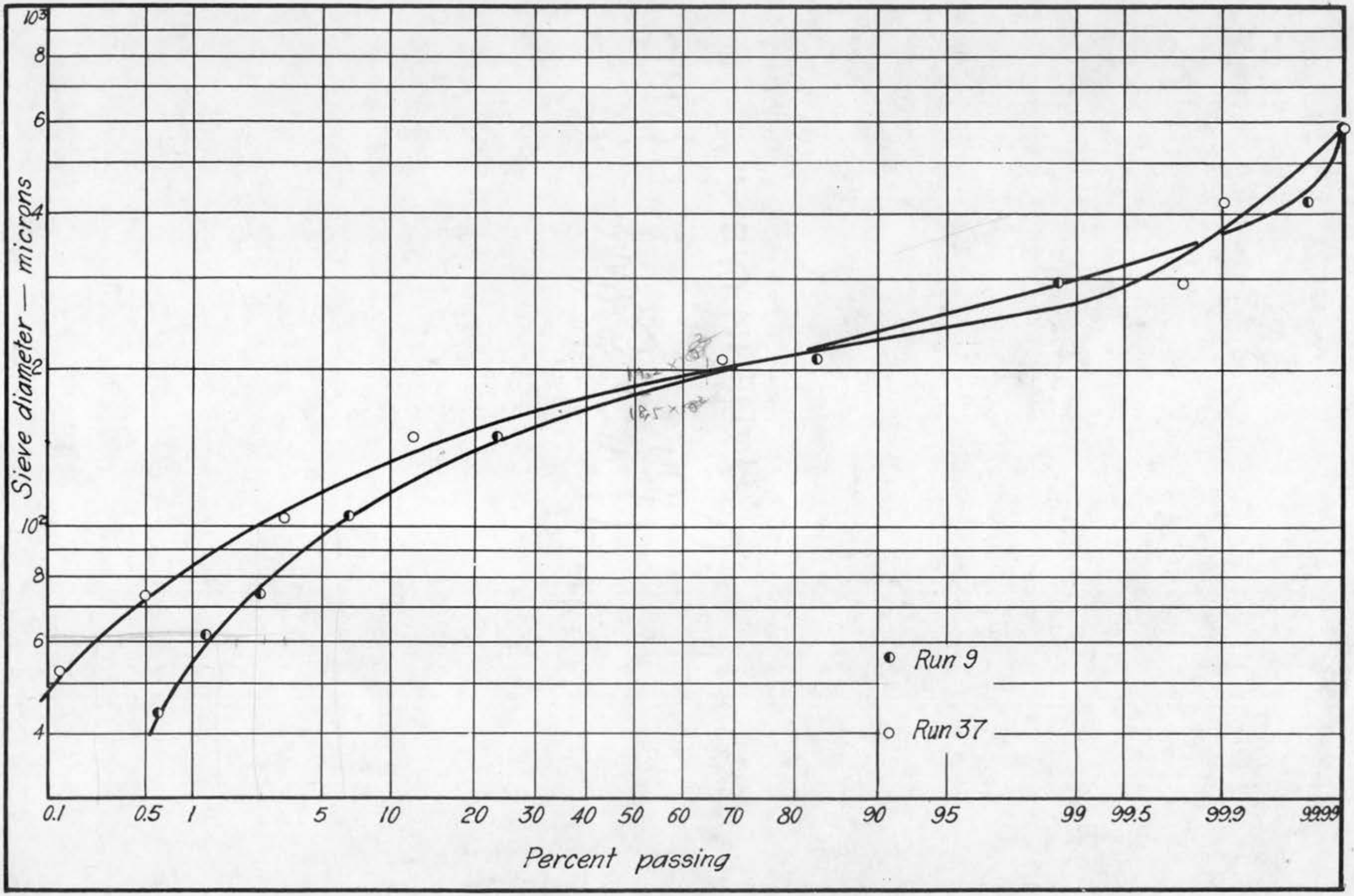

Fig. A1 Bed-material size distribution curves

1 micron = 1.0 x 10⁻⁶ m = 10⁻³ mm

19.2 x 10⁻³ x 10 = 0.192 mm

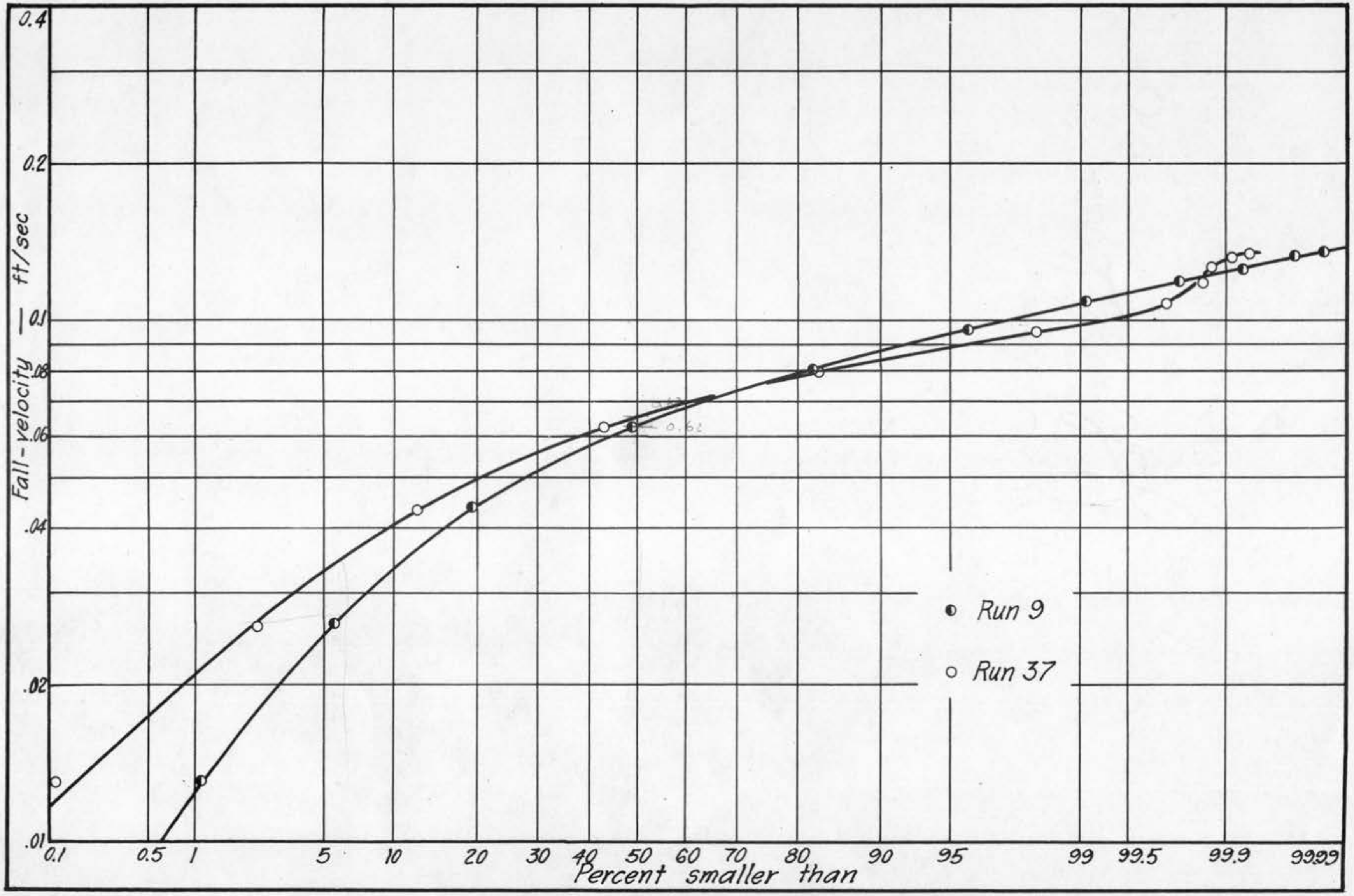

Fig. A2 Bed-material fall-velocity distribution curves

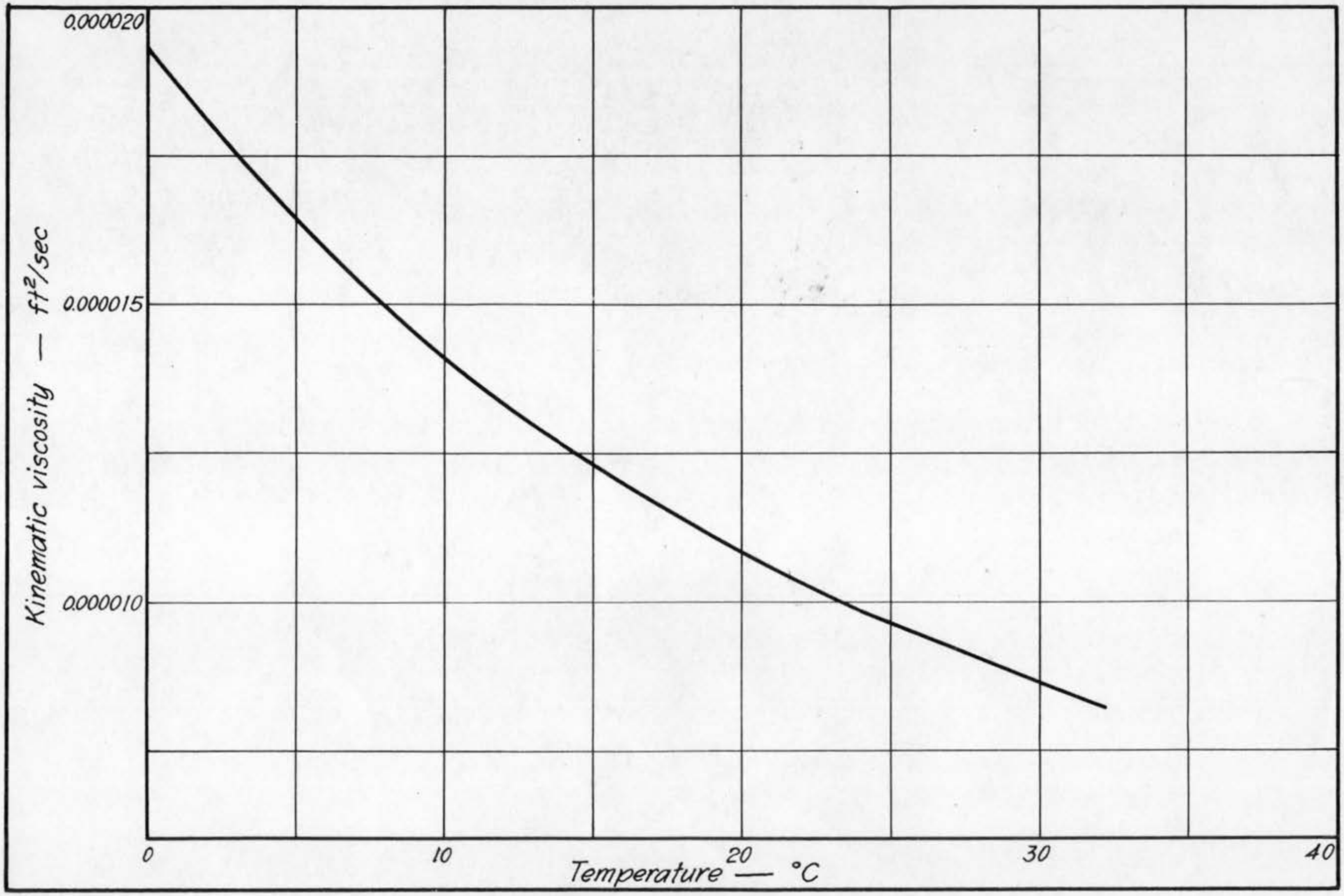

Fig. A3 Kinematic viscosity of water

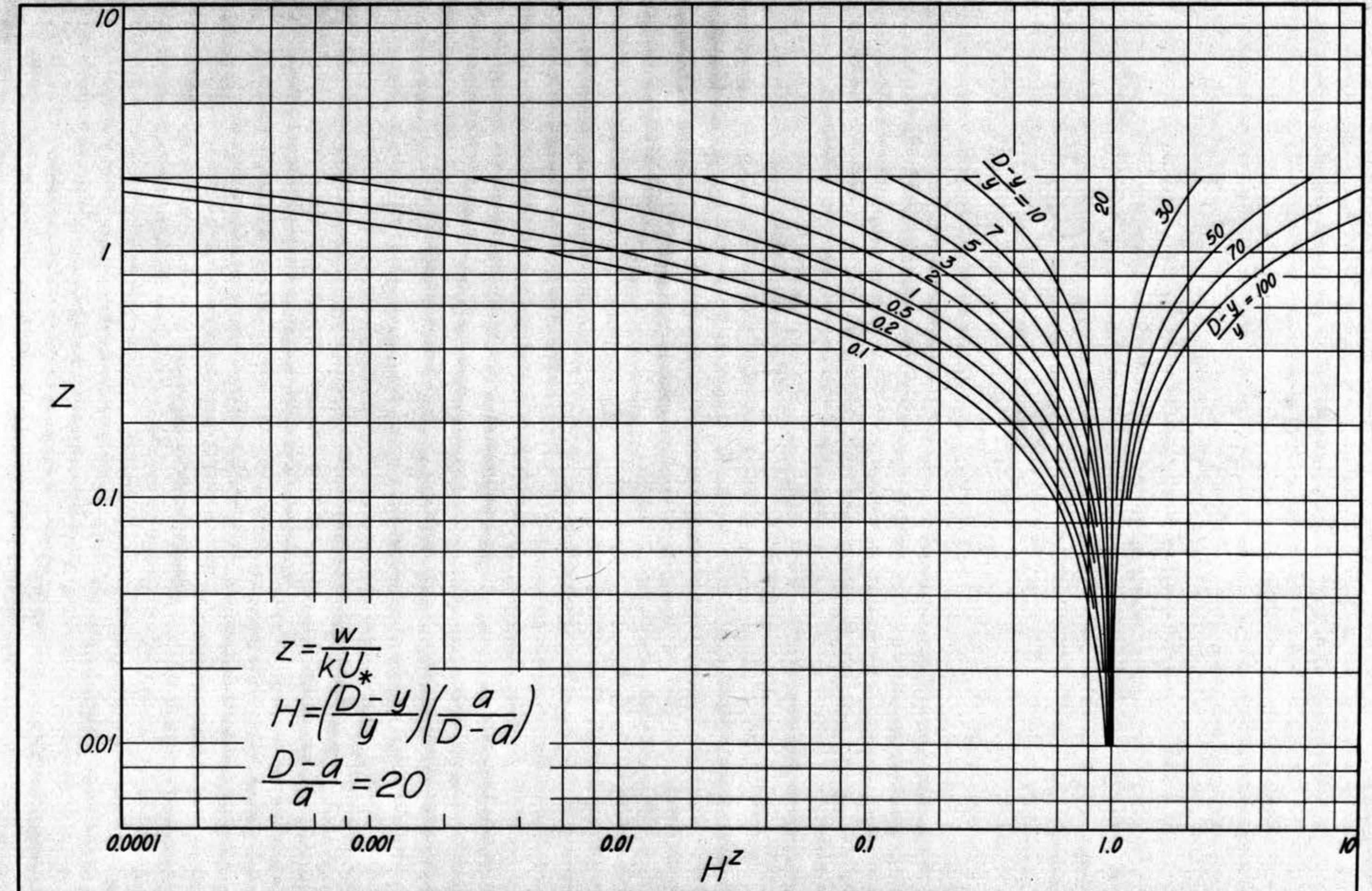

Fig. A4 Curves for the graphical integration of Eq 37